On the Origin and Differentiation of Melanophores in Zebrafish, *Danio rerio*

Dissertation
der Mathematisch-Naturwissenschaftlichen Fakultät
der Eberhard Karls Universität Tübingen
zur Erlangung des Grades eines
Doktors der Naturwissenschaften
(Dr. rer. nat.)

vorgelegt von
Christopher Michael Dooley
aus Burlington, Vermont, United States of America

Tübingen
2014

Tag der mündlichen Qualifikation: 06.06.2014

Dekan: Prof. Dr. W. Rosenstiel

1. Berichterstatter: Prof. Dr. C. Nüsslein-Volhard

2. Berichterstatter: Prof. Dr. R. Reuter

Acknowledgements

I would like to thank Janni for her generous support, encouragement and passion for science. Without her, this work would not have been possible. I would also like to thank Rolf Reuter for supervising this thesis and for the opportunity to teach in his practical courses, which I greatly enjoyed. I would also like to thank Robert Geisler for giving me a start and for his support.

For lots of great experiments, scientific conversations and much more I am grateful for having had the chance to work together with Alessandro.

I am grateful to Hans-Martin for teaching me many things and for always being there.

I would like to thank past members of the department; Mahendra, Matthew, Kellee, and Mitch for great scientific conversations and helping me to form ideas.

I would like to thank Silke for her help at different times and for helping me become fluent in German and also Ines, Iris, Chris and Host for help along the way.

I would like to thank fellow students; Madeleine, Katrin, Sven, Nic, Martina, Yi-Yen, Soeren, Andrey, Paolo, Simon and Xuefan for their help and support at different times.

I am thankful for comments and support for different parts of this work from Hans-Georg, Jana, Uwe, and Ajeet.

I am thankful to Brigitte for attempting some difficult experiments together and for the animal caretakers for providing and caring for our fish.

I would like to thank Heinz for his help in carrying out EMs and Gertrud for help photographing adult fish.

I am thankful to my family, Mom, Pam and Bryan, for supporting me while I was far away, even when times were tough.

Finally Janina, I am endlessly grateful for your understanding, care and support.

Contents

Acknowledgements **1**

List of publications presented **5**

Abbreviations **6**

Abstract **8**

Zusammenfassung **11**

OVERVIEW 1 .... **14**

Aim of this thesis: 19

INTRODUCTION 2 .... **20**

The Neural Crest **20**

2.1 Discovery 20

2.2 Identification of neural crest cells 22

2.3 Neural crest formation 24

2.4 Neural crest migration 25

2.5 Formation of the dorsal root ganglia 28

2.6 Neural crest gene regulatory network 30

2.7 Derivatives of neural crest 34

2.8 Haploid is just not enough – at least in mammals 35

2.9 Making a melanocyte – specification, differentiation and maturation of specific neural crest cells.............................. 36
2.10 Melanocyte specification – choosing a path................ 37
2.11 Melanocyte differentiation – the dark side of neural crest... 39
2.12 Pigmenting a human and pigmenting a fish – more than shades of grey... 42

RESULTS AND DISCUSSION 3.......................... 44

Publication 1:... 44
3.1 On the embryonic origin of adult melanophores.......... 44
3.1.1 Melanoblasts migrate along motor neurons 45
3.1.2 ErbB receptors are required for neural crest migration along the ventral medial pathway....................................... 49
3.1.3 Dorsal root ganglia are required for adult pigmentation 52
3.1.4 Ablation of embryonic melanophores activates melanophore precursors at the site of the dorsal root ganglia... 53
3.1.5 Dorsal root ganglia are an early established niche for adult melanophore progenitors... 56

3.1.6 *sparse like* encodes Kit ligand a and is expressed in migrating neural crest cells 56
3.1.7 Early Kit ligand a signaling is required for specific melanophore precursors and for the maintenance of embryonic melanophores 57
3.1.8 Distinct populations of melanophore progenitors and their specific migratory routes 60

Publication 2: **72**

3.2 On melanophore melanization **72**

CONCLUDING REMARKS 4 .... **88**

Bibliography **91**

Contributions **102**

Curriculum vitae **103**

List of publications **104**

List of publications presented

Publication 1:
Dooley CM, Mongera A, Walderich B, Nüsslein-Volhard C. (2013). **On the embryonic origin of adult melanophores: the role of ErbB and Kit signalling in establishing melanophore stem cells in zebrafish.** *Development* 140, 1003-1013

Publication 2:
Dooley CM, Schwarz H, Mueller KP, Mongera A, Konantz M, Neuhauss SC, Nüsslein-Volhard C, Geisler R. (2012). **Slc45a2 and V-ATPase are regulators of melanosomal pH homeostasis in zebrafish, providing a mechanism for human pigment evolution and disease.** *Pigment Cell Melanoma Res.* 26; 205–217

Abbreviations

BMP	Bone morphogenetic protein
dpf	days post-fertilization
cls	*colourless*
DRG	dorsal root ganglia
Dct	Dopachrome tautomerase
ECM	extra cellular matrix
EDN3	Endothelin-3
EDNRB	Endothelin receptor B
EGF	Epidermal growth factor
EMT	Epithelial–mesenchymal transition
FGF	Fibroblast growth factor
foxd3	Forkhead box D3
gfp	green fluorescent protein
H	hydrogen
hfp	hours post-fertilization
kita	*c-kit receptor a*
kitlga	*c-kit receptor ligand a*
Mab	monoclonal antibody
MCR	melanocortin receptor
mitfa	Microphthalmia-associated transcription factor
MSH	melanocyte-stimulating hormone
Na	sodium
NC	neural crest
nbt	neural beta-tubulin
OCA	oculocutaneous albinism
pax	Paired box
QCPN	quail non-chick perinuclear antigen
RPE	retinal pigment epithelium
RTK	receptor tyrosine kinase
SCF	stem cell factor
SNP	single nucleotide polymorphism

sox	Sry-related HMG box
TfAP2	Transcription factor apical protein 2
Tyr	Tyrosinase
Tyrp1	Tyrosinase related protein 1

Abstract

The neural crest is a vertebrate specific, developmentally transient population of pluripotent stem cells capable of crossing germ layer boundaries and differentiating into a multitude of different tissues. In Zebrafish, one of these cell types, the pigment cells of the body, first appear and differentiate in early embryos contributing to a stereotypical larval pigmentation pattern composed of melanophores, xanthophores and iridophores. At juvenile stages the larval pigmentation pattern undergoes a rapid transformation with the appearance of large numbers of newly arriving pigment cells that develop into the adult striped pattern of zebrafish skin. These melanophores arise from an undifferentiated cell population. Although ontogenetically derived from the neural crest, their exact source in juvenile and adult fish has remained unclear.

Here I present the source of the late appearing melanophores of the adult pattern to be derived from a stem cell population, set aside early in development at the future site of the dorsal root ganglia as part of the peripheral nervous system. The melanophore progenitors use the spinal nerves as migratory routes leading to the hypodermis at the periphery. Using

mutants, morpholino and small molecule inhibition, I dissect the specific roles of ErbB and Kit signaling in the establishment of the melanophore stem cells and the role of dorsal root ganglia as their niche. By combining blastula transplantation and live imaging techniques I have identified melanophore progenitor cells during regeneration becoming active at the site of the dorsal root ganglia. I have followed their lineage until melanization, thereby confirming their specific fate. Furthermore, I show the requirement of these melanophore stem cells for the adult pigment cell population.

Continuing along with melanophore maturation and differentiation, I have positionally cloned the zebrafish *albino* mutant and present mutations in *slc45a2* encoding a solute carrier protein as causing the phenotype. In humans, mutations in *SLC45A2* lead to oculocutaneous albinism type IV and single nucleotide polymorphisms (SNPs) at this locus are associated with skin color variation, but little is known about the function of *SLC45A2* in melanization. I present evidence for a role of *Slc45a2* in pH and ionic homeostasis inside melanosomes and show how variation of these conditions affects the key melanin producing enzyme, tyrosinase. I also show that mutations in *sandy/tyrosinase* lead to a destruction of melanosomes with toxic effects to neighboring tissues. Taken together these results provide insight into the large amount of variation in *SLC45A2* across many animals as opposed to the relative low variation associated with *TYROSINASE* in humans.

Zusammenfassung

Die Neuralleiste besteht aus einer Population von pluripotenten Stammzellen, die als embryonale Anlage bei der Entwicklung von Wirbeltieren entstehen. Zellen der Neuralleiste sind in der Lage, sich zu einer Vielzahl von Zelltypen zu differenzieren, wie unter anderem zu Pigmentzellen. In Zebrafischen erscheinen Pigmentzellen zuerst während der Embryonalentwicklung, und bilden ein typisches larvales Farbmuster aus. Später, während des jugendlichen Stadiums, entstehen eine Anzahl von neuen Pigmentzellen, die das Farbmusters des adulten Fisches bilden. Die Melanophoren dieses Musters entstammen einer undifferenzierten Zellpopulation, die von der Neuralleiste abgeleitet ist. Jedoch war ihr genauer Ursprung im jugendlichen und adulten Fisch bisher unbekannt.

Ich beschreibe hier, dass die Vorläuferzellen der adulten Melanophoren einer Stammzellpopulation entstammen, die bereits früh während der Entwicklung segmental neben den Ganglien (Dorsal Root Ganglion, DRG) des peripheren Nervensystems angelegt wird. Nach ihrer Aktivierung wandern die Melanophorenstammzellen dann entlang der Spinalnerven in die Haut des Fisches hinein. Durch Analyse verschiedener Zebrafischmutanten, Injektionen von

Morpholinos oder Nutzung von Hemmstoffen konnte ich die spezifischen Rollen der ErbB-und Kit-Signalwege bei der Anlage dieser Stammzellen am DRG und die Rolle des DRGs als Stammzellnische aufgliedern. Durch Transplantationsexperimente von Blastulazellen kombiniert mit Zeitrafferfilmen konnte ich die Aktivierung der Melanophorenstammzellen am DRG beobachten, ihre Entwicklung bis zum Zeitpunkt der Melanisierung verfolgen und somit ihre spezifische Herkunft nachweisen. Desweiteren zeige ich, dass diese Melanophorenstammzellen die adulten Melanophoren hervorbringen.

Im Zusammenhang mit meiner Analyse der Differenzierung von Melanophoren habe ich die *albino* Zebrafischmutation positional kloniert und zeige, dass Mutationen im Gen *slc45a2,* welches ein Transmembran-Transportprotein kodiert, den *albino* Phänotyp verursachen. Im Menschen führen Mutationen in *SLC45A2* zu okulokutanem Albinismus Typ IV. Polymorphismen an diesem Genlocus sind mit unterschiedlichen Hautfarben assoziiert, jedoch ist sehr wenig über die genaue Funktion von *SLC45A2* im Melanisierungsprozess bekannt. Ich zeige, dass *Slc45a2* möglicherweise eine Rolle bei der Kontrolle der pH- und ionischen Homöostase innerhalb der Melanosomen spielt, und demonstriere, wie eine Veränderung der Bedingungen ein Schlüsselenzym des Melaninstoffwechsels, Tyrosinase, beeinflussen. Weiterhin zeige ich, dass Mutationen in *sandy*/*tyrosinase* zur Zerstörung von Melanosomen und damit einhergehenden toxischen Effekten auf das umliegende Gewebe führen. Diese Ergebnisse erklären das Auftreten der vielfältigen bekannten Variationen in *SLC45A2* in vielen Tierarten, im Gegensatz zu der relativ seltenen Variation im *TYROSINASE* Gen.

Overview I

Pigment cells in developing vertebrates are derived from a transient and pluripotent embryonic cell population called the neural crest (NC). These cells arise at the border between the neural ectoderm and the epidermis during early development, migrate throughout the embryo, and give rise to widely diverse cell types, including chromatophores, the peripheral and enteric nervous system, ectomesenchymal tissues like the craniofacial skeleton and smooth muscle, to name a few.

NC specification and development is a multi-step process, which is orchestrated by BMP, Wnt and FGF signals at the border between neural and non-neural ectoderm inducing the cells there to become the neural crest. NC cells then delaminate and segregate from the neural epithelium of the developing neural tube and become migratory. NC cells disperse and migrate along specific pathways; for example, in the trunk the NC cells choose between two distinct pathways. Cells destined to become melanocytes migrate along the dorsolateral pathway between the ectoderm and the dermomyotome of the somites, whereas NC cells destined to become sympathetic chain and dorsal root ganglia take a ventromedial path between the myotome and the neural tube and notochord. Following delamination NC cells migrate, proliferate and differentiate into their final fates. Historically, the majority of initial neural crest studies were carried out in chick and mouse embryos. These studies have formed the basis of contemporary knowledge of NC development but it is important to point out that each vertebrate species has evolved its own nuances of neural crest development. For example, zebrafish like other fishes and amphibians have three pigment cell types. In addition to dark melanophores, it displays yellowish colored xanthophores and silver iridescent iridophores. It has been noted that in the zebrafish, pigment cells are capable of migrating along both trunk neural crest routes.

In the fishes, different pigment patterns arise during larval and adult stages. Larval pigmentation consists of three melanophore stripes along the dorsal and ventral myotomes and the horizontal myoseptum. Silver iridescent iridophores appear along with melanophores and yellowish xanthophores (Fig. 1). This pattern remains until the zebrafish goes through a metamorphosis as juveniles and begins to develop the adult pigment pattern at about three weeks of development. This process is marked by the appearance of new melanophores between the larval melanophore stripes. These "metamorphic" melanophores continue to appear for another three weeks and it is thought that a portion of this population is derived from cells retaining an undifferentiated stem cell like state, throughout the fish's life (Yang and Johnson, 2006).

A very well described example of pigment stem cells contained and maintained as undifferentiated melanoblast are those of the mammalian hair follicle bulge, which are called upon in every hair rejuvenating cycle (Tanimura et al., 2011). These cells represent one of only a limited number of examples of post embryonic developmental stem cells identified in their respective niche. Another source of melanoblasts recently described in chicken and mouse arise through a Schwann cell precursor intermediate from neural crest cells, which originally migrated along the ventral medially path. These two sources of melanocyte precursors represent fundamentally different cases: the first is an example of a classical stem cell-niche situation while the latter could be described as phenotypic switching.

Once a melanoblast has been specified it still requires a set of specific genes involved in its differentiation. For example, in order for a melanocyte to produce the dark pigment melanin it first must generate subcellular lysosomal-related vesicles called melanosomes. Within the melanosomes there is a stepwise synthesis of eumelanin from precursor substances such as tyrosine and dopamine. Fully differentiated melanophores of fish and amphibians are also capable of dynamically modulating the internal distribution of their melanosomes in response to environmental cues.

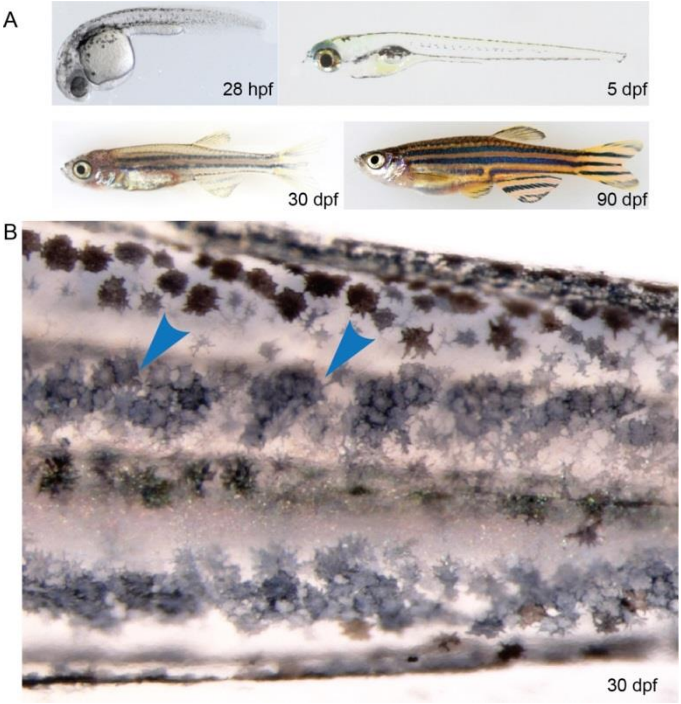

Figure 1: Pigment patterning of the zebrafish and the appearance of metamorphic melanophores. The first melanophores of both the RPE and the neural crest can easily be identified as they melanize at 28 hpf. At 5 dpf the larval pigmentation pattern consisting of a dorsal, medial and ventral stripes are now present. During metamorphosis, chromatophores continually appear until the first two juvenile stripes are readily visible at about 30 dpf. By 90 dpf the fish have assumed their adult morphology and pigment pattern (**A**). The continual addition of melanophores during juvenile stages appears to arise from undifferentiated precursors which can be seen as newly formed clusters in the flanks of juvenile fish (blue arrowheads). Their new melanophores appear bluish due to lower levels of melanin in contrast to the darker melanin of older melanophores (**B**).

Aim of this thesis:

The process of specifying, differentiating, maintaining and localizing a melanophore is highly complex and requires many different signals and factors in a specific temporal and spatial manner. This work intends to elucidate novel developmental elements of these processes by following melanophore ontogeny from the birth of their precursors in the neural crest to their final migration and differentiation throughout the body of the zebrafish.

Introduction 2

The Neural Crest

2.1 Discovery

The NC can be described as both the morphological structure consisting of the folds of the neural ectoderm along the dorsal neural tube during its invaginationes, and as the transient population of pluripotent stem cells, which are induced at the folds in developing vertebrates. Wilhelm His (1831-1904) was the first to identify a group of cells tucked between the future ectoderm and the dorsal neural tube that he termed the *Zwischenstrang* of a developing chicken embryo (His, 1868). His along with Arthur Milnes (1852-1893), who was the first to use the term 'neural crest' in 1879, independently discovered NC cells to be the source of spinal and cranial ganglia (Hall, 1999). A little more than a decade later Julia Platt (1857-1935) demonstrated that jaw cartilage and tooth dentine cells in salamander *Necturus maculosus* arose from an area of the ectoderm flanking the dorsal neural tube (Platt, 1897). These findings were largely rejected by her contemporaries because they were in direct conflict with the almost dogmatic acceptance of the germ-layer theory of the day. Almost 50 years would pass until Sven Hörstadius (1898-1996) along with others was able to show in detail and to convince the community that indeed NC cells were a source of mesenchyme giving rise to bones (Horstadius, 1950) (Raws, 1947).

These findings helped to lead to the abandonment of a rigid germ-layer theory and were not only important from a developmental but also from an evolutionary standpoint. In our modern era, it has been put forth by Brian Hall and others that NC is a fourth germ layer while ectoderm and endoderm can be considered primary germ layers and mesoderm and NC secondary germ layers (Hall, 1999). Just as the evolution of mesoderm has allowed for a vast expansion of body plans and structures seen in chordates, the NC is an invention of vertebrates which provides them with a pool of highly migratory progenitor cells capable of developing into many different cell types, which can be crafted and molded under the forces of development and evolution. (Hall, 1999).

2.2 Identification of neural crest cells

The ability to distinguish NC cells in a developing embryo and the faithful tracing through all possible derivatives has been intensely investigated since the initial discovery of the NC. It is astonishing that after more than a century of lineage studies, new crest derivatives are still being discovered. The study of NC cells poses a number of intrinsic challenges due to their highly migratory nature and the ability of NC cells to generate such a wide variety of different tissue types. Two major issues must be resolved in order to follow NC cells through their development; the first is the *in situ* (or *in vivo*) access to NC cells in the embryo and the second is the ability to mark these cells either physically (with dyes), molecularly or genetically.

The use of monoclonal antibodies (Mab) and avian models of NC (quail chick chimeras) created a number of influential advances in the 1980s and 1990s (Le Douarin, 1982, Le Douarin, 1986b). The discovery of the antibody HNK-1 (Vincent and Thiery, 1984) allowed the visualization of NC cells along their initial migratory routes shortly after they had left the dorsal neural tube. Although HNK-1 Mab is able to mark premigratory NC cells the signal diminishes in immunoreactivity in later NC cells and loses specificity.

Therefore it is not appropriate for long term labeling of NC derivatives. The construction of quail-chick chimeras through either grafting or injection of dissociated quail cells into chick allows for the long term tracking of NC cells and their derivatives (Le Douarin, 1986a, Le Douarin, 1986b) (Le Douarin, 1982). Transplanted quail cells are readily identified in their chick hosts by either nuclear morphological features or the QCPN (quail non-chick perinuclear antigen) Mab. Although these methods do allow for visualization *in toto* and at later stages with resolution at the single cell level they do not allow for *in vivo* experimentation.

Embryos of teleost fish, for example the zebrafish, are particularly well suited for studying NC early development and ontogeny. Being completely transparent and developing at a rapid pace in a simple petri dish zebrafish embryos are an ideal *in vivo* developmental model system. They can also be easily manipulated through basic embryological techniques such as heterotypic transplantation and ablation. Zebrafish NC cells are relatively large in size and can be observed within a developing embryo under simple light microscopy conditions. In initial NC fate-mapping experiments, Raible and Eisen took advantage of these qualities and described early NC cell differentiation by injecting vital dyes into NC cells followed by thorough observation through early development (Raible et al., 1992) (Raible and Eisen, 1994).

2.3 Neural crest formation

The first steps of NC specification occur during gastrulation as the presumptive areas of neural, ectodermal, epidermal and NC tissues are induced prior to neurulation. The forces of epidermalization and neurulation meet at the border of the neural and epidermal ectoderm, exactly where NC is induced (Raven, 1945). The establishment of the NC is a multi-step process where first inductive signals (*Bmp*, *Wnt*, *Fgf* and *Notch/Delta*) (Marchant et al., 1998) (LaBonne and Bronner-Fraser, 1998) (Cornell and Eisen, 2000, García-Castro et al., 2002) (Mayor et al., 1997) (Sauka-Spengler, 2008) establish the presumptive birthplace of NC at the neural plate borders by up regulation of important transcription factors of the *Msx*, *Pax* and *Zic* families (Saint-Jeannet et al., 1997) (Bang et al., 1997) (Deardorff et al., 2001) (Lewis et al., 2004, Sauka-Spengler, 2008). These transcriptional regulators then induce a second tier of transcription factors specific for NC cells such as *Snail*, *SoxE*, *FoxD3*, etc, and are also thought to play a role in the ensuing epithelial to mesenchymal transformation (EMT), where NC cells delaminate from the folds of the dorsal neural tube (Dutton et al., 2001, Monsoro-Burq et al., 2005) (Luo et al., 2003) (Sato et al., 2005, Sauka-Spengler et al., 2007) (Werner et al., 2007). Furthermore, these second tier factors also regulate expression of a third tier set of genes which play a role in migration and differentiation of NC cells into specific tissue types (Fig. 2B).

Neurulation of mammalian and avian embryos occurs through the invagination of the neural plate as it forms the neural tube. In contrast, in most teleosts (bony fishes) the neural tube is formed through a cavitation process, which intermediately produces a neural keel structure (Hall, 1999). Following the formation of the neural tube, regardless if via invagination or cavitation, NC cells undergo a loss of cell to cell adhesion. They degrade their basal lamina and modulate their intracellular components as the epithelial apical-basal polarity is lost and migration ensues, being the hallmark features of epithelial- mesenchymal transition (EMT) (Hall, 1999).

2.4 Neural crest migration

The initiation of NC cell migration occurs in a wave-like cranial to caudal progression. NC cells migrate ventrally along distinct paths within the developing embryo

(Horstadius, 1950, Weston, 1963) (Le Douarin, 1982, Dupin et al., 2006). Ectomesenchymal NC cells of the cranium migrate out in streams to populate the future jaw and nasal processes and will later contribute to bones, cartilage and connective tissue of the head. Non- ectomesenchymal NC cells also migrating in the anterior forming cranial ganglia, neurons, Schwann cells, pigment cells, etc. The specific paths these cells follow are largely the same across all vertebrates but the timing of migration of different NC cell types has been shown to vary (Fig. 2B) (Le Douarin, 1982) (Hall, 1999).

NC cells of the trunk migrate along two major paths typically referred to as the dorsolateral (or lateral) or the ventromedial (or medial) path (Le Douarin, 1982) (Raible et al., 1992) (Hall, 1999) (Kelsh et al., 2009). Commencement of migration along these paths again varies from species to species e.g.: NC cells in mouse begin migration along both routes simultaneously whereas in avian and teleost first the ventromedial NC cells migrate and after a delay the dorsolateral cells. NC cells migrating along the dorsolateral path move superficially between the epidermis and the somites forming more ventrally. Migration along this route is restricted to cells of a melanocyte fate in mammals and birds, and cells of chromatophore fates in fish and amphibians (Raws, 1947, Weston, 1963, Le Douarin, 1986a, Bronner-Fraser and Fraser, 1989, Erickson et al., 1992, Raible et al., 1992).

Cells migrating along the ventromedial path collect at specific points in a metamerized fashion along the ventral neural tube and then proceed further as streams of cells in a ventral direction. These cells migrate between the neural tube and the adjacent dermomyotome and sclerotome positioned laterally. The metameric array of the NC cell streams along this path directly determines the segmental arrangement of the future dorsal root ganglia, sympathetic ganglia and extending peripheral nerves and Schwann cells (Le Douarin, 1986a, Bronner-Fraser and Fraser, 1989). The positioning of these segmental streams was found to be restricted to the more rostral myotomal region in chick, while in a central position of the myotome teleosts; it has been correlated with the similar migratory path of the spinal motor axons. Guidance molecules involved in short range cell-cell interactions as well as long range diffusion gradients have been extensively studied in axonal guidance (Goodman and Shatz, 1993) (Keynes and Cook, 1995). These factors are thought to also play a role in NC migration. There is also emerging evidence that the axons themselves may play a role in NC migration (Mongera, Dooley, Nüsslein-Volhard unpublished data). The space between neural tube/notochord and somites are rich in

ECM and could allow for the neural crest themselves to shape their molecular surroundings as they pass through (Hall, 1999).

2.5 Formation of the dorsal root ganglia

NC cells migrating along the ventromedial path give rise to the dorsal root ganglia and autonomic ganglia, including sympathetic ganglia and parasympathetic ganglia (Weston, 1963, Le Douarin, 1982, Bronner-Fraser M, 1988). As these NC cells migrate through the somatic mesoderm, subpopulations of these cells coalesce at the presumptive site of the dorsal root ganglia. Other cells on the ventromedial route continue to migrate further where they accumulate above the dorsal aorta and give raise to the sympathetic ganglion chain. As the DRGs form there is crosstalk from one DRG anlagen to the next along the rostral-caudal axis. Once cells commit to a condensing DRG they take up positions as more quiescent interior cells or cells of the exterior which display active filopodia extensions to the surrounding environment (Kasemeier-Kulesa et al., 2005).

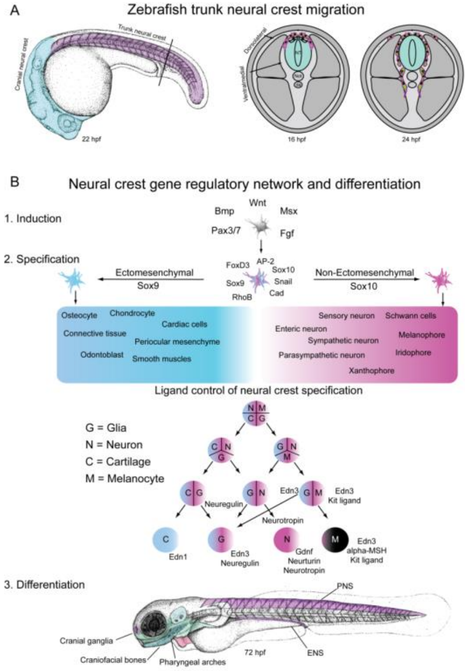
A
Zebrafish trunk neural crest migration
Cranial neural crest
Trunk neural crest
22 hpf
Dorsolateral
Ventralmedial
NT
Not
16 hpf
24 hpf
B
Neural crest gene regulatory network and differentiation
1. Induction
Wnt
Bmp
Msx
Pax3/7
Fgf
2. Specification
FoxD3
AP-2
Sox10
Snail
Cad
Sox9
RhoB
Ectomesenchymal
Sox9
Non-Ectomesenchymal
Sox10
Osteocyte
Chondrocyte
Cardiac cells
Connective tissue
Periocular mesenchyme
Odontoblast
Smooth muscles
Sensory neuron
Schwann cells
Enteric neuron
Sympathetic neuron
Melanophore
Parasympathetic neuron
Iridophore
Xanthophore
Ligand control of neural crest specification
G = Glia
N = Neuron
C = Cartilage
M = Melanocyte
N M C G
C N G
G N M
C G
G N
G M
Neuregulin
Edn3
Edn3
Kit ligand
Neurotropin
C
Edn1
G
Edn3
Neuregulin
N
Gdnf
Neurturin
Neurotropin
M
Edn3
alpha-MSH
Kit ligand
3. Differentiation
PNS
Cranial ganglia
Craniofacial bones
Pharyngeal arches
72 hpf
ENS

Figure 2: Neural crest induction, specification, migration and differentiation is orchestrated by a complex gene regulatory network. Neural crest development separates cranial neural crest development from trunk neural crest. The migration in the trunk occurs as a wave along the anterior to posterior axis beginning at about 14 hpf and completes at the tip of the tail at about 28 hpf (**A**). A gene regulatory network orchestrates each step of neural crest ontogeny. The stepwise process is the induction followed by speciation and then differentiation. Intrinsic factors push crest cells to adopt either an ectomesenchymal or a non-ectomesenchymal cell fate. NC cells encounter extracellular factors, e.g. ligands, along migratory routes can also play a role in pushing neural crest cells to adopt specific fates. Once a specific fate has been determined a further set of genes are activated to allow for the terminal differentiation. (**B**) **Adapted from(Martinez-Morales et al., 2007).*

2.6 Neural crest gene regulatory network

The events of NC induction, specification and final differentiation are coordinated through a complex set of intrinsic and extrinsic signals governed by a precise hierarchical gene regulatory network. Each of these steps employs a specific set of genes and signals, which guide NC cells to their terminal positions and fates (Sauka-Spengler, 2008).

Genes required for the induction of NC program the cells at the neural folds and bestow upon them properties of multipotency and migrational capacity. Neural crest cells at this point are true stem cells as they have been shown to be self-renewing as well as having the potential to differentiate into multiple derivatives (Stemple and Anderson, 1992). For example, acquisition of new cell surface receptors, metalloproteases and cell adhesion molecules allow the forming NC cells to receive new signals as well as to interact with their environment. Another important role of the inductive signals and their downstream targets is to initiate the expression of the second tier of the NC gene regulatory network which represent genes required for cell type specification of NC cells (Alfandari et al., 2001).

The NC specifiers (*Snail, SoxE, FoxD3 AP-2, Twist, c-Myc*) begin to specifically mark NC cells *in situ* and initiate a new regulatory state (Dottori et al., 2001, Britsch et al., 2001) (Knight et al., 2003, Sauka-Spengler, 2008). These genes play a major role in NC specification which is thought to occur directly in the dorsal neural tube or immediately following the initiation of migration. One of the first major tasks of this new state is to undergo the process of EMT so that these now mesenchymal cells are free to move out and investigate their surroundings (Le Douarin, 1982) (Hall, 1999, Strobl-Mazzulla and Bronner, 2012). Although the exact hierarchy still remains to be clarified, it has become clear that these transcription factors and signals regulate each other in specific ways whereby, specifying certain subtypes of NC cells is not only a matter of turning on and maintaining certain transcription factors but also turning off others.

NC cells are initially pluripotent cells, but this potency is thought to be consolidated in a process termed restrictive specification, which could function through different modes, for example through intrinsic mechanisms even before or during EMT (Hall, 1999) (Bronner-Fraser M, 1988). Furthermore, restriction through migrational processes has also been observed and could function in two particular modes (Le Douarin, 1986a, Bronner-Fraser and Fraser, 1989).

NC cells of certain fates are limited to specific migrational routes. For example in higher vertebrates there seems to be an overall inhibition of NC cells to migrate dorsolaterally with the exception of melanoblasts. Interestingly, lamprey NC cells only migrate dorsolaterally and lack ventromedial migrating NC cells as well as sympathetic ganglia (Sauka-Spengler et al., 2007). The other migrational mode is the restriction through extrinsic signals as NC cells migrate along their particular paths. These signals can be cell-to-cell interactions, membrane bound and soluble ligands, extracellular matrix (ECM) components. This process of restriction, reduces the number of pluripotent NC cells and lead them to multipotent, bipotent or specified cells.

One well-described example in zebrafish of the multiple responsibilities of a NC specifier can be seen in the role of the SoxE genes *sox9* and *sox10.* It has become clear that even though *sox9* and *sox10* are expressed throughout NC they play a major role in dividing NC cells into either a ectomesenchymal or non-ectomesenchymal fate respectively (Kelsh et al., 1996) (Akiyama et al., 2002). *colourless* (*cls*) mutants carry lesions in the *sox10* gene and NC cells of the trunk fail to migrate away from the dorsal neural tube, however the ectomesenchymal crest cells of the cranium remain normal. Conversely, the *sox9a* mutant *jellyfish,* presents severe cartilage differentiation defects (Yan et al., 2002).

Further examples of the interplay among NC specifiers is the roles of *sox10*, *foxD3* and *mitfa* in the differentiation of glia and melanophores (Lister et al., 1999). *sox10* is required early in the specification of glia and melanophores and Sox10 directly activates the expression of *mitfa,* which is a transcription factor required for the differentiation of melanophores (Dutton et al., 2001). If a cell is to remain specified along a glial fate, then the expression of *sox10* and *foxD3* is required to be maintained and expression of *mitfa* must be down regulated. Instead, for the specification of melanophores, *foxD3* must be repressed and high levels of *mitfa* are required (Curran et al., 2009) (Curran et al., 2010).

Extrinsic signals also play important roles in the specification of NC cells through receptor-ligand-mediated processes. Interactions with *neuregulins*, *endothelins* and *steel (SCF)* ligands (to name a few) play profound roles in pushing NC cells into specific fates while also acting as migrational cues and cell survival factors (Imokawa et al., 1992, Saldana-Caboverde and Kos, 2010, Lemmon and Schlessinger, 2010). Neuregulins and their binding partners, the Erbb/EGF receptor tyrosine kinases (RTK) class proteins, have previously been shown to participate in glia/Schwann cell migration and differentiation in mammals and zebrafish, while *steel*, also known as *kit ligand*, has been shown to guide melanoblasts and act as a cell survival factor in mouse (Parichy et al., 1999) (Rawls and Johnson, 2000) (Hultman et al., 2007).

As NC cells migrate, they invade areas rich in ECM, a fibrillar meshwork rich in hyaluronan, glycosaminoglycan, collagen, tenascin, laminin and fibronectin. These components help to facilitate the migration of NC cells by offering different surfaces to bind to. NC cells also deposit new components and modify the ECM, as they pass through, for example through metalloproteases (Hall, 1999).

2.7 Derivatives of neural crest

NC cells do not self-differentiate but require a complex set of interactions among their intrinsic factors (i.e. transcription factors) and extrinsic factors, in order to reach a terminal differentiated state. The culmination of intrinsic and extrinsic forces eventually determines the final fates of NC cells as they emerge from the dorsal neural tube to migrate out into the periphery. Over the last 150 years NC cells have been shown to give rise to craniofacial cartilage, smooth muscles, cardiac cells, sensory neurons, enteric neurons, sympathetic/parasympathetic neurons, Schwann cells, and chromatophores, to name the most important NC derivatives (Fig. 2 B). Of particular interest for the scope of this work is the relationship between the differentiation of neuronal, glial and chromatophore cell types which will be described in more detail in the following chapters.

2.8 Haploid is just not enough – at least in mammals

Waardenburg syndrome is associated with mutations in the transcription factors PAX3, SNAIL2, SOX10, MITF or the EDN3 – EDNRB signaling pathway (Pingault et al., 2010). Patients present a variety of symptoms ranging from craniofacial abnormalities, lack of pigment along the facial midline, heterchromia to bilateral isohypochromia and deafness. There are associations with other neural crest congenital defects such as Hirschsprung disease. These traits are inherited in mammals in an autosomal dominant manner and, has been shown to be caused by haploinsufficiency, i. e. one instead of two functional copies cause the mutant phenotype, with the exception of the EDN3 - EDNRB (Edery, 1996). Interestingly, the zebrafish *sox10* mutant *coulorless* and the *mitfa* mutant *nacre* are indistinguishable as heterozygotes compared to wild type siblings and it remains unclear why these processes in mammals are much more dosage sensitive than in fish (Dutton et al., 2001) (Lister et al., 1999).

2.9 Making a melanocyte – specification, differentiation and maturation of specific neural crest cells

All melanocytes of the body, with the exception of the retinal pigment epithelium (RPE), are either derived directly from melanoblasts migrating along the dorsolateral route or arise via a second population of cells capable of detaching from nerves. Irrespective to their particular ontogeny, melanocytes must be initially specified from their precursor cells predominantly through the action of the FoxD3, Sox10, Pax3 and Mitf transcription factors (Sauka-Spengler, 2008). Secondly, these specified cells further require modulation of extracellular signals such as Wnt, Edn, Kitlg, and other still unknown signals. This combination of intrinsic and extrinsic signals culminate in the activation of melanocyte specific genes, encoding *Tyr*, *Dct*, *Tyrp1* and *Pmel*, to only name a few, leading to the final maturation of a melanoblast to a melanized melanocyte (Thomas and Erickson, 2008).

2.10 Melanocyte specification – choosing a path

A traditional view of the melanocytic linage is that specification begins to take place very early, even before migration away of the cells from the dorsal neural tube. In the mouse, cells destined to become melanoblasts are the first to migrate away from the dorsal neural tube and move to migrational staging areas where they stall before proceeding underneath the ectoderm along the dorsolateral route (Weston, 1991). In avian and zebrafish embryos multipotent neural crest cells first migrate along the ventromedial path while crest destined to become melanoblasts migrates later along the dorsolateral path (Erickson et al., 1992, Raible et al., 1992). It is interesting to note that both vertebrates separate the directly forming melanoblasts are distinguished from the rest of the multipotent neural crest cells in a temporal and spatial manner.

Recently, a more complex picture of the neural crest melanocyte lineage has begun to emerge with the identification of neural crest derived melanoblasts migrating along nerves innervating the skin in mouse and chick (Adameyko et al., 2009). These late arriving melanocytes were shown to be derived from precursors, which had migrated along the ventromedial path. Using a Cre/LoxP-based system in the mouse Adameyko et al. were able to reveal that a considerable complement of dermal melanocytes were indeed derived from these nerve associated precursors. Therefore it was proposed that these cells are differentiated from common precursors of Schwann cells and melanocytes associated with the peripheral nerves.

Careful embryology and lineage tracing work carried out in zebrafish more than a decade earlier had already shown that melanoblasts were capable of traveling down the ventromedial path (Raible and Eisen, 1994). Indeed iridoblasts were also shown to follow this route (Kelsh et al., 2009). Much in line with the data from mouse and chick, a report of zebrafish adult melanophores emerging from the tips of nerves at the periphery during stripe formation described a much more developmentally important role of these cells (Budi et al., 2011). Taken together, these "migratory exceptions" initially observed in zebrafish melanophore migration have become more the rule for vertebrate melanocyte origins.

Melanocyte precursors migrate as undifferentiated cells called melanoblasts and only begin to differentiate as they approach their final destination. Mammalian melanoblasts require *Kit ligand* signalling to disperse across epidermal tissues and to colonize hair follicles (Jordan and Jackson, 2000). In humans, melanocytes are also capable of colonizing and remaining in the epidermis itself, where they form extensive dendritic connections to epidermal keratinocytes (Wehrle-Haller, 2003).

2.11 Melanocyte differentiation – the dark side of neural crest

The transcription factor Mitf not only plays a decisive role in the specification of melanocyte precursors but also directly regulates downstream genes involved in melanogenesis. This is carried out in complex coordination together with TfAP2, Sox10, Pax3 and is influenced by extrinsic signals such as Wnt and melanocyte stimulating hormone (MSH) and Mrc1. Through loss of function analysis Mitf has been shown to be necessary (Hodgkinson et al., 1993) (Lister et al., 1999) (Opdecamp et al., 1997) as well as sufficient to specify and differentiate melanocytes by misexpression experiments (Tachibana et al., 1996).

Melanogenesis begins with the expression of *Dopachrome tautomerase* (*Dct*), *Tyrosinase-related protein1* (*Tyrp-1*) and shortly thereafter *Tyrosinase* (*Tyr*); all enzymes directly involved in the conversion of Tyrosine and L-DOPA to melanin. These reactions occur in specialized membrane bound lysosome-related vesicles called melanosomes. As melanosomes mature, melanin is deposited along their internal fibrillar matrix until they become dark and solid vesicles (Thomas and Erickson, 2008). Melanosomes of melanocytes are then transported along cytoskeleton by the molecular motors kinesins, dynein and myosins to the tips of dendritic processes where they are exported to other tissues, for example keratinocytes in amniotes. In fish and amphibians melanosomes are retained within the cell and therefore these pigment cells are specifically called melanophores. Although not exported, melanosomes are dynamically trafficked in the same manner inside the cells in response to intrinsic and extrinsic stimuli (Raposo and Marks, 2002).

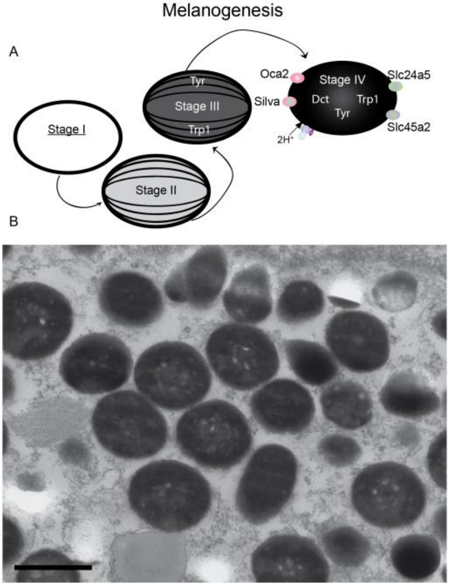

Figure 3: Melanosome maturation is classified into a four stage process leading to dark melanin-filled vesicles. Melanosomes are lysosome-related organelles housing the production of and later acting as the stores of melanin. Stage I melanosomes contain no melanin and can appear as empty vesicles. Vesicles arriving from the trans-Golgi network merge together with stage I melanosomes adding vital components such as fibril forming factors and enzymes such as tyrosinase and TYRP1. The internal environment of melanosomes is specific to the requirements of melanin producing enzymes. Melanin is initially synthesized along internal fibrils and the melanosomes are continually filled. Homeostasis of these conditions is achieved through a wide variety of solute carriers such as Slc45a2 and Slc24a5 along with other membrane bound components such as v-ATPase proton pumps (**A**). Mature melanosomes are about ~500nM in diameter, become dense with melanin and take on a sausage shaped form (**B**). Scale bar is 750nM

2.12 Pigmenting a human and pigmenting a fish – more than shades of grey

Although slight differences do exist among vertebrate melanin producing cells, there are deep similarities which make this system both powerful and fascinating to study. An example of this is the occurrence of albinism across vertebrate species. Oculocutaneous albinism (OCA) describes a group of rare human congenital diseases which can specifically be characterized by poor vision and a variable hypopigmentation phenotype. Reduction of pigmentation can occur in the eyes, skin and hair. In humans OCAI is the most common form of albinism and is caused by mutations in *TYROSINASE* (Spritz et al., 1988). Mutations in the same gene are the underlying cause of the *sandy* zebrafish mutant with a visually defective and hypopigmented phenotype (Page-McCaw et al., 2004).

Human skin color variation is another example of the similarities between zebrafish and human pigment biology and their ability to model each other. The zebrafish mutant *golden* was shown to carry mutations in the solute carrier *slc24a5* (Lamason et al., 2005). The same study also showed that missense mutations in the human *SLC24A5* gene were partly responsible for skin coluor variation between

Europeans and Africans. Nevertheless, despite the knowledge of more than 100 different genes associated with coat and skin color there still remains much to be resolved in order to fully understand the striking color variation seen across the vertebrates.

Results and discussion 3

Publication 1:

Dooley CM, Mongera A, Walderich B, Nüsslein-Volhard C. (2013). **On the embryonic origin of adult melanophores: the role of ErbB and Kit signalling in establishing melanophore stem cells in zebrafish.** *Development* 140, 1003-1013

3.1 On the embryonic origin of adult melanophores

The onset of this chapter begins with a simple question, *where do adult melanophores in zebrafish arise from?* With increasing body size, a zebrafish larvae progress through juvenile stages and then to adulthood; during this transition, there is an explosion in the number of chromatophores, creating the typical stripped pattern of the zebrafish. A vast collection of knowledge had laid out the ontological origins of all pigment cells of the body at the ridges of the neural tube, the birthplace of the neural crest, but the specific ontology between the birth and the final differentiation of melanophores and mammalian melanocytes remained largely unclear. It was observed that newly arising melanophores were derived *de novo* from unpigmented precursors (Parichy and Turner, 2003) but their actual source remained to be defined.

A two-pronged approach was undertaken, with the first to trace neural crest cells from their birthplace to their final differentiated state. Secondly, mutants lacking adult melanophore were analyzed to try to understand the role their responsible genes play in normal melanophore development.

3.1.1 Melanoblasts migrate along motor neurons

Streams of organized NC cells migrating along specific routes have been described in all investigated vertebrates. While the rostral-caudal position of these streams relative to the somite does vary between species, the migratory route of medially migrating neural crest cells overlaps with extending motor axons (Le Douarin, 1986a) (Raible et al., 1992) (Rickmann et al., 1985) (Krull, 2010) (Bonanomi and Pfaff, 2010). Organized streams of medially migrating neural crest cells labeled with GFP under the control of the *mitfA* promoter *Tg(mitfa:gfp)*, assume a distinct metamerized pattern by 16 hpf (Fig. 4, A-C). Time-lapse imaging of double transgenic *Tg(mitfa:gfp;nbt:DsRed)* fish allows for the simultaneous observation of both neural crest cells and developing motor axons (DsRed driven by the *b-tubulin* promoter which is specific for neurons) (Fig. 4, D-J). Neural crest cells initially migrate ventrally along the neural tube arriving at the positions of the motor neuron cells bodies (Fig. 4, D-E). Motor axons extend from the ventral base of the neural tube initially in a ventral direction and eventually extend out to the periphery. Following the axonal extension, *mitfa:gfp* positive NC cells of the medial path move along the motor axon in a ventral direction (Fig. 4, B-D). The first *mitfa:gfp* positive cells to migrate along the motor axons quickly reach the ventral trunk and disassociate from the motor axon (Dooley et al., 2013 Supplemental Fig. 1). Subsequently *mitfa:gfp* positive cells begin their differentiation into mature melanophores as they complete their ventral migration along the motor axon (Fig. 4, H-J). A small subset of *mitfa:gfp* positive cells, often a single cell in each segment, migrates only a short distance along the motor axon and then becomes stationary at the future site of the forming DRG (Fig. 4, D,G). These cells become quiescent, do not differentiate into melanophores, and often lose their GFP label.

Although the spatial-temporal association of migrating neural crest cells and the motor axons has been long noted (Le Douarin, 1986a) (Le Douarin, 1986b), these observations show a much more intimate association between the two cell types. Medial neural crest cells only commence their migration once the motor axon has begun to extend ventrally. Neural crest cells then specifically migrate along the motor axon and only disassociate once they reach the tip of the axon. Furthermore, the identification of a specific *mitfa:gfp* positive cell that migrates to the position of the future DRG is highly interesting in the context of its future developmental fate and will be further described in this work.

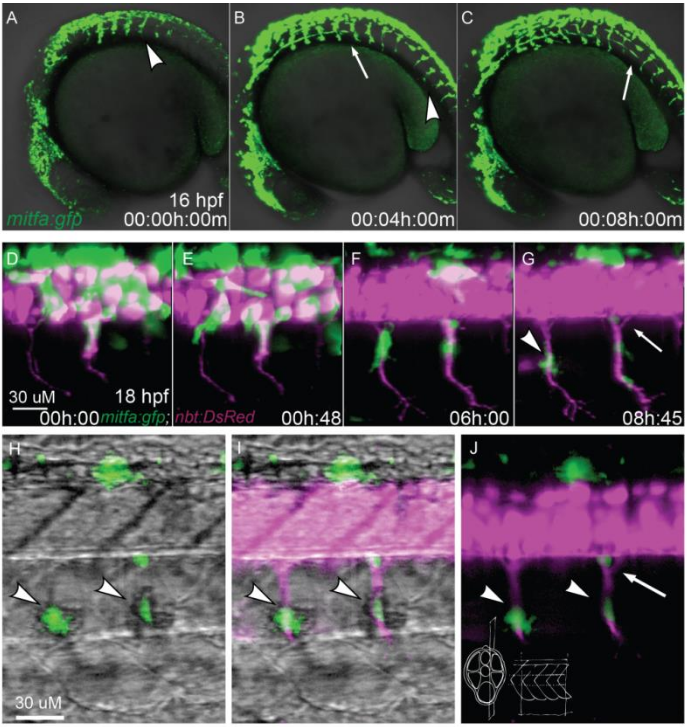

Figure 4: Ventromedial neural crest cells migrate along primary motor axons. Neural crest derived cells labeled with the *mitfa:gfp* transgene at the anterior most region of the trunk begin their medial migration at about 14 hpf. Organized streams of cells can be readily identified by 16 hpf (arrowhead, **A**). These streams initialize in an anterior to posterior fashion along the trunk over the next 12-14 hours of development (**A-C**). Migrating glia of the lateral line can also be seen as it moves anteriorly to posteriorly (arrow, **B-C**). Following ventromedial migration, neural crest cells specified for the dorsolateral pathway begin their migration (**C**). Lateral trunk view with optical sectioning to the level of the extending primary motor axons, labeled here with the *nbt:DsRed* transgene (**D-J**). *mitfa:gfp* positive cells can be identified as they migrate along primary motor axons. Some cells complete the ventral migration and move away from the tips of the motor axons. Other cells move to the future locations of the forming dorsal root ganglia (arrow, **G**). Melanophores of the ventral larval stripe begin to melanize as they complete their migration along the motor axon. The initial

melanin can be seen as part of the *mitfa:gfp* positive cells (arrowheads, **H**) and they are localized to the position of the motor axon (arrowheads, **J**). Cells located at the position of the forming dorsal root ganglia remain stationary (arrow, **J**) as the *mitfa:gfp* labeling begins to fade. A schematic depicting the level of the optical sectioning as well as the lateral view of the trunk (**J,** lower left). Adapted from Dooley et al. 2013

3.1.2 ErbB receptors are required for neural crest migration along the ventral medial pathway

ErbB receptors involved in the ventral medial migration of NC cells have been described using mutant *erbb3b*^{st48} in the *Tg(-4.9sox10:gfp)* background to facilitate the visualization of migrating neural crest cells (Honjo et al., 2008). Honjo et al. describe the neural crest cells failure to stop at specific points along their ventromedial path. They observed cells beginning a ventral migration but then changing directions. They interpreted this as the NC cells overshooting these points in their migration followed by the cells wandering off.

Closer inspection of *Tg(-4.9sox10:gfp;nbt:DsRed)* fish treated with the EGF inhibitor PD 168393 revealed motor axons already completely devoid of neural crest cells at 24 hpf (Dooley et al. 2013, Fig. 6 A-B). Time-lapse imaging of *Tg(-4.9sox10:gfp;nbt:DsRed)* further revealed that *sox10:gfp* positive cells are capable of moving to the motor axon cell bodies at the ventral neural tube but never initiate migration along the axon (Fig. 5 A-H). An example of normal migration in *Tg(-4.9sox10:gfp;nbt:DsRed)* is given in Dooley et al. 2013,. Supplemental Fig. 1.

Small molecule inhibition of EGF receptors functions indiscriminately on all ErbB receptors. Therefore, to uncover the role of specific ErbB receptors a genetic approach was taken. For this purpose *erbb2*^{t20604} embryos were time-lapse imaged in *Tg(mitfa:gfp;nbt:DsRed)* embryos. Just as with EGF inhibition, neural crest cells fail to migrate along motor axons (Fig. 5 I-N; Dooley et al. 2013 Supplemental movie Fig. 4).

Tg(mitfa:gfp;nbt:DsRed) embryos were also injected with *erbb3b* morpholino previously shown to phenocopy *erbb3b*$^{-/-}$ mutants (Budi et al., 2008). Although weaker than EGF receptor inhibition and *erbb2* knockouts, *erbb3b* morphants lack NC cells along the medial path (Dooley et al. 2013 Table 1, Fig. 6 C-E).

These observations are in contrast to the work published by Honjo et al. as the interpretation of my data implies a complete failure to migrate along motor axons while Honjo et al. propose a failure of cells to pause. Key to these differences is the ability to optically section live images from a lateral view and also the use of the *nbt:DsRed* transgene to visualize the motor axon. Defects in ErbB signaling does not affect neural crest migration along the dorsolateral path. A maximum image intensity projection of a cell moving along the dorsolateral path could easily be misinterpreted for a cell in the ventromedial path.

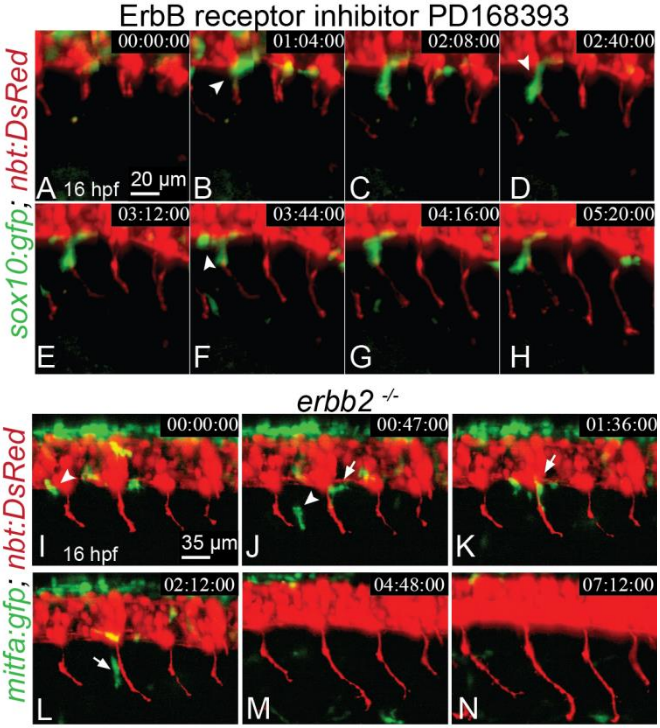
ErbB receptor inhibitor PD168393
sox10:gfp; nbt:DsRed
00:00:00
01:04:00
02:08:00
02:40:00
A 16 hpf
20 µm
B
C
D
03:12:00
03:44:00
04:16:00
05:20:00
E
F
G
H
erbb2 -/-
mitfa:gfp; nbt:DsRed
00:00:00
00:47:00
01:36:00
I 16 hpf
35 µm
J
K
02:12:00
04:48:00
07:12:00
L
M
N

Figure 5: Neural crest cells fail to migrate ventrally in lack of properly functioning ErbB receptors. Time-lapse imaging of *Tg(-4.9sox10:gfp;nbt:DsRed)* fish. Neural crest cells are capable of moving to the bodies of motor axon cells (arrowheads) but fail to migrate along extending motor axons when the EGF receptor inhibitor PD168393 is applied (**A-H**). In homozygous *erbb2*^{t20604} fish NC cells also fail to migrate properly along motor axons (**I-N**). In lack of a proper route a few neural crest cells move away from the motor neuron cell bodies in random directions (arrowhead, arrow).

3.1.3 Dorsal root ganglia are required for adult pigmentation

A defect in EGF receptor signaling also leads to the absence of DRGs in all of the above-mentioned cases. *erbb2*$^{-/-}$ fish are not viable, while knockouts in *erbb3b*$^{-/-}$ are (this work & (Budi et al., 2008)). Adult *erbb3b*^{t21441} fish display abnormal gaps in their adult pigment pattern (Dooley et al. 2013 Fig. 5 A). As these fish have a strongly reduced number of DRGs, there appeared to be a correlation between the presence absence of DRGs and adult pigmentation.

To test the potential association both a chemical and a physical ablation of the DRGs was carried out. Treatment of embryos for short pulses at different developmental stages with the EGF inhibitor causes a selective spatial-inhibition of neural crest migration along the anteroposterior axis. When neural crest cells fail to migrate, DRGs also fail to form. Embryos treated with the EGF inhibitor at earlier time points (12-16 hpf) displayed defects in the more anterior adult pigment patterns while embryos treated at later developmental stages (18-24 hpf) presented a more posterior phenotype (Dooley et al. 2013 Fig 5 B-E). Using a laser ablation system, 8 consecutive DRGs of 3 dpf larvae were ablated on the left side. Fish raised to adulthood showed a clear reduction of adult melanophores on the ablated left side (Dooley et al. 2013 Fig 5).

Failure to form dorsal root ganglia, as shown in the EGF inhibition experiments or ablation of the DRGs at 3 dpf, results in localized reduction of adult melanophores and gaps in the adult pigment pattern. Taken together, these experiments show that the dorsal root ganglia along with their associated cells are required for juvenile and adult melanophores.

3.1.4 Ablation of embryonic melanophores activates melanophore precursors at the site of the dorsal root ganglia

mitfa is required for the differentiation of melanophores from the neural crest lineage and mutations in this gene lead to embryonic and adult fish lacking all melanophores of the body (Lister et al., 1999). When *mitfa* morpholino is injected into zygotes it phenocopies *mitfa*$^{-/-}$ fish until about 3 dpf. After this time point, new melanophores begin to appear and eventually the melanophores are restored by about 5-7 dpf (Dooley et al 2013 Fig. 3 A-C). This indicates that melanophores are regenerated after *mitfa* knockdown.

In order to investigate where these regenerating melanoblasts arise from, *mitfa* morpholino was injected into *Tg(mitfa:gfp;nbt:DsRed)* zygotes followed by time-lapse imaging focusing on the DRGs. *mitfa:gfp* positive cells were identified as they emerged from DRGs of injected embryos at 60 hpf, they migrated in tight association along the spinal nerves (Fig.6 A-E).

To confirm that these newly appearing migrating cells had in fact emerged from the DRGs and were destined to take on a melanophore fate a more robust set of experiments was carried out to follow the linage from initiation to differentiation.

To knockdown *mitfa* expression, now, *albino* (*slc45a2*^{b4}) embryos producing unpigmented melanophores were injected at the one cell stage with the *mitfa* morpholino. These morphants were then used as hosts for blastula transplantation experiments. *Tg(mitfa:gfp)* embryos, injected with a rhodamine dextran at the one cell stage were subsequently used as donors. The logic behind this experiment was that all transplanted cells would be visible via the rhodamine dextran allowing for the identification of clones at appropriate locations. Labeled donor cells associated to the area of the DRGs could then be identified by the GFP label, and, in adults, by their dark pigmentation. With this approach it was possible to image previously quiescent melanophore progenitors becoming *mitfa:gfp* positive at the position of the DRGs. Newly active GFP positive cells began to migrate and to undergo a few cell divisions. Their daughter cells continued to migrate out to the periphery and began the process of melanization, thereby confirming their melanophore fate specification (Dooley et al. 2013 Fig. 4 A-H). Furthermore, when chimeric fish were grown to adulthood they displayed dark melanophore patches in the *albino* background the area of the larval DRG clones in their flanks (Dooley et al. 2013 Fig. 4 I-J).

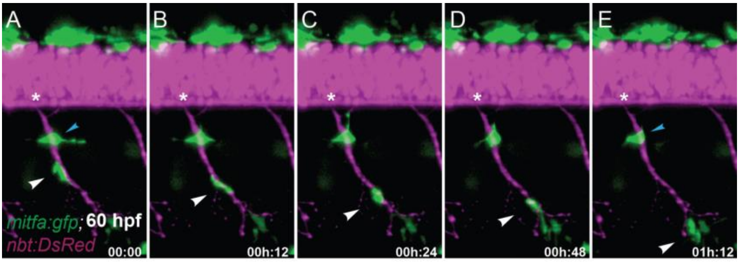

Figure 6: Recovering melanophores following *mitfa* morpholino knockdown emerge at the site of the dorsal root ganglia and migrate along spinal nerves. Lateral view with optical sectioning of *Tg(mitfa:gfp;nbt:DsRed)* embryos, which were injected with *mitfa* morpholino at the one cell stage. The position of the DRG is indicated by an *asterisk* in each frame. Following injections, embryos were imaged for several hours starting at 60 hpf. Cells carrying the *mitfa:gfp* label emerge from the DRG and migrate along spinal nerves (white arrowhead, **A-E**). Other *mitfa:gfp* positive cells extend filopodia but remain stationary over the course of time (blue arrowhead, **A-E**). Adapted from Dooley et al. 2013

3.1.5 Dorsal root ganglia are an early established niche for adult melanophore progenitors

Failure in the formation of the dorsal root ganglia or their ablation leads to a reduction of adult melanophores. When melanophore progenitors are prematurely activated after removal of embryonic melanophores, cells within the DRGs become active, and their progeny migrate along spinal nerves and begin to regenerate the larval melanophore population. These multiple lines of evidence make a compelling case for the DRG as a cellular niche containing undifferentiated melanophore progenitors. When activated, these cells have the potential to produce cells differentiating into melanophores. Another important aspect is that these cells are specified and set aside at an early developmental time point, most likely within the first 24 hpf.

3.1.6 *sparse like* encodes Kit ligand a and is expressed in migrating neural crest cells

Fish mutant for *sparse like* are adult viable but present a reduction in early embryonic melanophores as well as a dramatic reduction in adult melanophores (Dooley et al. 2013

Fig. 7 and Fig. 8 A). Positional cloning of the *sparse like* mutant revealed a premature stop in the *kit ligand a* gene. *kitlga's* receptor *kita* is a receptor tyrosine kinase also known as *c-Kit* in mammals and is required for melanophore/melanocyte development in amniotes. It shares the phenotype with *sparse like*. *kitlga* is expressed by neural crest cells as they migrate along the ventromedial path (Dooley et al. 2013 Fig. 8 B-D). This is a curious observation because the receptor for *kit ligand a*, *kita*, has been shown to be expressed in neural crest derived melanoblasts (Parichy et al., 1999, Hultman et al., 2007). Based on this evidence, neural crest cells themselves are providing *kitlga* along the ventromedial path and in doing so could be playing a role in the establishment of melanophore stem cells at the site of the future dorsal root ganglia.

3.1.7 Early Kit ligand a signaling is required for specific melanophore precursors and for the maintenance of embryonic melanophores

kitlga$^{-/-}$ fish develop a normal appearing peripheral nervous system and normal DRG. Melanophores specified for the dorsolateral pathway of the trunk initially differentiate into normal numbers but then immediately start to die and are all but absent by 5 dpf. Melanophores derived from ventromedial migrating neural crest cells belonging to the ventral larval stripe, medial larval stripe and yolk sac stripe fail to appear (Dooley et al. 2013 Fig. 7). As this phenotype is present in both *kita*$^{-/-}$ (*sparse*) and *kitlga* $^{-/-}$ (*sparse like*) loss of function alleles, this highlights firstly the specific interaction of Kita and its ligand Kitlga in the context of melanophores and secondly the different modes of action of Kita signaling. Melanophores have been classified into *kita*-dependent and *kita*-independent populations (Parichy et al., 1999). Melanophores of the dorsal larval stripe are *kita* independent in terms of their specification from the neural crest but are *kita*-dependent for their maintenance and survival. Melanophores of the ventromedial path are *kita* dependent for their specification from the neural crest lineage and in lack of this signaling fail to differentiate (Dooley et al. Fig. 7).

In adults, this picture becomes more complex. Adult *kita*$^{-/-}$ and *kitlga*$^{-/-}$ present a 90% reduction in melanophores of the flanks (Dooley et al. 2013 Fig. 7). Two likely situations could be occurring: the adult melanophores require *kita* signaling for their differentiation from melanophore progenitors to mature melanophores, or *kita* signaling is directly required for the establishment of adult melanophore progenitor cells. It is also possible that both situations are indeed the case simultaneously.

To add some insight to these possibilities, the following experiments were carried out. A morpholino specific for *kitlga* was injected into embryos at the single cell stage. Morpholinos have a limited time of action until it is eventually diluted out over the course of development; much like the injection of *mitfa* morpholino, which begins to lose its effect at about the third day of development (see above). Morphant *kitlga* fish phenocopy *kitlga*$^{-/-}$ fish all through embryonic development. Indeed, even at 20 dpf, *kitlga* morphant fish still fail to rescue their ventral, belly, lateral and yolk sac stripes, long after the effects of the morpholino have worn off. It is only at mid metamorphosis that melanophores begin to appear in the flanks possibly from a separate undefined source.

A possible explanation would be that early *kita* signaling is required for the establishment of larval and juvenile melanophore progenitors. Early perturbation of *kita* signaling leads to the failure in the establishment of melanophore progenitor cells. It is then only at the onset of metamorphosis that new melanophore progenitor cells can be produced by stem cells independently from early *kita* signaling.

3.1.8 Distinct populations of melanophore progenitors and their specific migratory routes

In summary of these new observations, an emerging picture of multiple melanophore classes begins to take form. Early melanophores of the dorsal larval stripe are both ErbB and Kita receptor signaling independent for their specification and differentiation but require Kita signaling for their maintenance once mature. Ventromedially migrating neural crest cells require ErbB signaling to properly follow along the extending motor axons. Defects in ErbB signaling result in the failure of medial NC crest migration, absence of dorsal root ganglia and overall defects in the peripheral nervous system. Melanophore progenitors derived from neural crest cells migrating along the ventromedial path require early embryonic Kita signaling for their establishment. The DRG act as niche for melanophore progenitor cells. Dorsal root ganglia and peripheral nervous system-associated melanophore progenitors persist and contribute to the majority of adult derived melanophores.

Development 140, 1003-1013 (2013) doi:10.1242/dev.087007
© 2013. Published by The Company of Biologists Ltd

On the embryonic origin of adult melanophores: the role of ErbB and Kit signalling in establishing melanophore stem cells in zebrafish

Christopher M. Dooley[1,2], Alessandro Mongera[1], Brigitte Walderich[1] and Christiane Nüsslein-Volhard[1,*]

SUMMARY

Pigment cells in vertebrates are derived from the neural crest (NC), a pluripotent and migratory embryonic cell population. In fishes, larval melanophores develop during embryogenesis directly from NC cells migrating along dorsolateral and ventromedial paths. The embryonic origin of the melanophores that emerge during juvenile development in the skin to contribute to the striking colour patterns of adult fishes remains elusive. We have identified a small set of melanophore progenitor cells (MPs) in the zebrafish (*Danio rerio*, Cyprinidae) that is established within the first 2 days of embryonic development in close association with the segmentally reiterated dorsal root ganglia (DRGs). Lineage analysis and 4D *in vivo* imaging indicate that progeny of these embryonic MPs spread segmentally, giving rise to the melanophores that create the adult melanophore stripes. Upon depletion of larval melanophores by morpholino knockdown of Mitfa, the embryonic MPs are prematurely activated; their progeny migrate along the spinal nerves restoring the larval pattern and giving rise to postembryonic MPs associated with the spinal nerves. Mutational or chemical inhibition of ErbB receptors blocks all early NC migration along the ventromedial path, causing a loss of DRGs and embryonic MPs. We show that the *sparse like* (*slk*) mutant lacks larval and metamorphic melanophores and identify *kit ligand a* (*kitlga*) as the underlying gene. Our data suggest that *kitlga* is required for the establishment or survival of embryonic MPs. We propose a model in which DRGs provide a niche for the stem cells of adult melanophores.

KEY WORDS: Kit ligand a, ErbB, Dorsal root ganglia, Melanophore stem cells

INTRODUCTION

Colour patterns are prominent features of many animals; they evolve rapidly and vary between closely related species, providing an important target for both natural and sexual selection (Darwin, 1871; Roulin, 2004; Hoekstra et al., 2006; Protas and Patel, 2008).

In vertebrates, all pigment cells of the body are derived from the neural crest (NC) except the pigmented retinal epithelium. The NC is an embryonic population of pluripotent migratory cells that contribute to a variety of organs and tissues. The NC is largely responsible for the emergence of many of the vertebrate-specific characteristics involved in head and body shape, protection and pattern diversity that evolved in this phylum over 550 million years (Gans and Northcutt, 1983).

The pigment patterns observed in birds and mammals are due to variations in melanin synthesis within a single type of chromatophore, the melanocyte. However, anamniotes and reptiles display several chromatophore types. In zebrafish, black melanophores, yellow xanthophores and silvery iridophores are arranged in distinct patterns in the hypodermis during larval and adult stages.

Although the early melanophores contributing to the larval pattern can be traced back directly to the migrating NC, the ontogeny of the melanophores that compose the continuously growing and expanding adult pattern during metamorphosis weeks later remains unclear. As the NC is no longer present, these cells must arise from hypothetical NC-derived stem cells that are set aside in the embryo (Rawls et al., 2001; Parichy et al., 2003; Yang and Johnson, 2006; Budi et al., 2011). These cells are quiescent during embryonic development but start to proliferate during juvenile development (Quigley et al., 2004; Mellgren and Johnson, 2004; Hultman et al., 2009).

Several zebrafish mutants in which melanophores are reduced or completely absent have been collected (Streisinger et al., 1986; Haffter et al., 1996; Kelsh et al., 1996; Lister et al., 1999). Mutations in the *colourless* (*cls*) gene, which encodes the HMG-box transcription factor Sox10, eliminate all three types of chromatophores as well as glia and the peripheral nervous system (Kelsh et al., 1996; Dutton et al., 2001). Mutations in genes such as *nacre* (*nac*; *mitfa* – Zebrafish Information Network), *sparse* (*spa*; *kita* – Zebrafish Information Network) and *sparse-like* (*slk*) specifically affect melanophores of the body whereas the other chromatophore types are present (Kelsh et al., 1996; Haffter et al., 1996; Lister et al., 1999). *mitfa* mutant fish lack all body melanophores throughout their lives. *mitfa* encodes a helix-loop-helix transcription factor (Elworthy et al., 2003). *mitfa* is expressed in melanoblasts at all stages of migration and differentiation (Lister et al., 1999). Interestingly, *mitfa* morphants, although completely deficient in early larval stripe formation, do recover and adopt normal larval and adult pigmentation (Mellgren and Johnson, 2004). This finding and evidence from temperature-sensitive *mitfa* alleles indicate that *mitfa* is not required for establishing or maintaining melanophore stem cells (Johnson et al., 2011). In juvenile fish, a population of postembryonic MPs expressing *mitfa* was described in the myotomes and associated with the Schwann cells of the spinal nerves and the DRGs (Budi et al., 2011). Although the proliferation and migration of these MPs ultimately gives rise to pigmented melanophores in the skin, the embryonic origin of postembryonic MPs remains unknown.

---

[1]Max-Planck-Institut für Entwicklungsbiologie, Spemannstr 35, 72076 Tübingen, Germany. [2]Wellcome Trust Sanger Institute, Wellcome Trust Genome Campus, Hinxton, Cambridge, CB10 1HH, UK.

*Author for correspondence (christiane.nuesslein-volhard@tuebingen.mpg.de)

Accepted 19 December 2012

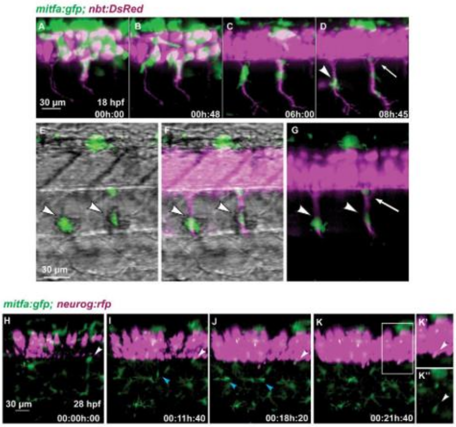

Fig. 1. Melanoblasts migrate along the motor neurons. (**A-G**) Time-lapse confocal imaging of a *Tg(mitfa:gfp;nbt:DsRed)* zebrafish embryo. Medially migrating GFP-positive cells (arrowhead in D) migrate along ventrally extending primary motor axons (DsRed) starting at 18 hpf. A portion of the area in D is shown in G, and in E,F with brightfield illumination. Arrowheads in E-G indicate melanoblasts melanising *in situ*. A GFP-positive cell remains at a ventral position of the neural tube (arrow in D,G). (**H-K″**) *Tg(mitfa:gfp;-8.4neurog1:nrfp)* embryo imaged starting at 28 hpf over a period of 22 hours. A GFP-positive cell (white arrowheads) located close to the ventral base of the neural tube remains at this position over the next 21 hours when the expression of nRFP marks the appearance of the DRG in the same region. A medially positioned cell (blue arrowhead in I) migrates out to the horizontal myoseptum and divides to form melanophores of the lateral stripe (blue arrowheads in J). (K′) Enlargement of the boxed region in K. (K″) Green channel only.

In adult *erbb3b* (also known as *hypersensitive*, *hps* and *picasso*) mutants, melanophores are drastically reduced but the larval melanophore pattern appears normal (Whitfield et al., 1996; Budi et al., 2008; Hultman et al., 2009; Hultman and Johnson, 2010). Mutations in *erbb3b* as well as in *erbb2* (*kitzelig*, *kiz*) not only cause defects in pigmentation, but also in the peripheral nervous system and lateral line glia (Lyons et al., 2005; Rojas-Muñoz et al., 2009). Morpholino and small molecule inhibitor studies show that both regenerating and adult melanophores require ErbB3b signalling during the first day of embryogenesis when NC cells delaminate and migrate (Budi et al., 2008; Hultman et al., 2009; Johnson et al., 2011; Budi et al., 2011). These findings support a model in which ErbB signalling is required in the early embryo to establish both the peripheral nervous system and the melanophore stem cells that later generate the adult melanophore pattern (Hultman et al., 2009; Hultman and Johnson, 2010).

kita mutant fish display a severe melanophore reduction. In larvae and juveniles, melanophores are almost completely absent. The adult fish display median longitudinal stripes that contain only ~15% of the normal number of melanophores (Johnson et al., 1995; Parichy et al., 1999; Hultman et al., 2007). In mice, mutations in *Kit* (also known as dominant-white spotting), in addition to a pigment phenotype, lead to an early failure in haematopoiesis, and homozygotes are embryonic lethal (Geissler et al., 1988). Similar phenotypes are observed in *Steel* (*Kitl*) mutant mice, which carry lesions at the *Kitlg* locus encoding the ligand of Kit. In mice, zebrafish and humans, *Kitlg* expression is required both for the migration and the survival of melanocyte precursors as well as later in the epidermis, where melanocyte precursors disperse throughout the entire embryo (Huang et al., 1992; Wehrle-Haller et al., 2001; Rawls and Johnson, 2003; Gu et al., 2009; Gu et al., 2011).

The *sparse like* (*slk*) mutant (Kelsh et al., 1996) displays a phenotype similar to that of *kita* mutants. We have positionally cloned *slk* and show that it encodes the zebrafish Kit ligand a. Both *kita* and *slk* (*kitlga*) mutants are viable and fertile; they display no defects in haematopoiesis, germ cell development or osteoclast development. The mutant phenotype of both genes suggests that larval and the majority of adult melanophores are Kitlga signalling dependent.

We present evidence for a distinct population of MPs associated with the DRGs. They require *slk* (*kitlga*) to function as stem cells. These melanophore stem cells are quiescent during larval life and activated in juveniles to give rise to the postembryonic MPs that distribute in a segmental fashion along the spinal nerves. Precocious activation is observed in embryos depleted of melanophores by *mitfa*-morpholino (MO) knockdown. Furthermore, their establishment, although not requiring Mitfa, depends on ErbB signalling in early embryonic development, which is required for migration of all NC cells including the MPs and DRG precursors along the ventromedial path. Our data suggest that DRGs serve as a niche for stem cells that generate melanophores contributing to the pigment pattern of adult fishes.

MATERIALS AND METHODS

Zebrafish husbandry and stocks

Zebrafish were maintained as described (Brand et al., 2002). Transgenic lines were provided by the following people: *Tg(mitfa:gfp)*^{w47} by James Lister, VCU Medical Center, Richmond, Virginia, USA; *Tg(−8.4neurog1:nRFP)*^{sh3}, *Tg(−4.9sox10:gfp)* by Robert Kelsh, University of Bath, Bath, UK; *Tg(nbt:DsRed)* by Madeleine van Drenth from the Max-Planck Institute for Developmental Biology, Tübingen, Germany. The following mutant alleles were used in this study: *alb*^{b4} (Streisinger et al., 1986), *erbb2*^{t20604} (*kiz*), *erbb3b*^{t21411} (*hps*) (Rojas-Muñoz et al., 2009), *mitfa*^{w2} (*nac*) (Lister et al., 1999), *kitlga*^{tc244b} (*slk*), *sox10*^{t3} (*cls*).

Mapping and cloning of *sparse like*

slk was mapped following Geisler et al. (Geisler et al., 2007) between markers z21055 (2.0 cM; LOD 63.1) and z3490 (2.3 cM; LOD 21.1) on chromosome 25. *kitlga* maps within the same interval. RNA was isolated from 48 hours post fertilisation (hpf) *slk* embryos using TRIzol (Life Technologies, Frankfurt, Germany) and processed into cDNA with Transcriptor High Fidelity cDNA Synthesis Kit (Roche Diagnostics Deutschland, Mannheim, Germany). The *kitlga* transcript was amplified, subcloned into pGEM-T (Promega, Mannheim, Germany) and sequenced.

RNA *in situ* hybridisation

A RT-PCR-based approach was used to generate probes for RNA *in situ* hybridisation. The PCR was performed using an antisense primer containing a T7-promoter sequence on its 5′-end. The DNA oligonucleotides used were: *kitlga*, 5′-TCTCGTTCCATATGAAGAAGTCAA-3′ and 5′-TAATACGACTCACTATAGGTCAGATATCCCCACATCTAATGG-3′ (Hultman et al., 2007). The PCR product included the target sequence flanked by the T7-promoter sequence, enabling us to synthesise an RNA riboprobe by *in vitro* transcription of the PCR product using T7-RNA polymerase (Fermentas, St Leon-Rot, Germany). Whole-mount *in situ* hybridisation (Thisse and Thisse, 2008) and antibody staining (Schulte-Merker, 2002) were performed as described. Anti-HuC/HuD (Honjo et al., 2008) was obtained from Life Technologies.

Generation of chimeric fish

Rhodamine dextran (Life Technologies) was injected into *Tg(mitfa:gfp)* donor eggs at the one-cell stage and about ten cells were transplanted at the blastula stage into *alb* recipients of the same age. The *alb* recipients had been injected at the one-cell stage with *mitfa* MO. Chimeric embryos were scored at 3 days post-fertilisation (dpf) and imaged using the LSM5 Live, Carl Zeiss Microimaging, Jena, Germany. Chimeras displaying donor-derived melanophores at the horizontal myoseptum were individually raised to adulthood and scored for darkly pigmented melanophores in the pale *alb* background.

Morpholino injection

MO injections were carried out as described (Nasevicius and Ekker, 2000) with the following amounts: *mitfa* 5.0 ng (*mitfa*-MO, 5′-CATGTTCAACTATGTGTTAGCTTC-3′), *kitlga* 5.0 ng (*kitlga*-MO, 5′-CTGGATAACAACACTCACCACTTCT-3′) (Hultman et al., 2007) and *erbb3b* 2.0 ng (erbb3b, 5′-TGGGCTCGAACTGGGTGGAAACAA-3′) (Budi et al., 2008). All MOs were obtained from Gene Tools LLC, Philomath, USA.

Inhibitor treatment

Embryos at somitic stages were dechorionated and placed in 10 µM of ErbB inhibitor (PD168393, Calbiochem, Merck KGaA, Darmstadt, Germany) at 28°C for 4 hours. Embryos were mounted in agarose (also containing 10 µM PD168393) and imaged for 24 hours.

DRG ablation

Tg(−8.4neurog1:nrfp)^{sb3} embryos at 3 dpf were anaesthetised and mounted in 0.6% low temperature melting agarose on glass-bottom dishes. Embryos were mounted laterally and four to eight DRGs of consecutive metamers were ablated using a 351-nm 100-Hz pulsed laser line on a FV1000 Olympus confocal microscope (Olympus Europa Holding, Hamburg, Germany).

TUNEL assay

Embryos were dechorionated and then fixed in 4% paraformaldehyde overnight at 4°C. Apoptosis staining was performed using the *In Situ* Cell Death Detection Kit (Roche Diagnostics Deutschland) according to the manufacturer's protocol.

Imaging

Embryos were dechorionated, anaesthetised in 0.004% tricaine and mounted in 0.6% low temperature melting agarose on glass-bottom dishes at 28°C. Live imaging was performed using a LSM5 Live confocal microscope (Carl Zeiss Microimaging). The data were analysed using IMARIS 6.1 software (Bitplane A6, Zurich, Switzerland). In some imaging experiments, the medial crest population was identified after removing the superficial optical sections with the function 'Crop 3D'. Adult fish were imaged using a Canon EOS 5d mark II (Canon Deutschland, Krefeld, Germany).

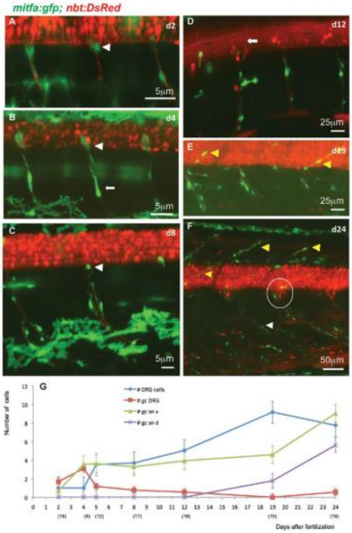

Fig. 2. Stationary MPs located at the DRGs give rise to MPs located along the spinal nerves. (**A-F**) Time-lapse confocal imaging of *Tg(mitfa:gfp;nbt:DsRed)* zebrafish individuals during larval development of consecutive ages. GFP-positive cells at the exit point of the spinal nerves (white arrowheads in A-C) appear to be stationary. Other GFP-positive cells of more elongated shapes are observed along the spinal nerves (e.g. arrow in B). Until 12 dpf (D), no GFP-positive cells can be seen along the dorsally extending spinal nerves (arrow in D), whereas at metamorphic stages (E,F) both the dorsally extending (yellow arrowheads) and the ventrally extending (white arrowhead) spinal nerves show an increased number of associated GFP-positive cells. The number of cells in each DRG (circled in F) has increased to about eight. (**G**) Average numbers of GFP-positive cells per hemisegment located at the DRGs, the ventral and dorsal spinal nerves as well as DRGs at increasing larval age (dpf). The numbers of hemisegments counted is indicated below the respective time points. gc DRG, green cells at DRG; gc sn v, green cells at spinal nerves ventral; gc sn d, green cells at spinal nerves dorsal.

RESULTS

Stationary MPs are associated with DRGs

A transgenic line expressing GFP under the control of the *mitfa* promoter (Lister, 2002) allows the 4D imaging and tracing of melanoblasts in early development. *mitfa:gfp* is initially broadly expressed among NC cells. Subsequently, its expression becomes more and more restricted to melanoblasts although it is also observed in other chromatophore types and glia (Curran et al., 2009). In the trunk, NC cells migrate along the ventromedial path

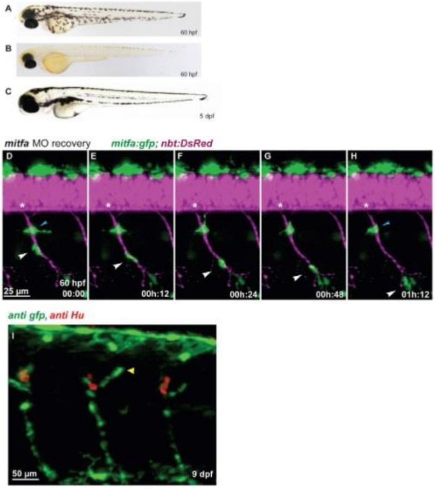

Fig. 3. Regenerating MPs emerge at the site of the DRGs and travel along the spinal nerves. (**A-C**) In contrast to wild type (A), *mitfa*-MO-treated zebrafish embryos (B) lack larval melanophore pigmentation until 60 hpf, but regenerate the larval melanophore stripes completely by day 5 (C). (**D-H**) *Tg(mitfa:gfp; nbt:DsRed)* embryo previously treated with *mitfa*-MO imaged for several hours starting at 60 hpf (digital sectioning). A GFP-positive cells (white arrowhead) migrates along the spinal nerve. Another cell remained stationary (blue arrowhead) but was later observed to migrate away. Asterisks indicate the position of the DRG. (**I**) In *mitfa* morphant larvae (9 dpf), the regenerating MPs form a string of *mitfa*-positive cells along the spinal nerves associated with the DRGs both dorsally (arrowhead) and ventrally.

in close association with primary motor neurons, labelled in Fig. 1A-G with a transgene expressing DsRed under the control of a neuron-specific promoter (*nβt:DsRed*) (supplementary material Movie 1). We identified some of the migrating GFP-positive cells as melanoblasts because they undergo melanisation while still associated with primary motor axons (Fig. 1E,F). We observe round stationary cells remaining at the motor axon exit point (Fig. 1G, arrow).

We followed *mitfa:gfp*-labelled cells together with RFP-labelled cells of neuronal origin under the control of a neurogenin promoter (*neurog:rfp*). Melanophores forming the lateral stripe also originate from *mitfa:gfp* cells following the ventromedial path at ~40 hpf, turning into the horizontal myoseptum and migrating towards the skin (Fig. 1H-K, blue arrowheads). Fig. 1K shows the appearance of the DRG precursor cell at 48 hpf located next to a *mitfa:gfp*-labelled cell that resided at this position for at least 21 hours.

The larval set of melanophores has differentiated by 3 dpf and GFP expression has largely ceased. Interestingly, at later time points we still observe GFP-labelled cells located close to the DRGs (Fig. 2A-C, arrowheads) and along the ventral motor neurons (Fig. 2B, arrow). Their elongated shape suggests that they are, at least in part, Schwann cells. Schwann cells along the lateral line also retain the *mitfa:gfp* label until late larval stages (data not shown).

Imaging larvae until metamorphosis (Fig. 2A-F) shows that the number of stationary cells at the site of the DRG expressing *mitfA:gfp* remains at the level of zero to one labelled cell per hemisegment. The number of labelled cells along the ventral spinal nerve (Fig. 2B, arrow) remains about four throughout larval development (Fig. 2G). No labelled cells along the dorsal spinal nerves (Fig. 2D, arrow) can be observed until metamorphosis, when the number of *mitfa:gfp*-labelled cells increases along the spinal nerves both dorsally and ventrally (Fig. 2E,F, arrowheads). This suggests that these are MPs emerging from the stationary cells at the DRG.

We propose that the DRG-associated stationary cells include melanophore stem cells producing MPs that later give rise to adult melanophores.

Recovering melanoblasts emerge at the DRG and migrate along the spinal nerves

Larval melanophores can regenerate if chemically or genetically ablated (Yang and Johnson, 2006; Hultman et al., 2009; Tryon et al., 2011). To investigate whether these newly formed melanophores originated from the putative DRG-associated stem cells, we depleted the directly differentiating melanophores with a *mitfa*-morpholino. (Mellgren and Johnson, 2004) and traced melanophore renewal by 4D *in vivo* imaging in the *Tg(mitfa:gfp)* line.

In the first 60 hpf, knockdown of Mitfa faithfully phenocopies the *nac* mutant phenotype as the *mitfa*-MO-treated embryos do not show pigmented melanophores. Strikingly, in subsequent stages, larval melanophore pigmentation recovers and by 5 dpf the larval melanophore pattern is completely restored (Mellgren and Johnson, 2004) (Fig. 3A-C). This indicates that knockdown of Mitfa during early development affects melanoblasts committed to direct differentiation, whereas the melanoblast population that restores the pattern is derived from melanophore stem cells that did not require Mitfa early in development (Hultman and Johnson, 2010).

In *mitfa*-MO embryos between 60 and 80 hpf, new *mitfa:gfp*-labelled melanoblasts appear. In time-lapse movies, we captured melanoblasts originating at the site of the DRG and migrating along the spinal nerves (Fig. 3D-H). We were able to follow *mitfa:gfp*-labelled cells in *mitfa*-MO individuals until late larval stages. Fig. 3I shows a stereotyped pattern of GFP-positive cells associated with DRG neurons (red) notably following both the dorsal (arrowhead) and ventral projections. This pattern resembles that observed later in juvenile wild-type fish, when *mitfa:gfp*-positive cells appear in close contact with the spinal nerves (Fig. 2E,F) (Budi et al., 2011).

To trace the migration and cell lineage of individual regenerating melanoblasts, we transplanted cells from *mitfa:gfp* embryos into *albino* (*slc45a2* – Zebrafish Information Network) mutant embryos treated earlier with *mitfa*-MO. This enabled us to select embryos in which donor cells (rhodamine-tracer positive) contributed to the DRGs. We imaged GFP-positive cells appearing at the location of donor-derived DRGs for 28 hours starting at 60 hpf. Fig. 4A-E (see also supplementary material Movies 2, 3) shows the migration of GFP-positive cells dividing several times while travelling along the sensory projections labelled in red. These cells originated from a single unlabelled cell that resides close to a DRG, begins to express GFP and undergoes a division giving rise to one daughter cell that remains at this location. The other daughter cell moves away, divides again and melanises once it reaches the ventral side of the myotome. In this clone, the migration of individual progeny of silent MPs could be traced along DRG-derived neurons to a location in the ventral stripe as well as into the dorsal stripe to differentiate into darkly pigmented melanophores (Fig. 4F-H).

We traced several GFP-labelled melanoblasts (n=8) that originate from the site of the DRGs, migrate along the spinal nerves and give rise to melanophores of larval stripes. We thus identified the MPs residing close to the DRG as progenitors of regenerating melanoblasts. From these transplantation experiments we selected chimeric animals displaying donor-derived melanophores located at the horizontal myoseptum and individually raised these to adulthood. In three out of five such cases, adult melanophores developed at the same location as the regenerated larval pigmentation (Fig. 4I,J). The chimeras displayed donor-derived melanophores in vertical streaks often spanning the entire pattern from dorsal to ventral. This indicates that MPs that give rise to the regeneration of the larval pigmentation also generate the adult melanophore pattern.

We conclude that in *mitfa*-MO-treated embryos the absence of differentiated melanophores induces premature activation of embryonic MPs located in close proximity to DRGs. This results in proliferation and migration of MPs that first restore a larval pattern, and eventually produce adult melanophores.

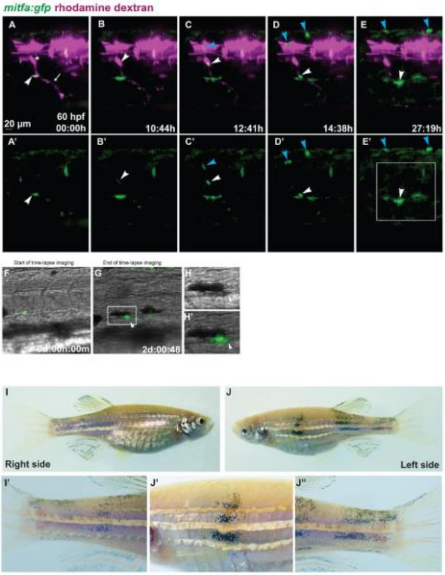

Fig. 4. Tracing individual MPs during regeneration in chimeric animals. Blastula transplantations were performed with *Tg(mitfa:gfp)* zebrafish embryos injected with rhodamine dextran as donors and *alb* embryos injected with *mitfa*-MO as recipients. (**A-E′**) Red and green channel are shown in A-E, green channel only in A′-E′. Starting at 60 hpf (A,A′), we imaged a clone appearing at the site of a rhodamine-labelled DRG (asterisk) from which a peripheral axon extends ventrally (arrow). The arrowhead in A,A′ points to a GFP-positive cell located at the ventral side of the myotome. Another labelled cell appears at 70 hpf at the site of the DRG (arrowhead in B,B′). This cell divides, and the two daughter cells migrate dorsally (blue arrowhead) and ventrally (white arrowhead) along a spinal nerve (C,C′). The dorsally migrating cell divides once (blue arrowheads in D-E′), its progeny arrive at the dorsal side of the larva. The ventrally migrating cell divides once (white arrowheads in D-E′). (**F-H′**) The daughter cells, after reaching a position along the ventral stripe close to a cell that arrived there earlier, melanise (arrowheads in G-H′). Complete time-lapse imaging is shown in supplementary material Movies 2, 3. The region marked in E′ is shown in more detail in G, and the boxed area in G is enlarged in H,H′. (**I-J″**) Chimeric adult fish that had developed several donor-derived melanophores at the lateral stripe in late larval stages. These display vertical streaks of donor-derived melanophores spanning the entire flank from dorsal to ventral, including the fins, enlarged in I′,J′,J″. These streaks appeared in the same rostrocaudal position as the larval melanophores.

ErbB receptors are required for the migration of all NC cells along the ventromedial path

To learn more about the role of DRGs in melanophore development, we examined mutants of the neuregulin receptors ErbB3b (also known as *hypersensitive*, *hps*) and ErbB2 (*kitzelig*, *kiz*) that lack DRGs and glia (Lyons et al., 2005; Honjo et al., 2008; Budi et al., 2008; Rojas-Muñoz et al., 2009). Whereas *erbb2* mutants are larval lethal, the *erbb3b* alleles are hypomorphs with variable expressivity and viability and mutant fish may survive to adulthood. Strikingly, large portions of the flank of *erbb3b* fishes are devoid of melanophores (Budi et al., 2008) (Fig. 5A). Small molecule inhibitor studies indicated that ErbB3b/ErbB2 signalling is required during the first day of embryogenesis for the subsequent development of metamorphic melanoblasts (Budi et al., 2008). A close correlation between the position of defects along the anteroposterior pattern in the adult fishes and the time window of inhibition coinciding with the developmental stage at which NC delaminates and migrates in the respective segments was shown by Budi et al. (Budi et al., 2008) in *sparse* (*kita*) mutant embryos for Kit-independent melanophores. We confirmed this correlation for wild type (Fig. 5B-E).

Honjo et al. (Honjo et al., 2008) reported that the lack of DRGs in *erbb3b* mutant embryos resulted from a failure of the NC cells to pause during migration towards the ventral side of the embryo. We performed 4D time-lapse imaging of NC labelled with *sox10:gfp* and neural tissue labelled with *nβt:DsRed*. In wild-type embryos, *sox10:gfp*-positive NC cells, after reaching the ventral side of the neural tube, continue to migrate in the conspicuous segmental streams along the primary motor neurons towards the ventral side of the embryo (Fig. 6A-A″). By contrast, no migration occurs in embryos treated with small molecule inhibitors of ErbB receptors, and NC cells are arrested dorsally to the neural tube (Fig. 6B-B″). The motor neurons remain uncovered by glial cells. A close-up at 36 hpf shows that embryonic *mitfa:gfp*-positive MPs are absent in inhibitor-treated embryos (Fig. 6C,D). Imaging of *mitfa:gfp* cells in the *erbb2* mutants showed that no NC migration occurs along the ventromedial path (supplementary material Movie 4). In *erbb3b* mutant embryos, some segments are completely devoid of migrating NC, whereas in others migration is normal (data not shown). Notably, migration of NC cells along the dorsolateral path is normal in *erbb* mutants or inhibitor-treated embryos (Fig. 6B′; supplementary material Movie 4). These observations indicate that ErbB signalling is required for NC migration specifically along the ventromedial path.

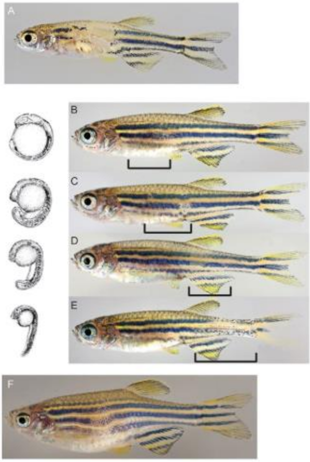

Fig. 5. The Role of ErbB signalling and the DRGs for adult melanophore pigmentation. (**A**) *hps/erbb3b*^{t21411} adult fish showing a dramatic regional reduction of melanophores. (**B-E**) Adult fish treated at successive stages of somitogenesis (left) with the ErbB inhibitor PD168393. The later the inhibitor was applied, the more posterior is the position of the defect (brackets). (**F**) Adult fish in which eight consecutive DRGs were laser-ablated at 3 dpf.

We investigated the recovery of melanoblasts in partial MO knockdowns of ErbB3b in *mitfa* morphants. We observed that some segments completely recovered the stream of GFP-positive cells associated with the DRG neurons, whereas others had a complete lack of such cells (Fig. 6E). There is a strong correlation between the presence of DRGs and recovered *mitfa:gfp*-positive cells whereas segments lacking a DRG do not usually display them (Table 1).

To examine further the role of DRGs, eight DRGs were laser ablated in wild-type larvae at 3 dpf. We observed a lower number of melanophores in the corresponding segments of the flank of the respective adult fishes and, thus, mild phenocopies of the *hps*/*picasso* mutant phenotype in eight out of ten cases (Fig. 5F).

These experiments support the notion that DRGs provide a niche for melanophore stem cells.

sparse like encodes Kit ligand a

We next investigated the role of Kitlga signalling in the establishment of melanophore progenitors. *spa* (*kita*) is required for the survival, migration and differentiation of melanoblasts at all stages of development. We identified the mutant *sparse like* (*slk*), (Kelsh et al., 1996) (Fig. 7) as affected in *kit ligand a* (*kitlga*) (Hultman et al., 2007). In both *spa* and *slk* mutants, late larval and metamorphic melanophores are absent (Fig. 7F-H). A population of Kitlga signalling-independent melanophores appears in adult fish (Fig. 7J). The mutant *slk* carries a stop codon in the *kitlga* gene (Fig. 8A). *kitlga* is expressed at very low levels in early embryos at the site of premigratory NC (Hultman et al., 2007) (data not shown). Its expression persists in segmental patches in cells under the epidermis on the dorsal side as well as in segmentally repeated expression domains close to the notochord (Hultman et al., 2007). This *kitlga* expression domain is absent in *sox10* mutant embryos and includes a subset of neural crest at the site of the developing PNS (Fig. 8B-D).

Table 1. Quantification of the association of DRGs and GFP-positive cells as shown in Fig. 6F

	Count	
DRG staining	Control	*erb3b*MO+*mitfa*MO
Hu+; *mitfa*:GFP+	190	138
Hu+; *mitfa*:GFP–	40	30
Hu–; *mitfa*:GFP+	2	5
Hu–; *mitfa*:GFP–	4	77
Total	236	250

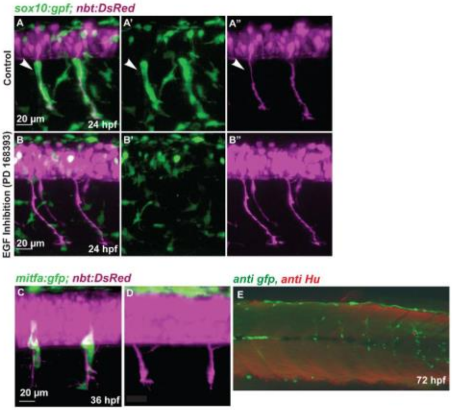

Fig. 6. NC migration along the ventromedial path is blocked by inhibition of ErbB receptors. (**A-B‴**) *Tg(sox10:gfp; nbt:DsRed)* zebrafish embryos at 24 hpf. (A,B) Red and green channel (merge); (A′,B′) green channel; (A″,B″) red channel. Medial NC cells (green) covering the primary motor axons (white arrowheads, A-A″) are absent after treatment with the ErbB inhibitor PD168393 (B-B″). (**C**,**D**) Confocal images of 36 hpf *Tg(mitfa:gfp; nbt:DsRed)* embryos. (C) Wild-type embryo. (D) Embryo treated with ErbB inhibitor at 16 hpf. (**E**) *Tg(mitfa:gfp)* embryos were injected with a double MO combination against *mitfa* and *erbb3b*. Larvae were stained at 8 dpf using anti-GFP (green) and anti-HU (red) antibody (white arrowheads). The association of DRGs (red) and GFP-positive cells was quantified (Table 1). In double *mitfa* and *erbb3b* knockdowns, of 82 metamers lacking HU positive cells only five (6%) develop a string of GFP-positive cells.

Kitlga signalling is required for embryonic MP formation

We imaged the site of DRG formation in *slk* embryos at 48 hpf. Fig. 9A-D shows the presence of *mitfa:gfp*-labelled cells located close to the progenitors of the DRGs. However, these cells often appear elongated and detached in *slk* mutants (Fig. 9B,D, arrowhead), suggesting that the stationary MPs are reduced or missing but *mitfA:gfp*-positive glia cells are retained. We observed the *mitfa:gfp*-labelled cells located along the spinal nerves in wild-type (Fig. 2) and *slk* mutant (data not shown) fish until metamorphosis. Although reduced in number, we do not observe a significant qualitative difference, presumably because the labelled cells are mostly glia. Interestingly, like in wild type, in *slk* mutants labelled cells along the dorsal spinal nerve are not observed before metamorphosis (data not shown). This indicates that in *slk* mutants, despite the absence of melanophores there is no precocious activation of MPs to produce regenerating melanoblasts, as seen in *mitfA*-MO-treated embryos (Fig. 3I). Embryos treated with *kitlga* MO do not show melanophore pigmentation and faithfully copy the mutant phenotype until late stages of larval development (Fig. 9G,H). Thus, in contrast to *mitfa*, *kitlga* morphants do not regenerate the larval melanophore population. This indicates that in

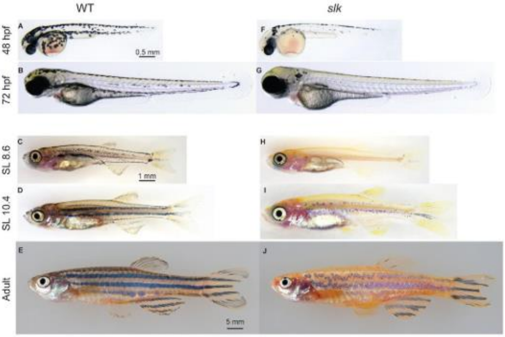

Fig. 7. The phenotype of *sparse like*^{tc244b} fish at different developmental stages. (**A-J**) The phenotype of wild-type (A-E) and *sparse like* (F-J) fish at different developmental stages. Unlike wild-type fish (C), *slk* fish are almost completely devoid of melanophores at the beginning of metamorphosis (H). Adult *slk* mutants (J) form stripes with strong reduction in melanophore number compared with wild-type siblings (E). SL, standard length.

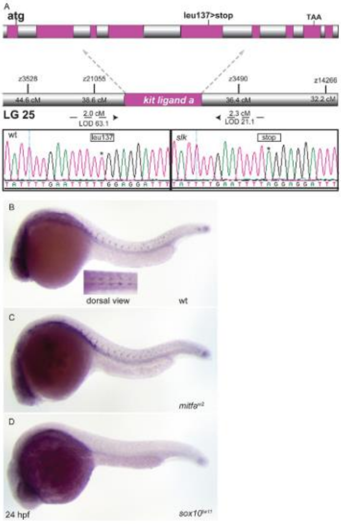

Fig. 8. *slk* encodes Kitlga and is expressed in NC cells. (**A**) *slk* mutants reveal a T to A base substitution in exon 5 of the *kitlga* transcript causing a premature stop codon. (**B-D**) *kitlga in situ* hybridisation. At 24 hpf, *kitlga* is expressed in NC cells migrating along the medial path. This expression domain is maintained in *mitfa* mutants (C) but not in *sox10* mutant embryos (D).

kitlga mutant embryos, embryonic MPs located at the DRG are missing or fail to function as stem cells. It also suggests that in normal development MPs are established during the first few days of embryogenesis when the MO knockdown is effective, under the control of Kitlga signalling.

In *slk* embryos, we do observe that *mitfa:gfp* cells undergo apoptosis before NC migration commences (Fig. 9C,D), reflecting the *slk* phenotype. This observation supports the notion that there is a population of melanoblasts in this dorsal location that is specified before migration along the dorsolateral route and that requires Kitlga signalling for its survival.

DISCUSSION

Identification of melanophore stem cells

Although the presence of embryonic melanophore stem cells (MSCs) had already been postulated (Budi et al., 2008; Johnson et al., 2011), their location remained elusive. We demonstrate that the embryonic MPs we observe during early development closely associated with the emerging DRGs are MSCs. These MSCs can be activated prematurely using MO knockdown of Mitfa to remove larval melanophores. The progeny of activated MSCs can be traced as they express *mitfa:gfp* and are mitotically active. They can regenerate all components of the larval melanophore pattern. Moreover, during migration along spinal nerves they form a chain of GFP-expressing cells, closely resembling postembryonic MPs reported by Budi et al. (Budi et al., 2011). Melanoblasts originating from these MPs migrate into the skin, melanise and arrange themselves in the striped pattern of the adult (Fig. 4). During normal development, activation of the quiescent melanophore stem cells occurs in late larval and juvenile stages (Fig. 2), giving rise to the adult melanophore pattern.

MSCs require ErbB signalling and are associated with the DRGs

Our live imaging confirms that NC migration along the ventromedial path occurs in close association with the extending primary motor axons (Banerjee et al., 2011). Melanoblasts of the larval pattern also migrate along this path, as shown by the direct tracing of *mitfa:gfp* cells that undergo melanisation (Fig. 1E,F). Mutations in *erbb2b* or treatment with drugs inhibiting ErbB receptors inhibit migration of NC cells along the ventromedial path. The close correlation between the position of adult pigmentation defects along the rostrocaudal axis and the time window of inhibiting migration of NC cells (Budi et al., 2008) (Fig. 5B-E) strongly supports the notion that the MSCs are also affected by the inhibitor. Both glia and melanoblasts express ErbB receptors (Lyons et al., 2005; Budi et al., 2008). Unlike glia, which require ErbB signalling during migration, proliferation and differentiation, in the case of the melanophores, once this migration has occurred, ErbB signalling is no longer required for the development of adult melanophores.

The stem cells we have identified are associated with the DRGs of the peripheral nervous system. ErbB-dependent NC migration also affects DRGs when perturbed. The progenitor cells of the DRGs settle at the exit point of the primary motor neurons adjacent to the ventral spinal cord (Carney et al., 2006). We found a close association of MSCs with the DRGs. Through ablation in the embryo we have provided evidence of the role of DRGs in the establishment of melanophore stem cells either as a niche, a source for the peripheral nerves on which MPs travel to the surface, or both.

So far, although we have ample evidence from lineage tracing that MSCs are located at the site of the DRGs, we do not exclude additional sites. Some of the *mitfa:gfp*-positive cells along ventral spinal nerves in larval stages (Fig. 2) might also function as MPs.

Kitlga signalling specifically affects melanophore stem cells

Our data indicate that the Kitlga pathway is specifically required for a progenitor population of melanophores whereas other NC-derived cell types are not affected. In *kitlga* embryos, the DRGs are formed and *mitfa:gfp*-positive cells are seen close to them and along the spinal nerves. Most, if not all, of these cells are presumably glial cells, and from the morphology we cannot unequivocally distinguish embryonic MPs and glia cells. These cells may include progenitors of Kitlga-independent adult melanophores that also migrate along the ventromedial path (Budi et al., 2008). The failure of the melanophore population to regenerate after *kitlga*-MO treatment means that they do not function as MSCs, and that MSCs require Kitlga signalling very early for their establishment. We observe cells that undergo apoptosis at a dorsal location, indicating that they are specified as

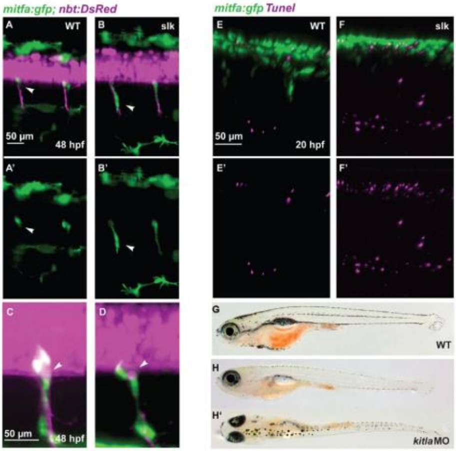

Fig. 9. Abnormal NC migration and apoptosis in *slk* embryos. (**A-B'**) GFP-positive cells in double transgenic *Tg(mitfa:gfp; nbt:DsRed)* wild-type (A,A') and *slk* mutant (B,B') embryos at 48 hpf. In the wild-type embryo, GFP-positive NC cells remain at the position of the DRG and have a rounded morphology (white arrowhead in A,A') whereas in *slk* mutants they are stretched along the nerves and appear to be migratory (white arrowheads in B,B'). A', B' show green channel only. (**C**,**D**) Magnification showing *mitfa:gfp*-labelled cells at the exit point of the spinal nerves at 48 hpf of wild-type (C) and *slk* mutant (D) embryos. The arrowheads point to DRGs. (**E-F'**) TUNEL staining in *Tg(mitfa:gfp)* embryos in wild-type (E,E') and *slk* (F,F') embryos at 20 hpf. E',F' show red channel only. (**G-H'**) Wild type (G) and *slk* morphant (H,H') at 20 dpf (5.7 mm SL).

melanoblasts prior to migration. Presumably most of these cells are melanoblasts destined to migrate along the dorsolateral route. *kitlga* is expressed early in NC cells located at the site of the future DRG and associated glia. It is tempting to speculate that, in addition to survival and migration, Kitlga has the function of a niche factor of MSCs. In this context, it is interesting to note that in mice, kit ligand (also known as steel factor) provides a niche factor for survival and migration of primordial germ cells (Gu et al., 2009).

We note that at the early time point, *kitlga* function distinguishes the various NC fates as in *slk* mutants only the melanophores are strongly reduced but there is no evidence that glia, peripheral nervous system or other chromatophore types are affected.

Melanophore progenitors migrate along a vertical path

In zebrafish, 4D imaging allows tracing of migrating cells and tissue with high resolution in time and space during embryonic and larval life. The premature activation of quiescent stem cells after *mitfa*-MO knockdown has enabled us to study the origin and migration of postembryonic regenerating MPs already in late larval stages. Regenerating melanophores are responsive to ErbB inhibition in the same time window in early development as adult melanophores (Hultman and Johnson, 2010; Johnson et al., 2011). Tracing regenerating melanophores in larval and adult chimeras confirmed the notion that both populations arise from the same stem cells (Fig. 4).

During metamorphosis, MPs originate at the DRGs and move along the spinal nerves both dorsally and ventrally. These cells populate individual segments with MPs that form a stream of labelled cells (Fig. 2E,F). In chimeric animals, during metamorphosis donor MPs populate the skin of albino recipients with melanophores in vertical streaks running from dorsal to ventral (Fig. 4; data not shown). This suggests that a segmental melanophore streak results from a single or a very small number of stem cells being seeded and that these can give rise to the entire population of MPs of a segment by spreading along the segmental spinal nerves, whereas little lateral spreading occurs. Fig. 10 illustrates schematically the paths taken by melanophore progenitors during embryogenesis (Fig. 10A-C) and metamorphosis (Fig. 10D-F).

Distinct classes of melanophore progenitors

On the basis of these observations, several classes of MPs can be distinguished. On the first day of development, a small number of MSCs that reside close to the DRGs in each segment is established. These are normally quiescent throughout larval life and do not require *mitfa*. They are dependent on Kitlga signalling for their function as MSCs. The development of MSCs depends on migration of NC cells along the ventromedial path and the establishment of the DRGs. This process requires ErbB2/3b receptor signalling during the first 18-24 hours of development.

In later larval and juvenile stages, another class of MPs appears as progeny of activated MSCs. These postembryonic MPs express *mitfa:gfp*, originate from the DRGs, proliferate and migrate along the spinal nerves. We do see melanising cells along the peripheral nerves in adult fishes, and propose that the MPs observed in extra hypodermal space (Budi et al., 2011) are in fact associated with nerve bundles running along myosepta. Both classes of MPs are present in *mitfa* mutants.

The DRG-associated MSCs give rise to the melanophores of the adult pattern. We presume but have not yet directly shown that these

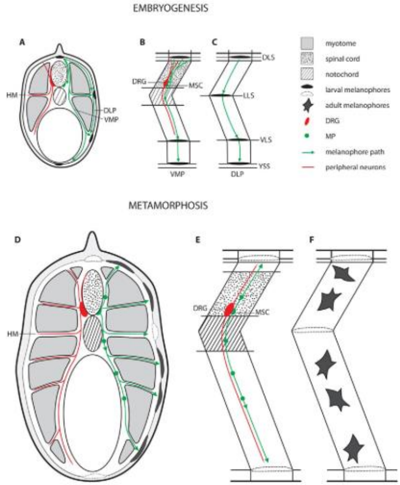

Fig. 10. Model of migration of melanophore progenitors during embryogenesis and metamorphosis. (**A**) Schematic cross-section through a trunk segment indicating the path of the peripheral neurons emerging from the DRG (left side). The migratory route taken by the melanoblasts along the ventromedial path (VMP) and the dorsolateral path (DLP) (right side). (**B**) Side view of the ventromedial path showing that melanoblasts contribute to the ventral larval stripes (VLS), they migrate through the horizontal myoseptum (HM) to form the lateral larval stripe (LLS). (**C**) Melanoblasts traveling along the dorsolateral path between somites and epidermis contribute to all three stripes. DLS, dorsal larval stripe; YSS, yolk sac stripe. (**D-F**) During metamorphosis adult melanophores arrive in the skin originating from melanophore progenitors (MPs) associated with the spinal nerves (red) that innervate the myotome via myosepta. These MPs are derived from embryonic melanophore stem cells (MSCs) located at the DRGs. The larval melanophores (dotted) later disappear.

have the capacity of self-renewal, as anticipated from stem cells. Failure in the establishment of MSCs cannot easily be repaired, as seen in the long-lasting effects of the early transient inhibition of the receptors of the ErbB signalling system, the DRG ablation, and the failure to recover the melanophore pattern in *kitlga* morphants. We propose that stem cell maintenance depends on the microenvironment provided by the DRG and associated glia as a stem cell niche, and speculate that one function of Kitlga signalling is to attract and to maintain them in this niche. The postembryonic MPs may be regarded as transient amplifying cells as they proliferate and provide the adults with the necessary supply of melanophores during stripe formation, growth and regeneration.

It is important to note that most, but not all, adult melanophores originate from these Kitlga signalling-dependent stem cells. During adulthood, *spa* and *slk* mutants develop a striped pattern displaying melanophores that do not require Kitlga signalling. Budi et al. (Budi et al., 2011) presented evidence for the existence of melanophore progenitor cells that develop from cells co-expressing *foxd3* and *mitfa*, possibly shared Schwann cell progenitors. A Schwann cell precursor origin of melanocytes derived from the ventromedial path of NC migration has also been observed in amniotes such as mice and chicken (Adameyko et al., 2009). Clonal analysis in adult zebrafish indicates that some melanophores share a lineage with iridophores (A. Singh, A.M. and C.N.-V., unpublished). Kitlga signalling-independent adult melanophores, however, require ErbB signalling at the same early time interval as the Kit-dependent MSCs (Budi et al., 2008), suggesting that these melanophore progenitors also travel along the ventromedial path. We do not yet know the embryonic origin of adult xanthophores or iridophores.

Although dorsolateral migration holds for some of the larval melanophores in zebrafish, adult melanophores arise from migration along nerves in a similar manner to the melanocyte progenitors described by Adameyko et al. (Adameyko et al., 2009) in mouse and chicken. We present evidence for a stem cell population that resides at the DRGs and that appears to be specific to melanophores. Although we expect the embryonic origin of adult melanophores to be common to fishes, it will be interesting to ascertain whether stem cells with a similar origin are also present in the amniotic vertebrates.

Acknowledgements
Sören Alsheimer, Ajeet Singh, Virgilio Failla and Christian Liebig provided excellent support in confocal microscopy and image processing. We thank Andrey Fadeev for assistance in adult fish photography. Robert Geisler and Ines Gehring provided technical support in the mapping of *slk*. We thank Jana Krauss and Ajeet Singh for discussion, and Robert Kelsh, Darren Gilmour, Simon Perathoner for valuable comments on earlier versions of the manuscript.

Funding
This research was funded by the Max-Planck Society, Germany.

Competing interests statement

The authors declare no competing financial interests.

Supplementary material

Supplementary material available online at
http://dev.biologists.org/lookup/suppl/doi:10.1242/dev.087007/-/DC1

References
Adameyko, I., Lallemend, F., Aquino, J. B., Pereira, J. A., Topilko, P., Müller, T., Fritz, N., Beljajeva, A., Mochii, M., Liste, I. et al. (2009). Schwann cell precursors from nerve innervation are a cellular origin of melanocytes in skin. *Cell* **139**, 366-379.

Banerjee, S., Gordon, L., Donn, T. M., Berti, C., Moens, C. B., Burden, S. J. and Granato, M. (2011). A novel role for MuSK and non-canonical Wnt signaling during segmental neural crest cell migration. *Development* **138**, 3287-3296.

Brand, M., Granato, M. and Nuesslein-Volhard, C. (2002). Raising and keeping zebrafish. In *Zebrafish: a Practical Approach* (ed. C. Nuesslein-Volhard and R. Dahm). Oxford: Oxford University Press.

Budi, E. H., Patterson, L. B. and Parichy, D. M. (2008). Embryonic requirements for ErbB signaling in neural crest development and adult pigment pattern formation. *Development* **135**, 2603-2614.

Budi, E. H., Patterson, L. B. and Parichy, D. M. (2011). Post-embryonic nerve-associated precursors to adult pigment cells: genetic requirements and dynamics of morphogenesis and differentiation. *PLoS Genet.* **7**, e1002044.

Carney, T. J., Dutton, K. A., Greenhill, E., Delfino-Machín, M., Dufourcq, P., Blader, P. and Kelsh, R. N. (2006). A direct role for Sox10 in specification of neural crest-derived sensory neurons. *Development* **133**, 4619-4630.

Curran, K., Raible, D. W. and Lister, J. A. (2009). Foxd3 controls melanophore specification in the zebrafish neural crest by regulation of Mitf. *Dev. Biol.* **332**, 408-417.

Darwin, C. (1871). *The Descent of Man, and Selection in Relation to Sex*. John Murray, London.

Dutton, K. A., Pauliny, A., Lopes, S. S., Elworthy, S., Carney, T. J., Rauch, J., Geisler, R., Haffter, P. and Kelsh, R. N. (2001). Zebrafish colourless encodes sox10 and specifies non-ectomesenchymal neural crest fates. *Development* **128**, 4113-4125.

Elworthy, S., Lister, J. A., Carney, T. J., Raible, D. W. and Kelsh, R. N. (2003). Transcriptional regulation of mitfa accounts for the sox10 requirement in zebrafish melanophore development. *Development* **130**, 2809-2818.

Gans, C. and Northcutt, R. G. (1983). Neural crest and the origin of vertebrates: a new head. *Science* **220**, 268-273.

Geisler, R., Rauch, G.-J., Geiger-Rudolph, S., Albrecht, A., van Bebber, F., Berger, A., Busch-Nentwich, E., Dahm, R., Dekens, M. P. S., Dooley, C. et al. (2007). Large-scale mapping of mutations affecting zebrafish development. *BMC Genomics* **8**, 11.

Geissler, E. N., Ryan, M. A. and Housman, D. E. (1988). The dominant-white spotting (W) locus of the mouse encodes the c-kit proto-oncogene. *Cell* **55**, 185-192.

Gu, Y., Runyan, C., Shoemaker, A., Surani, A. and Wylie, C. (2009). Steel factor controls primordial germ cell survival and motility from the time of their specification in the allantois, and provides a continuous niche throughout their migration. *Development* **136**, 1295-1303.

Gu, Y., Runyan, C., Shoemaker, A., Surani, M. A. and Wylie, C. (2011). Membrane-bound steel factor maintains a high local concentration for mouse primordial germ cell motility, and defines the region of their migration. *PLoS ONE* **6**, e25984.

Haffter, P., Odenthal, J., Mullins, M., and Lin, S. (1996). Mutations affecting pigmentation and shape of the adult zebrafish. *Dev. Genes Evol.* **206**, 260-276.

Hoekstra, H. E., Hirschmann, R. J., Bundey, R. A., Insel, P. A. and Crossland, J. P. (2006). A single amino acid mutation contributes to adaptive beach mouse color pattern. *Science* **313**, 101-104.

Honjo, Y., Kniss, J. and Eisen, J. S. (2008). Neuregulin-mediated ErbB3 signaling is required for formation of zebrafish dorsal root ganglion neurons. *Development* **135**, 2615-2625.

Huang, E. J., Nocka, K. H., Buck, J. and Besmer, P. (1992). Differential expression and processing of two cell associated forms of the kit-ligand: KL-1 and KL-2. *Mol. Biol. Cell* **3**, 349-362.

Hultman, K. A. and Johnson, S. L. (2010). Differential contribution of direct-developing and stem cell-derived melanocytes to the zebrafish larval pigment pattern. *Dev. Biol.* **337**, 425-431.

Hultman, K. A., Bahary, N., Zon, L. I. and Johnson, S. L. (2007). Gene duplication of the zebrafish kit ligand and partitioning of melanocyte development functions to kit ligand a. *PLoS Genet.* **3**, e17.

Hultman, K. A., Budi, E. H., Teasley, D. C., Gottlieb, A. Y., Parichy, D. M. and Johnson, S. L. (2009). Defects in ErbB-dependent establishment of adult melanocyte stem cells reveal independent origins for embryonic and regeneration melanocytes. *PLoS Genet.* **5**, e1000544.

Johnson, S. L., Africa, D., Walker, C. and Weston, J. A. (1995). Genetic control of adult pigment stripe development in zebrafish. *Dev. Biol.* **167**, 27-33.

Johnson, S. L., Nguyen, A. N. and Lister, J. A. (2011). mitfa is required at multiple stages of melanocyte differentiation but not to establish the melanocyte stem cell. *Dev. Biol.* **350**, 405-413.

Kelsh, R. N., Brand, M., Jiang, Y. J., Heisenberg, C. P., Lin, S., Haffter, P., Odenthal, J., Mullins, M. C., van Eeden, F. J., Furutani-Seiki, M. et al. (1996). Zebrafish pigmentation mutations and the processes of neural crest development. *Development* **123**, 369-389.

Lister, J. A. (2002). Development of pigment cells in the zebrafish embryo. *Microsc. Res. Tech.* **58**, 435-441.

Lister, J. A., Robertson, C. P., Lepage, T., Johnson, S. L. and Raible, D. W. (1999). nacre encodes a zebrafish microphthalmia-related protein that regulates neural-crest-derived pigment cell fate. *Development* **126**, 3757-3767.

Lyons, D. A, Pogoda, H.-M., Voas, M. G., Woods, I. G., Diamond, B., Nix, R., Arana, N., Jacobs, J., and Talbot, W. S. (2005). Erbb3 and Erbb2 are essential for schwann cell migration and myelination in zebrafish. *Curr. Biol.* **15**, 513-524.

Mellgren, E. M. and Johnson, S. L. (2004). A requirement for kit in embryonic zebrafish melanocyte differentiation is revealed by melanoblast delay. *Dev. Genes Evol.* **214**, 493-502.

Nasevicius, A. and Ekker, S. C. (2000). Effective targeted gene 'knockdown' in zebrafish. *Nat. Genet.* **26**, 216-220.

Parichy, D. M., Rawls, J. F., Pratt, S. J., Whitfield, T. T. and Johnson, S. L. (1999). Zebrafish sparse corresponds to an orthologue of c-kit and is required for the morphogenesis of a subpopulation of melanocytes, but is not essential for hematopoiesis or primordial germ cell development. *Development* **126**, 3425-3436.

Parichy, D. M., Turner, J. M. and Parker, N. B. (2003). Essential role for puma in development of postembryonic neural crest-derived cell lineages in zebrafish. *Dev. Biol.* **256**, 221-241.

Protas, M. E. and Patel, N. H. (2008). Evolution of coloration patterns. *Annu. Rev. Cell Dev. Biol.* **24**, 425-446.

Quigley, I. K., Turner, J. M., Nuckels, R. J., Manuel, J. L., Budi, E. H., MacDonald, E. L. and Parichy, D. M. (2004). Pigment pattern evolution by differential deployment of neural crest and post-embryonic melanophore lineages in Danio fishes. *Development* **131**, 6053-6069.

Rawls, J. F. and Johnson, S. L. (2003). Temporal and molecular separation of the kit receptor tyrosine kinase's roles in zebrafish melanocyte migration and survival. *Dev. Biol.* **262**, 152-161.

Rawls, J. F., Mellgren, E. M. and Johnson, S. L. (2001). How the zebrafish gets its stripes. *Dev. Biol.* **240**, 301-314.

Rojas-Muñoz, A., Rajadhyksha, S., Gilmour, D., van Bebber, F., Antos, C., Rodríguez Esteban, C., Nüsslein-Volhard, C. and Izpisúa Belmonte, J. C. (2009). ErbB2 and ErbB3 regulate amputation-induced proliferation and migration during vertebrate regeneration. *Dev. Biol.* **327**, 177-190.

Roulin, A. (2004). The evolution, maintenance and adaptive function of genetic colour polymorphism in birds. *Biol. Rev. Camb. Philos. Soc.* **79**, 815-848.

Schulte-Merker, S. (2002). Looking at Embryos. In *Zebrafish: a Practical Approach* (ed. C. Nuesslein-Volhard and R. Dahm), pp. 39-58. Oxford: Oxford University Press.

Streisinger, G., Singer, F., Walker, C., Knauber, D. and Dower, N. (1986). Segregation analyses and gene-centromere distances in zebrafish. *Genetics* **112**, 311-319.

Thisse, C. and Thisse, B. (2008). High-resolution in situ hybridization to whole mount zebrafish embryos. *Nat. Protoc.* **3**, 59-69.

Tryon, R. C., Higdon, C. W. and Johnson, S. L. (2011). Lineage relationship of direct-developing melanocytes and melanocyte stem cells in the zebrafish. *PLoS ONE* **6**, e21010.

Wehrle-Haller, B., Meller, M. and Weston, J. A. (2001). Analysis of melanocyte precursors in Nf1 mutants reveals that MGF/KIT signaling promotes directed cell migration independent of its function in cell survival. *Dev. Biol.* **232**, 471-483.

Whitfield, T. T., Granato, M., van Eeden, F. J., Schach, U., Brand, M., Furutani-Seiki, M., Haffter, P., Hammerschmidt, M., Heisenberg, C. P., Jiang, Y. J. et al. (1996). Mutations affecting development of the zebrafish inner ear and lateral line. *Development* **123**, 241-254.

Yang, C.-T. and Johnson, S. L. (2006). Small molecule-induced ablation and subsequent regeneration of larval zebrafish melanocytes. *Development* **133**, 3563-3573.

Publication 2:

Dooley CM, Schwarz H, Mueller KP, Mongera A, Konantz M, Neuhauss SC, Nüsslein-Volhard C, Geisler R. (2012). **Slc45a2 and V-ATPase are regulators of melanosomal pH homeostasis in zebrafish, providing a mechanism for human pigment evolution and disease.** *Pigment Cell Melanoma Res.* 26; 205–217

3.2 On melanophore melanization

The genetic foundations of both cellular differentiation and natural variation are major fields of investigation and it is of particular interest when a single locus can be shown to play a direct and conclusive role in both. The zebrafish *albino* mutant presents a classical oculocutaneous albinism (OCA), where both the RPE of the eyes and the melanophores of the skin lack melanin. Positional cloning of the *albino* mutant revealed mutations in the solute carrier *slc45a2*. Mutations in the human ortholog of this gene are responsible for OCA4 (Newton et al., 2001), while single nucleotide polymorphisms both in coding as well as in non-coding areas of this locus are highly correlated with natural human pigment variation (Sabeti et al., 2007). Although an association of *SLC45A2* and pigmentation has been previously described, very little was known about the actual role of the solute carrier in melanization.

When visualized using electron microscopy, melanosomes in *albino* mutants were present but contained only minimal amounts of melanin. In contrast, *sandy* mutants (*tyrosinase*/OCA1) or phenylthiourea (a copper chelator) treated fish failed to form proper melanosomes. These observations suggest that in the absence of functional tyrosinase toxic products are produced that cause a breakdown of melanosomes.

V-ATPases act as pumps pushing protons across membranes in an ATP-dependent manner and mutations in different protein subunits of these pumps are associated with pigment defects (Nuckels et al., 2009). To gain further insight into a possible role of *SLC45A2* in melanosome homeostasis morpholino knockdown and small molecule inhibition of V-ATPase were carried out and lead to a rescue of melanization in *albino* fish. Thiss lead to an increase in melanine production.

By specifically blocking the proton-pumping action of its V_1 subunit, the amount of protons transferred into melanosomes becomes reduced. This increase in pH is then sufficient to reinstate and rescue melanin production in *albino* mutants.

These findings suggest that a normal function of Slc45a2 acting as a Na^+/H^+ exchanger, together with Slc24a5 (*golden*) is necessary for the maintenance of appropriate pH and ionic conditions for the activity of *Tyrosinase* inside melanosomes. Furthermore, as slight variations in the function of Slc45a2 directly lead to variations in melanin production without the deleterious consequences observed in *tyrosinase* mutants, it becomes clear why *SLC45A2* has been repeatedly associated with human skin color variation as well as pigment variation throughout vertebrates.

PIGMENT CELL & MELANOMA RESEARCH

Volume 26, Number 2, March 2013 Pages 157–284

The official journal of
INTERNATIONAL FEDERATION OF PIGMENT CELL SOCIETIES · SOCIETY FOR MELANOMA RESEARCH

PIGMENT CELL
& MELANOMA
Research

Volume 26 · Number 2 · March 2013

Melanosomal pH Regulators
Hermansky-Pudlak Syndrome
Evading Senescence in Melanoma Progression

WILEY
www.pigment.org

Slc45a2 and V-ATPase are regulators of melanosomal pH homeostasis in zebrafish, providing a mechanism for human pigment evolution and disease

Christopher M. Dooley[1]*, Heinz Schwarz[1], Kaspar P. Mueller[2], Alessandro Mongera[1], Martina Konantz[1,†], Stephan C. F. Neuhauss[2], Christiane Nüsslein-Volhard[1] and Robert Geisler[1,‡]

1Max Planck Institute for Developmental Biology, Tübingen, Germany **2**Institute of Molecular Life Sciences, University of Zurich, Zürich, Switzerland *Current address: The Wellcome Trust Sanger Institute, The Wellcome Trust Genome Campus, Hinxton, UK †Current address: Department of Hematology, Oncology, Immunology, Rheumatology and Pneumology, University of Tübingen Medical Center II, Tübingen, Germany ‡Current address: Institute of Toxicology and Genetics, Karlsruhe Institute of Technology, Eggenstein-Leopoldshafen, Germany

CORRESPONDENCE Christopher M. Dooley, e-mail: chris.dooley@sanger.ac.uk and Robert Geisler, e-mail: robert.geisler@kit.edu

KEYWORDS slc45a2/albinism/V-ATPase/melanosome/melanocyte/retinal pigment epithelium/skin color variation

PUBLICATION DATA Received 11 September 2012, revised and accepted for publication 22 November 2012, published online 3 December 2012

doi: 10.1111/pcmr.12053

Summary

We present here the positional cloning of the *Danio rerio albino* mutant and show that the affected gene encodes Slc45a2. The human orthologous gene has previously been shown to be involved in human skin color variation, and mutations therein have been implicated in the disease OCA4. Through ultrastructural analysis of the melanosomes in *albino* alleles as well as the tyrosinase-deficient mutant *sandy*, we add new insights into the role of *Slc45a2* in the production of melanin. To gain further understanding of the role of *Slc45a2* and its possible interactions with other proteins involved in melanization, we further analyzed the role of the V-ATPase as a melanosomal acidifier. We show that it is possible to rescue the melanization potential of the *albino* melanosomes through genetic and chemical inhibition of V-ATPase, thereby increasing internal melanosome pH.

Introduction

Body pigmentation in vertebrates has an important function in camouflage, kin recognition, and sexual selection as well as shielding the skin from sunlight. Large-scale genetic screens in mouse and zebra fish have identified a great number of genes that affect melanin-dependent body pigmentation. Pigmentation of the skin results from melanocytes originating in the neural crest (NC), while pigmented retinal epithelium (RPE) arises from the neuroectoderm of the developing optic cup. In zebra fish, a mutation in the *nacre/mitfa* gene eliminates all NC–derived melanophores causing the body of the mutant to appear yellow due to a lack of the black stripes, while the RPE is normally pigmented (Lister et al., 1999). In contrast, other genes specifically affect the pigmentation of the melanocytes of the body as well as the RPE, suggesting that they are involved in the production and

Significance

Our findings show that Slc45a2 and V-ATPase along with Slc24a5 control pH and ionic homeostasis within melanosomes. In our model, a reduction in the efficiency of Slc45a2 has a quenching effect on the activity of tyrosinase by lowering the melanosomal pH while still maintaining the integrity of the melanosomes avoiding the toxic effects seen in tyrosinase mutants. These findings offer new clues to the molecular basis of melanin biosynthesis as well as providing a potential mechanism for human skin color variation.

© 2012 John Wiley & Sons A/S

while at the same time NC-derived body melanophores also start to become visible, and both are completely dark by 48 hpf (Figure 1A). The first described zebra fish *albino* mutant, *alb*^{b4}, which was described by Streisinger more than 25 yr ago (Streisinger et al., 1986), fails to melanize by 48 hpf and appears to lack melanin in both RPE- and NC-derived melanophores (Figure 1B). Although multiple *albino* alleles have been generated in previous screens (Kelsh et al., 1996), we decided to isolate additional alleles to generate a more complete series. For example, *alb*^{ti225} (Figure 1E, H), *alb*^{tj20e} (data not shown) from the Tübingen 1996 screen (Kelsh et al., 1996). and the newly identified *alb*^{tnr52} (Figure S1E) show the same strong larval phenotype as *alb*^{b4} (Figure 1G) but *alb*^{ti225} shows a slightly weaker phenotype than *alb*^{b4} as an adult (Figure 1E). An allele of particular interest, *alb*^{tnr39}, was identified in our screen in which the melanophores of both the body and the RPE of transheterozygous *alb*^{tnr39}/*alb*^{b4} larvae have greatly reduced melanin, but the cells are still readily visible (Figure 1F, I). This suggests that both cell types are capable of producing at least small amounts of melanin by 78 hpf. As adults, the body melanophores of *alb*^{tnr39}/*alb*^{b4} seem to contain almost no melanin, but the dark eyes of the RPE are an obvious contrast to the stronger *alb*^{b4} allele (Figure 1F). Finally, transheterozygous larval fish *alb*^{b4}/*alb*^{tm83a} (Figure 1J) have melanophores with slightly reduced melanin, but as an adult, the homozygous *alb*^{tm83a} allele is practically indiscernible from wild type. Figure 1 shows the pigmentation phenotype of representative alleles. Table 1 presents a summary of the *alb* alleles investigated in this study and their corresponding sequences (Figure S2A–F).

Table 1. Overview of *albino* alleles characterized in this study

Allele	Mutation type	Change	Source
alb^{b4}	Nonsense	[c.1386G>T; p. G461X]	Streisinger
alb^{ti20e}	Nonsense	[c.1270T>A; p. Y423X]	Tübingen 1996 screen
alb^{ti225}	Missense	[c.182G>A; p.G61R]	Tübingen 1996 screen
alb^{tm83a}	In-frame deletion	[c.184_186del; p. S62del]	Tübingen 1996 screen
alb^{tnr39}	Missense	[c.1545A>G; p. Q516R]	New allele
alb^{tnr52}	Deletion	[c.1244_1451del; p. Y415X]	New allele

albino Fish present reduced visual acuity

Visual acuity is highly reduced in humans afflicted with different forms of albinism, so we asked whether the visual resolution of adult *alb*^{b4}, *alb*^{tnr52}, and *alb*^{tnr39} alleles was affected when compared to a collection of different wild-type and pigment mutant fish. Previous studies have shown that the *sandy* mutant presents a specific visual phenotype with impaired light adaption ability that is fundamentally different from that of *albino*, but *sandy* also displays an erratic optokinetic response (OKR; Page-McCaw et al., 2004). The OKR is a series of stereotypic eye movements evoked by movements in the surrounding, such as a moving grate of black and white stripes (Brockerhoff et al., 1995; Mueller and Neuhauss, 2010). Visual acuity can be assessed by determining the minimal

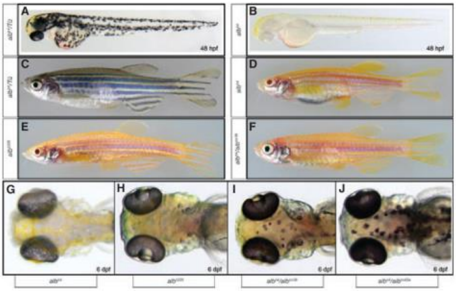

Figure 1. Neural crest–derived and retina pigment melanophores fail to pigment properly in *alb* mutants. At 48 hpf, the melanophores of the neural crest (NC) and retinal epithelium (RPE) are completely melanized in heterozygous siblings (A), whereas *alb*^{b4} fails to produce any visible melanin but developing iridophores become more obvious on the dorsal aspect of the trunk (B). The lack of melanization persists to adulthood in the mutant as compared to heterozygous siblings (C–D). *alb*^{ti225} presents as an adult an almost complete, but pale melanization (E), while the *alb*^{tnr39}/*alb*^{b4} transheterozygous adult lacks visible melanin in the body but retains noticeable amounts in the RPE (F). As a larva, *alb*^{ti225} (H) is indistinguishable from *alb*^{b4}, (G) but *alb*^{tnr39}/*alb*^{b4} larvae display lightly melanized melanophores (I). *alb*^{b4}/*alb*^{tm83a} present an almost wild-type amount of melanin (J).

© 2012 John Wiley & Sons A/S

spatial frequency of the stimulus that is able to evoke the OKR (Haug et al., 2010). We measured in an automated fashion the temporal-to-nasal OKR slow-phase velocity of the right eye of *alb*^{b4} (n = 12), *alb*^{tnr52} (n = 13), and *alb*^{tnr39} (n = 9) fish along with a collection of wild-type fish as well as the *golden* and *nacre* mutants in response to changing contrast or spatial frequency of the optokinetic stimulation (Figure 2A, D). We could not detect any difference in contrast sensitivity of *alb*^{b4}, *alb*^{tnr52}, *alb*^{tnr39}, and other fish (Figure 2E) showing that all fish are fully capable of seeing and responding to the stripe pattern (see methods). However, we were able to establish a significant difference in spatial resolution (Figure 2F) in the range from 0.2 to 0.35 cycles/degree. The average gain of *alb*^{b4} *and alb*^{tnr52} is significantly lower than that of the wild-type control group but not for *alb*^{tnr39} fish (*alb*^{b4}: $P < 0.001$). Therefore, we conclude that similar to *sandy*, visual acuity of both *alb*^{b4} and *alb*^{tnr52} fish is reduced compared to wild-type fish. While, unlike in *albino* mutants, the light adaptation phenotype of *sandy* may involve a defect in network adaptation (Page-McCaw et al., 2004), the similar OKR phenotypes of *sandy* and *albino* strengthen the case for a common root cause of the visual phenotypes of both mutants and further point to a direct link between RPE melanization and visual acuity.

albino Encodes the 12-transmembrane domain transporter SLC45A2

Through genome scanning with a set of SSLP markers (Geisler et al., 2007), we rough mapped the *alb*^{b4} locus to an interval between the markers z4492 and z4425, about 36–39 cM from the top of chromosome 21 (Figure 3A). By analyzing all annotated genes present in this genomic interval, we identified the 12-transmembrane domain transporter Slc45a2 as a probable candidate, which is also the causative disease gene of OCA4, has been implicated in human skin color variation and has been characterized as affected in the medaka *b* mutant (Fukamachi et al., 2001). The entire coding sequence localized to BAC CH211-71C16 (accession CR749169; Figure 3A). We sequenced the cDNA transcripts of *alb*^{b4} along with their wild-type siblings and identified a G to T transversion in exon 6, which leads to a premature stop codon after AA 461. Further analysis of strong alleles also revealed a nonsense mutation in *alb*^{tj20e} at AA 423 and a deletion of exon 6 in *alb*^{tnr52} causing a stop codon at AA 414 at the end of exon 5 (Figure 3A, C).

In the hypomorphic allele *alb*^{tm83a}, an in-frame deletion removing S62 was detected, as well as two missense mutations causing a G61R and a Q516R replacement, in the alleles *alb*^{ti225} and *alb*^{tnr39}, respectively. The missense mutation, *alb*^{ti225}, displays a glycine to arginine change at amino acid 61, thereby placing a much larger basic side chain directly next to a conserved serine. This mutation causes a strong phenotype, which might be explained by its interfering in interactions between the intravesicular chains that form an end of the transporter, this in turn might drastically perturb the protein's transporting function. To better visualize the location of the lesions in the various *alb* alleles, we used the known structure of the glycerol-3-phosphate transporter from *Escherichia coli*

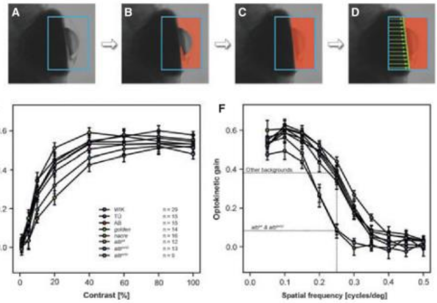

Figure 2. *alb* mutants display reduced visual ability. Schematic representation of the algorithm for detection of eye orientation (exemplified for the right eye). (A) a rectangle is drawn around the lens of the eye, (B) the area within the rectangle is thresholded to extract the brightest part, (C) the convex hull is drawn around the detected area, and (D) starting from the left side, the program searches for an approximately vertical edge, which corresponds to the rim of the right eye. In total, eight different strains were analyzed: three wild-type backgrounds WIK, TU, AB as well as homozygous mutants *nacre* (*mitfa*$^{-/-}$), *golden* (*slc24a5*$^{-/-}$), *albino*^{b4}, *albino*^{tnr52}, and *albino*^{tnr39}. Average temporal-to-nasal gain of the right eye of adult fish from the listed backgrounds measured with increasing contrast (E) and spatial frequency (F) of the optokinetic stimulation. Dotted lines emphasize the more than twofold difference in optokinetic gain between *albino* stops and other backgrounds.

© 2012 John Wiley & Sons A/S

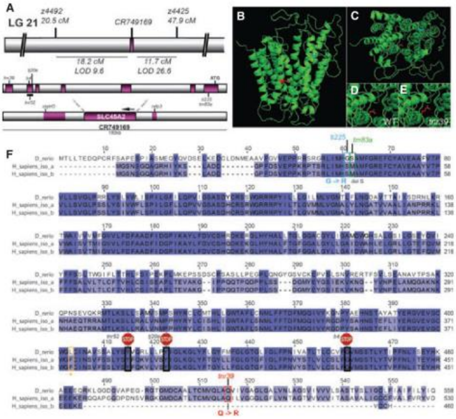

Figure 3. Mapping and positional cloning of the *alb* mutant reveal mutations in the solute carrier Slc45a2. The *alb*^{b4}, mutation was mapped to linkage group 21 using the presented microsatellite markers (above), which gave a predicted interval (below) of about 30 cM. The BAC CR74969 lies within this interval and contains all seven exons of the coding sequence of Slc45a2. Two additional transcripts, *clqtrf3* and *rxfp3*, are also contained within the BAC. The positions of the identified lesions of the *albino* mutants are displayed in reference to their positions among the exons. The deletion of exon 6 in *alb*^{tnr52} is represented by the black bar (A). The modeled 3D ribbon structure is shown in two orientations, and the missense mutations *alb*^{tnr39} (red) and *alb*^{ti225} (blue) are mapped onto the structure (B). A blow up looking through the central pore clearly displays how the side chain of R^{516}, in *alb*^{tnr39}, projects into the center of the pore (C, E) in contrast to Q^{516} in the wild type (D). The protein homology of *Danio rerio* as compared to the two known human isoforms is shown with each identified lesion mapped, respectively (F).

(1pW4_A) as a template (probability of true template 99.95%, E-value < 1.1e−24) to model the three-dimensional structure of SLC45A2 (Figure 3B). All 12-transmembrane domains fold in to form an almost pore-like structure. Interestingly, the three hypomorphic missense alleles (*alb*^{ti225}, *alb*^{tm83a}, and *alb*^{tnr39}) all show lesions in these transmembrane domains (Figure 3B, F). The position of all alleles as well as an alignment with the two known human isoforms is displayed in Figure 3F.

To further confirm that the identified lesions in *slc45a2* are causative for the *alb* phenotype, we intended to rescue the phenotype through BAC injections at the one cell stage. The entire *slc45a2* coding sequence is contained by the BAC along with two other genes, *clqtrf3* and *rxfp3*. Following injection, we identified several darkly pigmented melanophores in larval fish (Figure 4A, B). This indicates that the BAC contains the complete coding sequence of the responsible gene but also all the regulatory elements required to drive the gene's expression in the body melanophores.

Even though BAC injection was able to rescue *alb* melanophores in a mosaic fashion to a melanization level indistinguishable from wild type, there still remained at least two other complete coding sequences on the BAC. We therefore isolated and injected zebra fish *slc45a2* RNA that resulted in rescue of melanization of both melanophore and RPE by 48 hpf (Figure 4C). Next, we were interested whether human SLC45A2 RNA would also be able to rescue the zebra fish *albino* mutant. The 72 hpf larvae injected with human SLC45A2 RNA show a weak but distinguishable melanization (Figure 4D, E).

Furthermore, we then knocked down the *slc45a2* function through morpholino injection and noted a dose-dependent reduction in the melanophores' ability to pigment both RPE and NC-derived melanophores (Figure 4F–I).

Expression of *slc45a2* is restricted to melanophores

We carried out whole-mount in situ hybridization with *slc45a2* riboprobe on wild-type and *nacre* (*mitfa*$^{-/-}$) embryos at 24 and 48 hpf. In wild-type larvae, staining can be seen in the melanophores of the RPE as well as the melanophores of the migrating NC (Figure 4J, K). In *nacre* embryos, which lack all NC-derived melanophores but where the melanophores of the RPE and the other

© 2012 John Wiley & Sons A/S

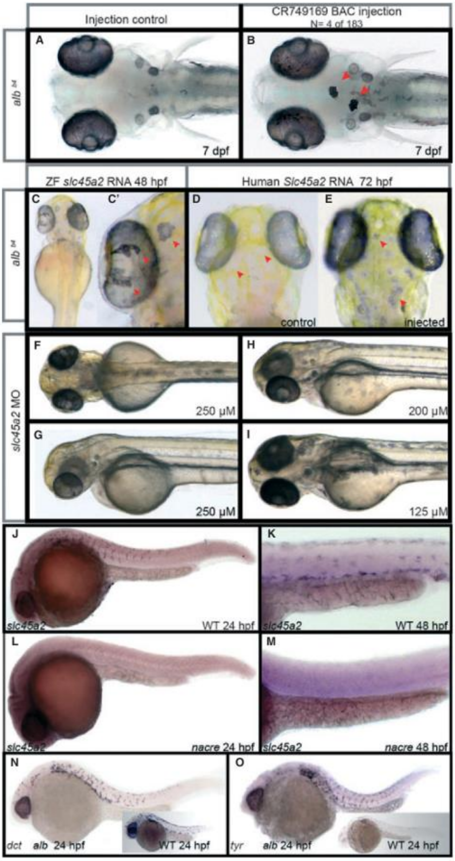
Injection control
CR749169 BAC injection
N= 4 of 183
alb b4
A
B
7 dpf
7 dpf
ZF slc45a2 RNA 48 hpf
Human Slc45a2 RNA 72 hpf
alb b4
C
C'
D
E
control
injected
slc45a2 MO
F
H
250 µM
200 µM
G
I
250 µM
125 µM
J
K
slc45a2
WT 24 hpf
slc45a2
WT 48 hpf
L
M
slc45a2
nacre 24 hpf
slc45a2
nacre 48 hpf
N
O
dct alb 24 hpf
WT 24 hpf
tyr alb 24 hpf
WT 24 hpf

Figure 4. Rescue of melanocyte melanization, morpholino knockdown, and expression of *slc45a2* and melanoblast markers in *albino* mutants. BAC CR749169 injection shows complete rescue of melanophores (red arrows) on the dorsal aspect of the head (A, B). Injection of zebra fish wild-type *slc45a2* mRNA leads to melanization of melanophores of both the neural crest and retinal epithelium (RPE; red arrows; C and C′), while mRNA injection of human *Slc45a2* leads to weak melanization (red arrows D, E). Morpholino knockdown of the *slc45a2* transcript abolishes almost all melanin synthesis at a concentration of 250 μM, shown here at two different imaging angles (F, G), but some residual pale melanophores can still be seen. At lower morpholino concentrations, the melanophore intensity increases (H, I). Expression of *slc45a2* is in cells typical of melanoblasts of the migrating neural crest (NC) and RPE at 24 hpf (J) and still remains in melanophores of PTU-treated wild-type larvae at 48 hpf (K). Expression is abolished in the *nacre* mutant at both 24 and 48 hpf in NC-derived but not in RPE melanoblasts (L–M). Melanoblasts are otherwise present in *albino* mutants as the melanoblast-specific markers *dct* and *tyr* are still expressed at similar levels as in wild type (N, O).

chromatophore types are present, the expression of *slc45a2* in the NC–derived melanophores is abolished and no other cell type of the trunk expresses *slc45a2*, whereas expression remains in the RPE (Figure 4L, M). This shows that *slc45a2* is expressed in no other NC-derived tissue.

We were unable to identify multiple isoforms of *slc45a2*, leaving the most likely explanation for the

© 2012 John Wiley & Sons A/S

separate regulation of *slc45a2* in RPE and NC melanophores to be the result of the paralogs *mitfb* and *mitfa,* respectively. It would be of interest to further investigate whether in zebra fish, the expression in these cell types is mediated by two distinct promoter sequences, as has previously been shown in medaka (Fukamachi et al., 2008; Shimada et al., 2002) .

To confirm the presence of melanoblasts in *alb*^{b4}, the expression patterns of the melanoblast markers *dct* and *tyr* were investigated by whole-mount in situ hybridization. This experiment shows that in *alb,* NC-derived melanoblasts are present and distributed normally. The presence of melanophores lacking visible pigmentation persists in fully developed fish and mutant fish exhibit the typical zebra fish striping pattern, indicating that the basic cellular differentiation of the melanophores is normal but their ability to properly synthesize melanin is impaired (Figure 4N, O). Based on these data, we conclude that the function of Slc45a2 is specific to the melanophores and cells of the RPE.

Slc45a2 is vital for melanosome function and maturation but is not required for melanosome stability

We investigated the melanosomes of *alb* mutants at the ultrastructural morphological level. We chose to analyze the melanosomes of the RPE because of its compact nature and because the packing of melanosomes around the photoreceptor membranes allowed for a robust comparison between different mutants. In 3–4 dpf wild-type larvae, the melanosomes of the RPE have formed fully pigmented stage IV vesicles, which are completely filled with dense black melanin (Figure 5A–C). When sectioned and visualized by EM, the cylinder-shaped melanosomes appear for the most part transversely cut as round circles with some small chipping to their brittle melanin resulting in white gaps.

alb^{b4} mutant RPE forms vesicles resembling melanosome stages I–II in a slightly reduced number as compared to wild type with a slightly higher amount of variability in their size. These melanosomes appear almost empty; however, a very small amount of melanin, which is predominantly localized to the central regions of the vesicle, can be detected (Figure 5A–F). This is also obtained in the analysis of another premature stop allele *alb*^{ti20e} (Figure 5I). The stage II–III melanosomes of the weak *alb*^{ti225} allele contain slightly more melanin than *alb*^{b4}, but their pigment is also pale when compared to wild type (Figure 5G). The amount of melanization of the melanosomes increases in *alb*$^{b4/tnr39}$ with the central region becoming more densely filled and smaller circular satellite positions typical of stage III melanosomes also becoming melanized (Figure 5J). The amount of melanin production continues to increase in the stage III–IV melanosomes of the weaker *alb* hypomorphs but even the melanosomes of *alb*$^{b4/tm83a}$, the weakest *alb* allelic combination, still form highly irregularly sized and shaped melanosomes with reduced melanin accumulations (Figure 5H).

We also found that the *golden* (*slc24a5*) mutant exhibits weaker melanization with reduced melanosomes as previously described (Lamason et al., 2005). However, when compared to *golden* melanosomes (Figure 5K–M), all *alb* alleles show less pigmentation and higher variability, as well as lack of the regular structural characteristics of the late stages of melanosome maturation (stage III–IV).

Formation of melanosomes is tyrosinase dependent

To compare the melanosome morphology of *albino* to a tyrosinase-negative melanosome, we also examined the zebra fish *tyrosinase* mutant *sandy.* In contrast to *golden* and *albino,* the RPE cells of *sandy* mutants fail to form stage I melanosomes as well as any obvious lysosome- or melanosome-like vesicles (Figure 5N–P). In *sandy,* the photoreceptor membranes are also not developed properly at this time point. As tyrosinase's function is dependent on copper ions (Matoba et al., 2006), the copper chelator PTU is a frequently used chemical to inhibit the melanization of melanophores. Upon ultrastructural analysis of PTU-treated fish, we found that some stage I melanosomes are present but appear to be highly irregular and seemed to be in the process of collapsing (Figure 5Q–S). The photoreceptor membranes resembled those found in *sandy* mutants. Taken together, these results indicate that the presence of a functional tyrosinase is required for the formation and/or maintenance of melanosomes.

Knockdown of V-ATPase V1H1 subunit causes lightening of melanocytes in wild type and rescues melanization in albino

The V-ATPase complex had previously been described to play a role in the development and pigmentation of the zebra fish eye but we wanted to determine whether it was directly playing a role in melanosome biogenesis (Navarro et al., 2008; Nuckels et al., 2009). First, we assessed the function of *atp6v1h* by means of morpholino knockdown in wild-type fish. The V_1H protein has been shown to play a crucial role in the catalytic activity of the proton pump but does not play a role in the V_1 assembly (Nishi and Forgac, 2002). In this way, using a morpholino knockdown of the *atp6v1h* transcript, we are able to specifically inhibit the proton pump through genetic means without having an effect on the assembly of the V_1 complex. After injection, melanocytes initially appear paler and then begin to round up by 48 hpf when compared to controls (Figure 6A, B). Knockdown of *atp6v1h* carried out in the hypomorphic *alb*^{tnr39} allele showed noticeable darkening of the melanocytes at 48 hpf as well as the rounding up phenotype also seen in wild-type background. The null allele of *albino*^{b4} did not show a noticeable increase in melanin at 48 hpf (data not shown), but there was an obvious increase in melaniza-

© 2012 John Wiley & Sons A/S

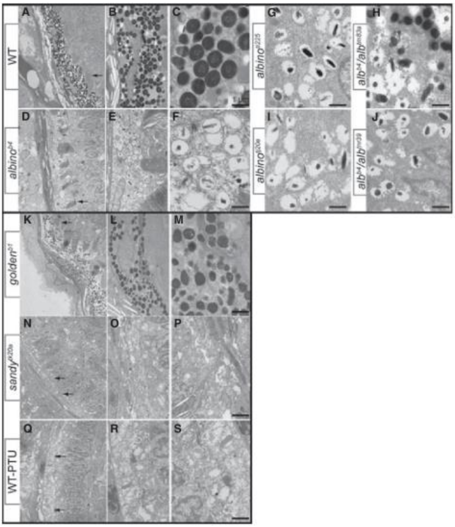

Figure 5. Melanosome ultrastructure reveals melanosomes of normal size and shape but dramatically reduced melanization in *alb* mutants. The melanosomes of the retinal epithelium (RPE) were investigated at 3.5 dpf on the ultrastructural level (A–S). Wild-type melanosomes of the RPE are tightly packed around the developing photoreceptor membranes and filled with dark electron dense melanin (A–C). The melanosomes of the alb^{b4} mutant are present in normal size and number but lack almost all melanin (D–F), and the photoreceptor membranes are of normal nature (arrows). Other *albino* alleles show varying degrees of melanin inside their melanosomes (G–J). For comparison, the *golden* mutant displays melanosomes of diminished melanin content (K–M). The *sandy* mutant completely lacks melanosomes and presents only very few vesicle-like structures (N–P) with abnormal developing photoreceptor membranes (arrows). The *sandy* phenotype is phenocopied through PTU treatment with some premelanosome-like vesicles (star; Q–S).

tion by 4 dpf when compared to injected controls (Figure 6E–H). By specifically knocking down the *atp6v1h* subunit, we show that it is possible to rescue the melanin producing capacity of both *albino* hypomorphs and null mutants.

V-ATPase inhibition through bafilomycin rescues melanization in albino mutants

To further confirm that the rescue of *albino* melanin production was specifically due to only the inactivation of the V_1 proton pump portion of the V-ATPase complex, we inhibited the pump through use of bafilomycin. Melanosomes are lysosome-related vesicles and are acidified through the activity of V-ATPases. These organelle acidifiers can be selectively inhibited through the application of bafilomycin that has previously been shown for zebra fish lysosomes (Peri and Nüsslein-Volhard, 2008) to increase the vesicle pH of their targets (Smith et al., 2004). We applied bafilomycin to 24 hpf developing alb^{b4} embryos over night at 25°C and found a dramatic melanization of both the NC-derived melanophores as well as the RPE (Figure 6J). Ultrastructural analysis of bafilomycin-treated embryos shows that the darkening seen in these embryos is indeed directly due to the increase in melanin within the melanosomes (Figure 6K). Therefore, we conclude that the melanosomes of *albino* fish are capable of producing melanin but lack the proper pH to do so. This suggests that the function of Slc45a2 is required for the expulsion of protons from the melanosomes in agreement with its previously proposed role as a proton exchanger. By increasing the pH of the melanosome, we suggest that the optimal pH of tyrosinase is approached and melanin production is resumed.

Discussion

The genetics of pigmentation and furthermore skin and coat color variation are highly complex and often involve multiple loci. A number of polymorphisms in the tyrosinase gene have been identified in humans but have failed to be convincingly associated with specific skin color variants. In recent years, the variation in human skin color has been shown to be tightly associated with the solute carriers SLC24A5 and SLC45A2. In the case of Slc45a2, the amino acid variation L374F can be found almost solely in people of European decent, while another polymorphism, E272K is more predominant in Japanese and Chinese populations. Positional cloning of the zebra fish

© 2012 John Wiley & Sons A/S

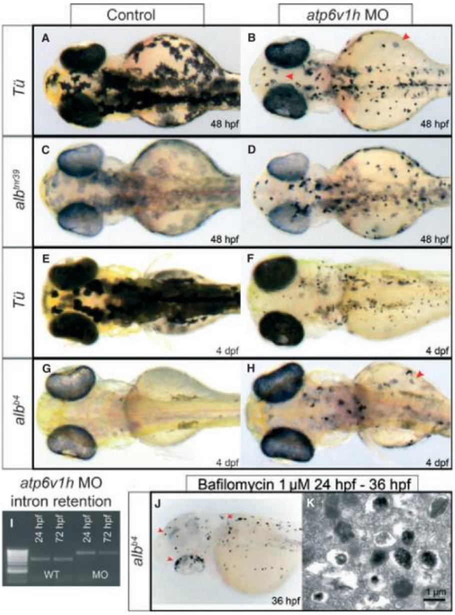

Figure 6. Knockdown or inhibition of V-ATPase complex causes rescue of *albino* melanization. Morpholino knockdown of *atp6v1h* was carried out in *Tü*, *alb*^{tnr39}, and *alb*^{b4} alleles and compared to injected controls. At 48 hpf, injected Tü fish have lighter melanocytes (arrowhead) that eventually round up and appear as small dots (A, B). The *alb*^{tnr39} shows a darkening of the melanocytes at 48 hpf as well as the rounding up seen in wild-type morphants (C, D). *atp6v1h* morphant phenotype persists at 4 dpf in wild-type larvae (E, F), and a noticeable darkening of melanocytes in the *alb*^{b4} morphant larvae can also be detected (arrowhead) before the rounding up of the melanocytes (G, H). *atpv1h1* morpholino specificity is demonstrated via intron retention at both 24 and 72 hpf. Treatment with bafilomycin at 24 hpf causes a dramatic increase in melanin in melanophores of both the body as well as the retinal epithelium (arrowheads) (H). Ultrastructural analysis of bafilomycin-treated embryos shows an increase in the content of melanin, which is found localized to the interior of the melanosomes (K).

golden mutant revealed the affected gene to encode the potassium-dependent sodium–calcium exchanger SLC24A5, leading to a reduction in melanosome size, number, and melanin density.

Here, we present evidence that a second solute carrier previously implicated in skin color variation, *slc45a2*, is the causative gene for the zebra fish *albino* phenotype. Three alleles exhibiting a premature stop codon (i.e. *alb*^{b4}, *alb*^{tj20e}, *alb*^{tnr52}) consistently show phenotypes that are indistinguishable from one another both as living fish and upon evaluation of the ultrastructural morphology of their melanosomes. *alb* nonsense alleles present a reduction in melanin density of the melanosomes themselves where the melanosomes of these *alb* alleles are highly similar to stage I melanosomes. Both also retain the ability to produce melanin albeit in the case of the *alb* stop alleles at very low levels.

This is in contrast to the more or less complete lack of melanosomes that we have observed in the tyrosinase mutant *sandy*. Furthermore, after treatment with PTU, which chelates copper ions required for the proper folding of tyrosinase protein, we also observe a similar drastic reduction in melanosomes. Taken together, this indicates that the formation and/or stability of the melanosomes is dependent on the transmembrane tyrosinase's presence but probably not on its function. The *sandy* mutant has been described to have a delayed ability to adapt to bright light when challenged with long periods of darkness during the day (Page-McCaw et al., 2004). This failure was thought to be localized to the retinal neural network, postsynaptic to the photoreceptors. Our ultrastructural analysis of *sandy* has shown an almost complete lack of melanosomes or vesicle-like structures in the RPE as well as improperly developed photoreceptor membranes. It has been proposed that L-DOPA, which is normally localized in the melanosomes, is also secreted from the RPE and is further processed to dopamine and acts in a paracrine fashion along with melatonin to modulate light

© 2012 John Wiley & Sons A/S

adaptation, providing a mechanism for the effect of *sandy*. Our observations suggest morphological changes in the RPE as an alternative mechanism that may at least contribute to this effect.

Through our analysis of various alleles, we show that modification of Slc45a2 can cause an intermediate reduction in melanosome melanization. The *alb*$^{b4/tnr39}$ allele replaces a glycine with a much larger and positively charged arginine, which based on structural predictions, projects into the channel. This extended side chain could then be in a position to inhibit the passage of the transporter's normal substrate.

V-ATPases are made up of two major subunits the V_1 and the V_0, which can be coupled and decoupled from each other. The V_0 is initially found in the vesicle membrane along with the associated protein AP1 where it plays a role in the sorting and fusing of vesicles. At a downstream time point, the V_1 can be coupled to the V_0 turning the entire complex into an ATP-dependent proton pump (Figure 7A). By means of our *atp6v1h1* knockdown, we also show that the V-ATPase is specifically responsible for the acidification of melanosomes and by means of rescue of the *albino* phenotype interaction with *slc45a2*. The *catastrophe* mutant, caused by mutations at the *atp6vo0d1* locus, has previously been shown to have significant ultrastructural melanosomal defects as well as to also be particularly sensitive to copper deprivation (Madsen and Gitlin, 2008).

The function of Slc45a2 has been proposed to be linked to the production of melanin in either of two different roles: first, the proper trafficking and sorting of tyrosinase to the melanosome, and second, the maintenance of a specific pH within the melanosomes themselves (Graf et al., 2005; Lucotte et al., 2010). Our findings support the second possibility.

The differentiation of melanosomes may require a dynamic range of pH and ionic conditions at different time points. Initially, a low pH may be required for the proper sorting required to form stage I melanosomes. As the melanosomes mature, a change in the pH and ionic conditions may be required in order for the optimal activity of tyrosinase to be achieved (Figure 7B). We have observed that the melanosomes of all *albino* alleles have in principle a normal structure, making a role for Slc45A2 in membrane trafficking less likely, but with varying degrees of hypopigmentation. Also, Konantz et al. (in preparation) have shown that Slc45a2 is specifically localized to the melanosomes. The activity of tyrosinase is known to be dependent on the secretion of H^+ from the melanosomes, so that varying the internal pH of the vesicle would have a direct effect on enzymatic activity. While the optimal pH of tyrosinase is 7.3, an acidic environment would render it almost inactive (Smith et al., 2004). It has been demonstrated that the activity of tyrosinase of light-colored melanocytes can be increased through the application of compounds such as bafilomycin, which block the activity of the organelle acidifier, V-ATPase, thereby raising the pH of the melanosomes (Smith et al., 2004). We show that increasing the pH of the melanosome through the use of bafilomycin or through knockdown of *atp6v1h* partially rescues the *albino* phenotype, suggesting that the functional role of Slc45a2 is related to the maintenance of melanosome pH. The Na^+/H^+ exchanger Slc45a2 removes H^+ from the melanosome by exchange with Na^+, which is then cycled back out of the melanosome by the cation exchanger Slc24a5 (Figure 7C). In this way, Slc45a2 plays a crucial role in the pH and ionic homeostasis within the melanosome. Our ultrastructural analysis of both *sandy*- and PTU-treated embryos highlights the importance of both

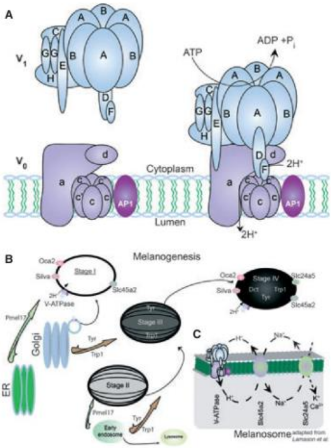

Figure 7. An overview of V-ATPase V_1, V_0 coupling, and melanosomal homeostasis. Initially, the V_0 subunit of the V-ATPase is found in the vesicle membrane where it plays a role in vesicle fusions and sorting. At a later point in vesicle maturation, it can reversibly bind the V_1 subunit. Together, both subunits form the complete V-ATPase complex capable of ATP-dependent proton pumping across the membrane (A). Melanosomes are thought to arise either directly from the ER itself or through a more complex post-Golgi, endocytic route. The maturing melanosomes are continually fused with vesicles as they pass stage I and stage II premelanosomes and begin to display the characteristic Pmel17 fibrils. As tyrosinase and Tyrp1 are added and becomes active in stage III melanosomes, the production of melanin is commenced until a fully mature and black granule is formed (B). Maintenance of ionic and pH conditions can be achieved through epistatic interactions on the melanosome membrane. By acting as a Na^+/H^+ exchanger, Slc45a2 plays both a role in maintaining the proper Ca^{2+} flux passing through Slc24a5 and in maintaining an optimal pH for the activity of tyrosinase (C).

© 2012 John Wiley & Sons A/S

tryosinase and the copper that it requires to fold properly in melanosomal integrity. A reduction in the efficiency of Slc45a2 as an exchanger as seen in the *albino*^{tnr39} allele is expected to have a quenching effect on the activity of tyrosinase. At the same time, the integrity of the melanosomes is maintained in *albino* mutants avoiding the toxic effects of their disruption seen in *sandy* mutants. In this way, the activity of tyrosinase can be controlled and stabilized within the melanosomes in large part through the function of SLC45A2, which mediates the melanosome pH. A similar effect may be postulated for the European and African variants of the human Slc45a2 ortholog, providing a molecular basis for human skin color variation.

Methods

Zebra fish husbandry

Zebra fish were maintained as described (Nüsslein-Volhard, 2002).

Adult OKR

Optokinetic response of adult *alb*^{b4}, *alb*^{tnr52}, *alb*^{tnr39}, and other backgrounds zebra fish was measured as previously described (Mueller and Neuhauss, 2010). To enable automatic detection of the orientation of the unpigmented *alb*^{b4} eyes, the algorithm of the software had to be slightly modified (Figure 2). In addition, we used the projector (PLV-Z3000, SANYO Electric Co. Ltd., Osaka, Japan) to achieve better black values, higher contrast, and higher spatial resolution.

We measured temporal-to-nasal OKR slow-phase velocity of the right eye of adult fish in response to changing contrast or spatial frequency of the optokinetic stimulation. Angular velocity of the stimulation was left constant at 12 degree/s. In case of changing contrast, spatial frequency was held constant at 0.1 cycles/degree, and in case of changing spatial frequency, contrast was held constant at 70%.

Statistical analysis was performed using PASW Statistics 18 (SPSS Inc., Chicago, IL, USA). We used repeated measures ANOVAS with the contrast (repeated measures ANOVA, $F_{2,34} = 0.741$, $P = 0.484$) or the spatial frequency as within-subjects effect and the genotype as between-subjects effect (repeated measures ANOVA, $F_{2,34} = 4.840$, $P = 0.014$). Where appropriate, Dunnett's one-tailed post hoc test was used to compare the means of *alb*^{b4} and *alb*^{tnr39} fish against the wild-type control group (WIK).

Mapping and cloning of albino

Mapping of *albino* was carried out as described in Geisler et al. (2007). To validate candidate genes, total RNA was prepared from both wild-type and mutant embryos or clipped fins using TRIzol Reagent (Invitrogen, Darmstadt, Germany) with an added chloroform extraction before precipitation. For separation of phases, phase lock tubes (PLG 1.5 ml Heavy; Eppendorf, Hamburg, Germany) were used according to the manufacturer's protocol. Reverse transcription was performed using total RNA, oligo(dT) primer, and Superscript III reverse transcriptase (Invitrogen) according to standard procedures.

3D modeling using HHPRED

3D modeling was performed using HHPRED (http://toolkit.tuebingen.mpg.de/hhpred) with standard parameters. Briefly, eight iterations of PSI-BLAST were performed using the amino acid sequence of SLC45A2 from *Danio rerio* from the pdb70_24Apr10 database. A local alignment mode was used, and secondary structure was scored. The highest score was found for glycerol-3-phosphate transporter from *E. coli* (1pW4_A). This structure was used as a template for the 3D modeling. The model was visualized with MacPyMol (The PyMOL Molecular Graphics System, Schrödinger, LLC, New York, NY, USA).

Allele screen

Mutagenesis was performed as described before (Mullins et al., 1994) with the addition of clove oil to minimize stress (Rohner, unpublished). Mutagenesis was performed every week for a total of five times. Female albb4 were then crossed to ENU-treated males, and their progeny were then screened at 72 h for albino-like phenotypes. Those larvae were segregated, raised to adults, and then genotyped based on cDNA.

Morpholino injection

The antisense morpholinos for *slc45a2* and *atp6v1h* are both ATG morpholinos and were obtained from Gene Tools with the following sequences: *slc45a2*_atg:GCTGGTCCTCAGTAAGAAGAGTCAT and *atp6v1h*_atg:ATATTTAAGGAGCTGCTTCCTCTGC as well as the intron retention morpholino *atp6v1h1*_2ret3:CGGGAAGAATGCAATATTAACCTGA. *atp6v1h1* knockdowns were primarily carried out using the *atp6v1h1_atg* morpholino, but all experiments were also repeated using the *atpv1h1_2ret3* morpholino to demonstrate transcript specificity.

BAC injection

The BAC CH211-71C16 (CR749169) was purified using the Large–Construct Kit (QIAGEN, Hilden, Germany) according to manufacturer's instructions and then injected into the one cell stage at a concentration of 20 ng/μl.

RNA rescue

The zebra fish *slc45a2* cDNA sequence BC154627 was used as a reference to design the following oligos: SLC(zeb)f1 5′-TCT TAC CAT CCA GAA CCA TGA CT-3′ and SLC(zeb)r1 5′-TTG AGG CTT ATT CTG TAC ATC ACA T-3′. The product was ligated into the pCS2^{+} vector. The resulting plasmid was verified by sequencing and was then linearized using NotI, and mRNA was produced using the mMESSAGE mMACHINE® SP6 Kit (Ambion, Kaufungen, Germany). Injections were carried out at the one cell stage at a concentration of 400 ng/μl. Rescue using the human RNA was performed exactly as above but with the following oligos for cloning: SLC(hum)f1-ACG TCA AAT CCA GTT TGA AAC AC and SLC(hum)r1-TCT GAG GTT AGG GTC ATT GTC TC.

In situ hybridization

An RT-PCR-based approach was used to generate probes for in situ hybridization. The PCR was carried out using an antisense primer, containing a T7 promoter sequence on its 5′-end. The PCR product then included the target sequence flanked by the T7 promoter sequence, so that an RNA riboprobe could be synthesized by in vitro transcription of the PCR product using the T7-RNA polymerase (Fermentas). The DNA oligos that were used are as follows: Slc45A2: 5′-tgtttggaagggaattctgc-3′ and 5′-TAATACGACTCACTATAGGcactccaaacatcaccacca-3′ along with 5′-cactccaaacatcaccacca-3′ and 5′-TAATACGACTCACTATAGGtgtttggaagggaattctgc-3′, which allows for the creation of both sense and antisense riboprobes. The *tyr* and *dct* riboprobes were generated using the following oligos: tyr-for-T7: 5′-TAATACGACTCACTATAGGGAGATGGTTTTGGCCAGATTTAGG-3′ tyr-rev: 5′-CAGCTCCTCAGCTCGTCTCT-3′; dct-for-T7: 5′-TAATACGACTCACTATAGGGAGAACATAGCCGGTCTGTTGTCC-3′ dct-rev: 5′-

© 2012 John Wiley & Sons A/S

ACTTCTTCGTCTGGCAGCAT-3′, respectively. Whole-mount in situ hybridization was carried out as previously described (Nüsslein-Volhard, 2002).

Ultrastructure analysis of melanosomes

For ultrastructural analysis by transmission electron microscopy (TEM), larvae were fixed in 4% formaldehyde and 2.5% glutaraldehyde in PBS (pH 7.2) at 4°C overnight. After postfixation with 1% osmium tetroxide, samples were rinsed with water, block stained with 1% uranyl acetate for 1 h on ice, dehydrated in a graded series of ethanol, infiltrated with Epon, and polymerized at 60°C for 48 h. Ultrathin sections stained with uranyl acetate and lead citrate were viewed in a Philips CM10 electron microscope at 60 kV. In addition, toluidine blue–stained Epon sections of 0.5 or 3 μm thickness were prepared for light microscopy.

Bafilomycin treatment

Bafilomycin was dissolved in DMSO according to Peri and Nüsslein-Volhard (2008) and was then applied to embryos in final concentrations ranging from 0.1 μM to 1 mM at 16, 24, 28, and 32 hpf overnight at 25°C to find the most effective condition, which was determined to be 1 μM applied at 16 hpf over night at 25°C.

Acknowledgements

C.D. and R.G. would like to acknowledge Ines Gehring for technical assistance as well as Simon Perathoner and Nicolas Rohner for providing mutagenized fish and Matthew Harris and Mitch Levesque for many enlightening discussions. The authors would also like to thank an anonymous reviewer for helpful comments on this manuscript. This work was supported by the European Commission's 6th Framework Programme (ZF-MODELS project, contract no. LSHG-CT-2003-503496) and 7th Framework Programme (ZF-HEALTH project, grant agreement HEALTH-F4-2010-242048).

Author contribution

C.D. conceived and designed the experiments. C.D., H.S., K.M., A. M., and M.K. performed the experiments. C.D., C.N.V., and R.G. analyzed the data. S.N. contributed reagents/materials/analysis tools. C.D., C.N.V., and R.G. wrote the manuscript.

References

Braasch, I., Schartl, M., and Volff, J.-N. (2007). Evolution of pigment synthesis pathways by gene and genome duplication in fish. BMC Evol. Biol. *7*, 74.

Brockerhoff, S.E., Hurley, J.B., Janssen-Bienhold, U., Neuhauss, S. C., Driever, W., and Dowling, J.E. (1995). A behavioral screen for isolating zebrafish mutants with visual system defects. Proc. Natl Acad. Sci. USA *92*, 10545–10549.

Dell'Angelica, E.C. (2003). Melanosome biogenesis: shedding light on the origin of an obscure organelle. Trends Cell Biol. *13*, 503–506.

Du, J., and Fisher, D.E. (2002). Identification of Aim-1 as the underwhite mouse mutant and its transcriptional regulation by MITF. J. Biol. Chem. *277*, 402–406.

Fernandez, L.P., Milne, R.L., Pita, G., Aviles, J.A., Lazaro, P., Benitez, J., and Ribas, G. (2008). SLC45A2: A novel malignant melanoma-associated gene. Hum. Mutat. *29*, 1161–1167.

Fukamachi, S., Shimada, A., and Shima, A. (2001). Mutations in the gene encoding B, a novel transporter protein, reduce melanin content in medaka. Nat. Genet. *28*, 381–385.

Fukamachi, S., Kinoshita, M., Tsujimura, T., Shimada, A., Oda, S., Shima, A., Meyer, A., Kawamura, S., and Mitani, H. (2008). Rescue from oculocutaneous albinism type 4 using medaka slc45a2 cDNA driven by its own promoter. Genetics *178*, 761–769.

Geisler, R., Rauch, G.-J., Geiger-Rudolph, S. et al. (2007). Large-scale mapping of mutations affecting zebrafish development. BMC Genomics *8*, 11.

Gentleman, R.C., Carey, V.J., Bates, D.M. et al. (2004). Bioconductor: open software development for computational biology and bioinformatics. Genome Biol. *5*, R80.

Graf, J., Hodgson, R., and van Daal, A. (2005). Single nucleotide polymorphisms in the MATP gene are associated with normal human pigmentation variation. Hum. Mutat. *25*, 278–284.

Graf, J., Voisey, J., Hughes, I., and van Daal, A. (2007). Promoter polymorphisms in the MATP (SLC45A2) gene are associated with normal human skin color variation. Hum. Mutat. *28*, 710–717.

Haffter, P., Odenthal, J., Mullins, M. et al. (1996). Mutations affecting pigmentation and shape of the adult zebrafish. Dev. Genes. Evol. *206*, 260–276.

Haug, M.F., Biehlmaier, O., Mueller, K.P., and Neuhauss, S.C. (2010). Visual acuity in larval zebrafish: behavior and histology. Front. Zool. *7*, 8.

He, L., Vasiliou, K., and Nebert, D.W. (2009). Analysis and update of the human solute carrier (SLC) gene superfamily. Hum. Genomics *3*, 195–206.

Hirata, M., Nakamura, K.-I., Kanemaru, T., Shibata, Y., and Kondo, S. (2003). Pigment cell organization in the hypodermis of zebrafish. Dev. Dyn. *227*, 497–503.

Kelsh, R.N., Brand, M., Jiang, Y.J. et al. (1996). Zebrafish pigmentation mutations and the processes of neural crest development. Development *123*, 369–389.

Lamason, R.L., Mohideen, M.-A.P.K., Mest, J.R. et al. (2005). SLC24A5, a putative cation exchanger, affects pigmentation in zebrafish and humans. Science *310*, 1782–1786.

Lister, J.A. (2002). Development of pigment cells in the zebrafish embryo. Microsc. Res. Tech. *58*, 435–441.

Lister, J.A., Robertson, C.P., Lepage, T., Johnson, S.L., and Raible, D.W. (1999). nacre encodes a zebrafish microphthalmia-related protein that regulates neural-crest-derived pigment cell fate. Development *126*, 3757–3767.

Lucotte, G., Mercier, G., Diéterlen, F., and Yuasa, I. (2010). A decreasing gradient of 374F allele frequencies in the skin pigmentation gene SLC45A2, from the north of West Europe to North Africa. Biochem. Genet. *48*, 26–33.

Madsen, E.C., and Gitlin, J.D. (2008). Zebrafish mutants calamity and catastrophe define critical pathways of gene-nutrient interactions in developmental copper metabolism. PLoS Genet. *4*, e1000261.

Matoba, Y., Kumagai, T., Yamamoto, A., Yoshitsu, H., and Sugiyama, M. (2006). Crystallographic evidence that the dinuclear copper center of tyrosinase is flexible during catalysis. J. Biol. Chem. *281*, 8981–8990.

Mueller, K.P., and Neuhauss, S.C.F. (2010). Quantitative measurements of the optokinetic response in adult fish. J. Neurosci. Methods *186*, 29–34.

Mullins, M., Hammerschmidt, M., Haffter, P., and NussleinVolhard, C. (1994). Large-scale mutagenesis in the zebrafish – in search of genes-controlling development in a vertebrate. Curr. Biol. *4*, 189–202.

Navarro, R.E., Ramos-Balderas, J.L., Guerrero, I., Pelcastre, V., and Maldonado, E. (2008). Pigment dilution mutants from fish models with connection to lysosome-related organelles and vesicular traffic genes. Zebrafish *5*, 309–318.

Newton, J.M., Cohen-Barak, O., Hagiwara, N., Gardner, J.M., Davisson, M.T., King, R.A., and Brilliant, M.H. (2001). Mutations

© 2012 John Wiley & Sons A/S

in the human orthologue of the mouse underwhite gene (uw) underlie a new form of oculocutaneous albinism, OCA4. Am. J. Hum. Genet. *69*, 981–988.

Nishi, T., and Forgac, M. (2002). The vacuolar (H+)-ATPases–nature's most versatile proton pumps. Nat. Rev. Mol. Cell Biol. *3*, 94–103.

Nuckels, R.J., Ng, A., Darland, T., and Gross, J.M. (2009). The vacuolar-ATPase complex regulates retinoblast proliferation and survival, photoreceptor morphogenesis, and pigmentation in the zebrafish eye. Invest. Ophthalmol. Vis. Sci. *50*, 893–905.

Nüsslein-Volhard, C., and Dahm, R. (2002). Zebrafish: A Practical Approach. (New York: Oxford University Press).

Page-McCaw, P.S., Chung, S.C., Muto, A., Roeser, T., Staub, W., Finger-Baier, K.C., Korenbrot, J.I., and Baier, H. (2004). Retinal network adaptation to bright light requires tyrosinase. Nat. Neurosci. *7*, 1329–1336.

Peri, F., and Nüsslein-Volhard, C. (2008). Live imaging of neuronal degradation by microglia reveals a role for v0-ATPase a1 in phagosomal fusion in vivo. Cell *133*, 916–927.

Raposo, G., and Marks, M.S. (2007). Melanosomes–dark organelles enlighten endosomal membrane transport. Nat. Rev. Mol. Cell Biol. *8*, 786–797.

Rees, J.L. (2003). Genetics of hair and skin color. Annu. Rev. Genet. *37*, 67–90.

Reischauer, S., Levesque, M.P., Nusslein-Volhard, C., and Sonawane, M. (2009). Lgl2 executes its function as a tumor suppressor by regulating ErbB signaling in the zebrafish epidermis. PLoS Genet. *5*, e1000720.

Sabeti, P.C., Varilly, P., Fry, B. et al. (2007). Genome-wide detection and characterization of positive selection in human populations. Nature *449*, 913–918.

Shimada, A., Fukamachi, S., Wakamatsu, Y., Ozato, K., and Shima, A. (2002). Induction and characterization of mutations at the b locus of the medaka, Oryzias latipes. Zool. Sci. *19*, 411–417.

Smith, D.R., Spaulding, D.T., Glenn, H.M., and Fuller, B.B. (2004). The relationship between Na(+)/H(+) exchanger expression and tyrosinase activity in human melanocytes. Exp. Cell Res. *298*, 521–534.

Streisinger, G., Singer, F., Walker, C., Knauber, D., and Dower, N. (1986). Segregation analyses and gene-centromere distances in zebrafish. Genetics *112*, 311–319.

Sturm, R.A., Teasdale, R.D., and Box, N.F. (2001). Human pigmentation genes: identification, structure and consequences of polymorphic variation. Gene *277*, 49–62.

Summers, C.G. (1996). Vision in albinism. Trans. Am. Ophthalmol. Soc. *94*, 1095–1155.

Supporting information

Additional Supporting Information may be found in the online version of this article:

Figure S1. Comparison of the phenotype of alb^{b4}/alb^{tm83a} transheterozygotes (A) and in late juveniles (12 mm) (B) with the phenotype of alb^{tm83a} homozygotes (C–D). In addition the adult alb^{tnr52} is shown (E).

Figure S2. Sequencing traces of all presented allele are presented here (A–F).

© 2012 John Wiley & Sons A/S

Concluding remarks 4

Vertebrates have evolved key innovations compared to more basal protochordates including an increased numbers of genes through genome duplications, a more complex head and brain, cartilage and bone, ectodermal placodes and the neural crest. It has been proposed by Gans and Northcutt (Gans and Northcutt, 1983) that these features enabled early vertebrate ancestors to move beyond filter feeding and to adapt to a more active lifestyle. The question of how the neural crest itself evolved remains a highly debated topic, although recently some exciting results have been brought forth from *Ciona intestinalis*, a non-vertebrate chordate (Abitua, 2012). *Ciona intestinalis* possesses a cephalic melanocyte lineage, very similar to neural crest-derived melanocytes. When *Twist* is ectopically expressed in these cells using a *Mitf* promoter, melanocytes can be reprogrammed and become migrating ectomesenchyme. If these interpretations hold to be true, this would mean that the melanocyte gene regulatory network predates the evolution of the neural crest, making melanocytes the first neural crest cells.

Directly from their birth at the ridges of the dorsal neural tube, neural crest cells display an intimate association with neuronal tissue. They use primary motor axons as migratory paths and establish residences as part of the dorsal root ganglia. During metamorphosis or upon melanophore ablation, the melanophore progenitors are activated deep in the body and begin migrating towards distant tissues. *How do they know when to become active and where to migrate to?* One could imagine an intriguing scenario where the spinal nerves play an important role in communicating with pigment cells of the periphery back to stem cells residing in the dorsal root ganglia. The role of long range signaling molecules such as hormones can also not be ruled out, or some yet undefined signaling system.

Melanocytes play a major role in vertebrate natural variation. As humans we place great value in skin, hair and eye color, unfortunately at times also with negative intentions. The white tiger, which has recently been shown to harbor mutations in *SLC45A2* but is considered by some to be a natural variant, it is an interesting case of variation versus genetic defect (Xu et al., 2013). Mutations in *SLC45A2* in both humans and fish lead to decreased visual acuity. Although Xu et al. did not test the vision of the white tigers, as this would be understandably difficult and most likely traumatizing for these big cats, a cost of their beautiful white fur is possibly a reduction in their sight.

By following melanophores from their developmental birthplace to their final destination as members of intricate stripes along the flanks of the zebrafish, it has been possible to gain further insight into their ontogenetic paths and the factors required for them to reach their destination.

Bibliography

Abitua, P. B. W., Eileen; Navarrete, Ignacio A.; Levine, Michael 2012. Identification of a rudimentary neural crest in a non-vertebrate chordate. *Nature,* 492, 3.

Adameyko, I., Lallemend, F., Aquino, J. B., Pereira, J. A., Topilko, P., Müller, T., Fritz, N., Beljajeva, A., Mochii, M., Liste, I., Usoskin, D., Suter, U., Birchmeier, C. & Ernfors, P. 2009. Schwann cell precursors from nerve innervation are a cellular origin of melanocytes in skin. *Cell,* 139, 366-79.

Akiyama, H., Chaboissier, M.-C., Martin, J. F., Schedl, A. & de Crombrugghe, B. 2002. The transcription factor Sox9 has essential roles in successive steps of the chondrocyte differentiation pathway and is required for expression of Sox5 and Sox6. *Genes & Development,* 16, 2813-2828.

Alfandari, D., Cousin, H., Gaultier, A., Smith, K., White, J. M., Darribère, T. & DeSimone, D. W. 2001. Xenopus ADAM 13 is a metalloprotease required for cranial neural crest-cell migration. *Current Biology,* 11, 918-930.

Bang, A. G., Papalopulu, N., Kintner, C. & Goulding, M. D. 1997. Expression of Pax-3 is initiated in the early neural plate by posteriorizing signals produced by the organizer and by posterior non-axial mesoderm. *Development,* 124, 2075-2085.

Bonanomi, D. & Pfaff, S. L. 2010. Motor axon pathfinding. *Cold Spring Harb Perspect Biol,* 2, a001735.

Britsch, S., Goerich, D. E., Riethmacher, D., Peirano, R. I., Rossner, M., Nave, K.-A., Birchmeier, C. & Wegner, M. 2001. The transcription factor Sox10 is a key regulator of peripheral glial development. *Genes & Development,* 15, 66-78.

Bronner-Fraser, M. & Fraser, S. 1989. Developmental potential of avian trunk neural crest cells in situ. *Neuron,* 3, 755-766.

Bronner-Fraser M, F. S. 1988. Cell lineage analysis reveals multipotency of some avian neural crest cells. *Nature,* 335, 3.

Budi, E. H., Patterson, L. B. & Parichy, D. M. 2008. Embryonic requirements for ErbB signaling in neural crest development and adult pigment pattern formation. *Development,* 135, 2603-14.

Budi, E. H., Patterson, L. B. & Parichy, D. M. 2011. Post-embryonic nerve-associated precursors to adult pigment cells: genetic requirements and dynamics of morphogenesis and differentiation. *PLoS Genet,* 7, e1002044.

Cornell, R. A. & Eisen, J. S. 2000. Delta signaling mediates segregation of neural crest and spinal sensory neurons from zebrafish lateral neural plate. *Development,* 127, 2873-2882.

Curran, K., Lister, J. A., Kunkel, G. R., Prendergast, A., Parichy, D. M. & Raible, D. W. 2010. Interplay between Foxd3 and Mitf regulates cell fate plasticity in the zebrafish neural crest. *Dev Biol,* 344, 107-18.

Curran, K., Raible, D. W. & Lister, J. A. 2009. Foxd3 controls melanophore specification in the zebrafish neural crest by regulation of Mitf. *Dev Biol,* 332, 408-17.

Deardorff, M. A., Tan, C., Saint-Jeannet, J.-P. & Klein, P. S. 2001. A role for frizzled 3 in neural crest development. *Development,* 128, 3655-3663.

Dottori, M., Gross, M. K., Labosky, P. & Goulding, M. 2001. The winged-helix transcription factor Foxd3 suppresses interneuron differentiation and promotes neural crest cell fate. *Development,* 128, 4127-4138.

Dupin, E., Creuzet, S. & Douarin, N. 2006. The Contribution of the Neural Crest to the Vertebrate Body. *In:*

SAINT-JEANNET, J.-P. (ed.) *Neural Crest Induction and Differentiation.* Springer US.

Dutton, K. A., Pauliny, A., Lopes, S. S., Elworthy, S., Carney, T. J., Rauch, J., Geisler, R., Haffter, P. & Kelsh, R. N. 2001. Zebrafish colourless encodes sox10 and specifies non-ectomesenchymal neural crest fates. *Development,* 128**,** 4113-25.

Edery, P. A., Tania; Amiel, Jeanne; Pelet, Anna; Eng, Charis; Hofstra, Robert M.W.; Martelli, Helene; Bidaud, Christelle; Munnich, Arnold; Lyonnet, Stanislas 1996. Mutation of the endothelin-3 gene in the Waardenburg-Hirschsprung disease (Shah-Waardenburg syndrome). *Nat Genet,* 12**,** 2.

Erickson, C. A., Duong, T. D. & Tosney, K. W. 1992. Descriptive and experimental analysis of the dispersion of neural crest cells along the dorsolateral path and their entry into ectoderm in the chick embryo. *Developmental Biology,* 151**,** 251-272.

Gans, C. & Northcutt, R. G. 1983. Neural Crest and the Origin of Vertebrates: A New Head. *Science,* 220**,** 268-273.

Garcí a-Castro, M. n. I., Marcelle, C. & Bronner-Fraser, M. 2002. Ectodermal Wnt Function as a Neural Crest Inducer. *Science,* 297**,** 848-851.

Goodman, C. S. & Shatz, C. J. 1993. Developmental mechanisms that generate precise patterns of neuronal connectivity. *Cell,* 72, Supplement**,** 77-98.

Hall, B. 1999. *The neural crest in development and evolution.,* Berlin, Springer.

His, W. 1868. *Untersuchen ueber die erste Anlage des Wirbelthierleibes.* , Lepizig, Vogel.

Hodgkinson, C. A., Moore, K. J., Nakayama, A., Steingrímsson, E., Copeland, N. G., Jenkins, N. A. & Arnheiter, H. 1993. Mutations at the mouse microphthalmia locus are associated with defects in a gene encoding a novel basic-helix-loop-helix-zipper protein. *Cell,* 74**,** 395-404.

Honjo, Y., Kniss, J. & Eisen, J. 2008. Neuregulin-mediated ErbB3 signaling is required for formation of zebrafish dorsal root ganglion neurons. *Development*, dev.022178v1.

Horstadius, S. 1950. *The neural crest: Its properties and derivatives in the light of experimental research,* New York, Oxford University Press.

Hultman, K. A., Bahary, N., Zon, L. I. & Johnson, S. L. 2007. Gene Duplication of the zebrafish kit ligand and partitioning of melanocyte development functions to kit ligand a. *PLoS Genet,* 3, e17.

Imokawa, G., Yada, Y. & Miyagishi, M. 1992. Endothelins secreted from human keratinocytes are intrinsic mitogens for human melanocytes. *Journal of Biological Chemistry,* 267, 24675-24680.

Jordan, S. A. & Jackson, I. J. 2000. MGF (KIT Ligand) Is a Chemokinetic Factor for Melanoblast Migration into Hair Follicles. *Developmental Biology,* 225, 424-436.

Kasemeier-Kulesa, J. C., Kulesa, P. M. & Lefcort, F. 2005. Imaging neural crest cell dynamics during formation of dorsal root ganglia and sympathetic ganglia. *Development,* 132, 235-245.

Kelsh, R. N., Brand, M., Jiang, Y. J., Heisenberg, C. P., Lin, S., Haffter, P., Odenthal, J., Mullins, M. C., van Eeden, F. J., Furutani-Seiki, M., Granato, M., Hammerschmidt, M., Kane, D. A., Warga, R. M., Beuchle, D., Vogelsang, L. & Nüsslein-Volhard, C. 1996. Zebrafish pigmentation mutations and the processes of neural crest development. *Development,* 123, 369-89.

Kelsh, R. N., Harris, M. L., Colanesi, S. & Erickson, C. A. 2009. Stripes and belly-spots -- a review of pigment cell morphogenesis in vertebrates. *Semin Cell Dev Biol,* 20, 90-104.

Keynes, R. & Cook, G. M. W. 1995. Axon guidance molecules. *Cell,* 83, 161-169.

Knight, R. D., Nair, S., Nelson, S. S., Afshar, A., Javidan, Y., Geisler, R., Rauch, G.-J. & Schilling, T. F. 2003. lockjaw encodes a zebrafish tfap2a required for early neural crest development. *Development,* 130, 5755-5768.

Krull, C. E. 2010. Neural crest cells and motor axons in avians: Common and distinct migratory molecules. *Cell Adh Migr,* 4.

LaBonne, C. & Bronner-Fraser, M. 1998. Neural crest induction in Xenopus: evidence for a two-signal model. *Development,* 125, 2403-2414.

Lamason, R. L., Mohideen, M.-A. P. K., Mest, J. R., Wong, A. C., Norton, H. L., Aros, M. C., Jurynec, M. J., Mao, X., Humphreville, V. R., Humbert, J. E., Sinha, S., Moore, J. L., Jagadeeswaran, P., Zhao, W., Ning, G., Makalowska, I., McKeigue, P. M., O'donnell, D., Kittles, R., Parra, E. J., Mangini, N. J., Grunwald, D. J., Shriver, M. D., Canfield, V. A. & Cheng, K. C. 2005. SLC24A5, a putative cation exchanger, affects pigmentation in zebrafish and humans. *Science,* 310, 1782-6.

Le Douarin, N. 1986a. Cell line segregation during peripheral nervous system ontogeny. *Science,* 231, 1515-1522.

Le Douarin, N. M. 1982. *The Neural Crest,* Cambridge, Cambridge University Press.

Le Douarin, N. M. 1986b. Investigations on the Neural Cresta. *Annals of the New York Academy of Sciences,* 486, 66-86.

Lemmon, M. A. & Schlessinger, J. 2010. Cell Signaling by Receptor Tyrosine Kinases. *Cell,* 141, 1117-1134.

Lewis, J. L., Bonner, J., Modrell, M., Ragland, J. W., Moon, R. T., Dorsky, R. I. & Raible, D. W. 2004. Reiterated Wnt signaling during zebrafish neural crest development. *Development,* 131, 1299-1308.

Lister, J. A., Robertson, C. P., Lepage, T., Johnson, S. L. & Raible, D. W. 1999. nacre encodes a zebrafish microphthalmia-related protein that regulates neural-crest-derived pigment cell fate. *Development,* 126, 3757-67.

Luo, T., Lee, Y.-H., Saint-Jeannet, J.-P. & Sargent, T. D. 2003. Induction of neural crest in Xenopus by transcription factor AP2α. *Proceedings of the National Academy of Sciences,* 100, 532-537.

Marchant, L., Linker, C., Ruiz, P., Guerrero, N. & Mayor, R. 1998. The inductive properties of mesoderm suggest that the neural crest cells are specified by a BMP gradient. *Developmental Biology,* 198, 319-329.

Martinez-Morales, J.-R., Henrich, T., Ramialison, M. & Wittbrodt, J. 2007. New genes in the evolution of the neural crest differentiation program. *Genome Biology,* 8, R36.

Mayor, R., Guerrero, N. & Martı́ nez, C. 1997. Role of FGF andNogginin Neural Crest Induction. *Developmental Biology,* 189, 1-12.

Monsoro-Burq, A.-H., Wang, E. & Harland, R. 2005. Msx1 and Pax3 Cooperate to Mediate FGF8 and WNT Signals during Xenopus Neural Crest Induction. *Developmental Cell,* 8, 167-178.

Newton, J. M., Cohen-Barak, O., Hagiwara, N., Gardner, J. M., Davisson, M. T., King, R. A. & Brilliant, M. H. 2001. Mutations in the human orthologue of the mouse underwhite gene (uw) underlie a new form of oculocutaneous albinism, OCA4. *Am J Hum Genet,* 69, 981-8.

Nuckels, R. J., Ng, A., Darland, T. & Gross, J. M. 2009. The vacuolar-ATPase complex regulates retinoblast proliferation and survival, photoreceptor morphogenesis, and pigmentation in the zebrafish eye. *Invest Ophthalmol Vis Sci,* 50, 893-905.

Opdecamp, K., Nakayama, A., Nguyen, M. T., Hodgkinson, C. A., Pavan, W. J. & Arnheiter, H. 1997. Melanocyte development in vivo and in neural crest cell cultures: crucial dependence on the Mitf basic-helix-loop-helix-zipper transcription factor. *Development,* 124, 2377-2386.

Page-McCaw, P. S., Chung, S. C., Muto, A., Roeser, T., Staub, W., Finger-Baier, K. C., Korenbrot, J. I. & Baier, H. 2004. Retinal network adaptation to bright light requires tyrosinase. *Nat Neurosci,* 7, 1329-36.

Parichy, D. M., Rawls, J. F., Pratt, S. J., Whitfield, T. T. & Johnson, S. L. 1999. Zebrafish sparse corresponds to an orthologue of c-kit and is required for the morphogenesis of a subpopulation of melanocytes, but is not essential for hematopoiesis or primordial germ cell development. *Development,* 126, 3425-36.

Parichy, D. M. & Turner, J. M. 2003. Zebrafish puma mutant decouples pigment pattern and somatic metamorphosis. *Dev Biol,* 256, 242-57.

Pingault, V., Ente, D., Dastot-Le Moal, F., Goossens, M., Marlin, S. & Bondurand, N. 2010. Review and update of mutations causing Waardenburg syndrome. *Human Mutation,* 31, 391-406.

Platt, J. B. 1897. The development of the cartilaginous skull and of the branchiaaland hypoglossol musculature in Necturs. . *Morphol Jb,* 25, 87.

Raible, D. W. & Eisen, J. S. 1994. Restriction of neural crest cell fate in the trunk of the embryonic zebrafish. *Development,* 120, 495-503.

Raible, D. W., Wood, A., Hodsdon, W., Henion, P. D., Weston, J. A. & Eisen, J. S. 1992. Segregation and early dispersal of neural crest cells in the embryonic zebrafish. *Developmental Dynamics,* 195, 29-42.

Raposo, G. & Marks, M. S. 2002. The Dark Side of Lysosome-Related Organelles: Specialization of the Endocytic Pathway for Melanosome Biogenesis. *Traffic,* 3, 237-248.

Raven, C. P. a. K., J. 1945. Induction by medial and lateral pieces of the archenteron roof, with special reference to the determination of the neural crest. *Acta Neerl. Morph. Norm. Path.,* 5.

Rawls, J. F. & Johnson, S. L. 2000. Zebrafish kit mutation reveals primary and secondary regulation of melanocyte development during fin stripe regeneration. *Development,* 127**,** 3715-24.

Raws, M. E. 1947. Origin of pigment cells from the neural crest in the mouse embryo. *Physiol. Zool.,* 20**,** 18.

Rickmann, M., Fawcett, J. W. & Keynes, R. J. 1985. The migration of neural crest cells and the growth of motor axons through the rostral half of the chick somite. *J Embryol Exp Morphol,* 90**,** 437-55.

Sabeti, P. C., Varilly, P., Fry, B., Lohmueller, J., Hostetter, E., Cotsapas, C., Xie, X., Byrne, E. H., McCarroll, S. A., Gaudet, R., Schaffner, S. F., Lander, E. S., Consortium, I. H., Frazer, K. A., Ballinger, D. G., Cox, D. R., Hinds, D. A., Stuve, L. L., Gibbs, R. A., Belmont, J. W., Boudreau, A., Hardenbol, P., Leal, S. M., Pasternak, S., Wheeler, D. A., Willis, T. D., Yu, F., Yang, H., Zeng, C., Gao, Y., Hu, H., Hu, W., Li, C., Lin, W., Liu, S., Pan, H., Tang, X., Wang, J., Wang, W., Yu, J., Zhang, B., Zhang, Q., Zhao, H., Zhao, H., Zhou, J., Gabriel, S. B., Barry, R., Blumenstiel, B., Camargo, A., Defelice, M., Faggart, M., Goyette, M., Gupta, S., Moore, J., Nguyen, H., Onofrio, R. C., Parkin, M., Roy, J., Stahl, E., Winchester, E., Ziaugra, L., Altshuler, D., Shen, Y., Yao, Z., Huang, W., Chu, X., He, Y., Jin, L., Liu, Y., Shen, Y., Sun, W., Wang, H., Wang, Y., Wang, Y., Xiong, X., Xu, L., Waye, M. M. Y., Tsui, S. K. W., Xue, H., Wong, J. T.-F., Galver, L. M., Fan, J.-B., Gunderson, K., Murray, S. S., Oliphant, A. R., Chee, M. S., Montpetit, A., Chagnon, F., Ferretti, V., Leboeuf, M., Olivier, J.-F., Phillips, M. S., Roumy, S., Sallée, C., Verner, A., Hudson, T. J., Kwok, P.-Y., Cai, D., Koboldt, D. C., Miller, R. D., et al. 2007. Genome-wide detection and characterization of positive selection in human populations. *Nature,* 449**,** 913-8.

Saint-Jeannet, J.-P., He, X., Varmus, H. E. & Dawid, I. B. 1997. Regulation of dorsal fate in the neuraxis by Wnt-1 and Wnt-3a. *Proceedings of the National Academy of Sciences,* 94**,** 13713-13718.

Saldana-Caboverde, A. & Kos, L. 2010. Roles of endothelin signaling in melanocyte development and melanoma. *Pigment cell & melanoma research,* 23**,** 160-170.

Sato, T., Sasai, N. & Sasai, Y. 2005. Neural crest determination by co-activation of Pax3 and Zic1 genes in Xenopus ectoderm. *Development,* 132**,** 2355-2363.

Sauka-Spengler, T., Meulemans, D., Jones, M. & Bronner-Fraser, M. 2007. Ancient Evolutionary Origin of the Neural Crest Gene Regulatory Network. *Developmental Cell,* 13**,** 405-420.

Sauka-Spengler, T. B.-F., Marianne 2008. A gene regulatory network orchestrates neural crest formation. *Nat Rev Mol Cell Biol,* 9.

Spritz, R., Strunk, K., Oetting, W. & King, R. 1988. RFLP for TaqI at the human tyrosinase locus. *Nucleic Acids Research,* 16**,** 9890.

Stemple, D. L. & Anderson, D. J. 1992. Isolation of a stem cell for neurons and glia from the mammalian neural crest. *Cell,* 71**,** 973-985.

Strobl-Mazzulla, P. H. & Bronner, M. E. 2012. Epithelial to mesenchymal transition: New and old insights from the classical neural crest model. *Seminars in Cancer Biology,* 22**,** 411-416.

Tachibana, M., Takeda, K., Nobukuni, Y., Urabe, K., Long, J. E., Meyers, K. A., Aaronson, S. A. & Miki, T. 1996. Ectopic expression of MITF, a gene for Waardenburg syndrome type 2, converts fibroblasts to cells with melanocyte characteristics. *Nat Genet,* 14**,** 4.

Tanimura, S., Tadokoro, Y., Inomata, K., Binh, N. T., Nishie, W., Yamazaki, S., Nakauchi, H., Tanaka, Y., McMillan, J. R., Sawamura, D., Yancey, K., Shimizu, H. & Nishimura, E. K. 2011. Hair Follicle Stem Cells Provide a Functional Niche for Melanocyte Stem Cells. *Cell Stem Cell,* 8**,** 177-187.

Thomas, A. J. & Erickson, C. A. 2008. The making of a melanocyte: the specification of melanoblasts from the neural crest. *Pigment cell & melanoma research,* 21**,** 598-610.

Vincent, M. & Thiery, J.-P. 1984. A cell surface marker for neural crest and placodal cells: Further evolution in peripheral and central nervous system. *Developmental Biology,* 103**,** 468-481.

Wehrle-Haller, B. 2003. The role of Kit-ligand in melanocyte development and epidermal homeostasis. *Pigment Cell Res,* 16**,** 287-96.

Werner, T., Hammer, A., Wahlbuhl, M., Bösl, M. R. & Wegner, M. 2007. Multiple conserved regulatory elements with overlapping functions determine Sox10 expression in mouse embryogenesis. *Nucleic Acids Research,* 35**,** 6526-6538.

Weston, J. 1991. Sequential segregation and fate of developmentally restricted intermediate cell populations in the neural crest lineage. *Curr Top Dev Biol.,* 25**,** 20.

Weston, J. A. 1963. A radioautographic analysis of the migration and localization of trunk neural crest cells in the chick. *Developmental Biology,* 6**,** 279-310.

Xu, X., Dong, G.-X., Hu, X.-S., Miao, L., Zhang, X.-L., Zhang, D.-L., Yang, H.-D., Zhang, T.-Y., Zou, Z.-T., Zhang, T.-T., Zhuang, Y., Bhak, J., Cho, Yun S., Dai, W.-T., Jiang, T.-J., Xie, C., Li, R. & Luo, S.-J. 2013. The Genetic Basis of White Tigers. *Current Biology,* 23**,** 1031-1035.

Yan, Y.-L., Miller, C. T., Nissen, R., Singer, A., Liu, D., Kirn, A., Draper, B., Willoughby, J., Morcos, P. A., Amsterdam, A., Chung, B.-c., Westerfield, M., Haffter, P., Hopkins, N., Kimmel, C. & Postlethwait, J. H. 2002. A zebrafish sox9 gene required for cartilage morphogenesis. *Development,* 129, 5065-5079.

Yang, C.-T. & Johnson, S. L. 2006. Small molecule-induced ablation and subsequent regeneration of larval zebrafish melanocytes. *Development,* 133, 3563-3573.

Contributions

Publication 1:

Dooley CM, Mongera A, Walderich B, Nüsslein-Volhard C. (2013). **On the embryonic origin of adult melanophores: the role of ErbB and Kit signalling in establishing melanophore stem cells in zebrafish.** *Development* 140, 1003-1013

The project was conceived by and designed by Dooley CM with assistance from Nüsslein-Volhard C. The majority of experiments were carried out by Dooley CM with assistance of Walderich B with some transplantations (Fig 4). Further transplantations were carried out by Walderich B (Fig 2) and dorsal root ganglia ablation carried out by Mongera A (Fig 5F). Publication 1 was primarily written by Nüsslein-Volhard C. with the assistance of Dooley CM.

Publication 2:

Dooley CM, Schwarz H, Mueller KP, Mongera A, Konantz M, Neuhauss SC, Nüsslein-Volhard C, Geisler R. (2012). **Slc45a2 and V-ATPase are regulators of melanosomal pH homeostasis in zebrafish, providing a mechanism for human pigment evolution and disease.** *Pigment Cell Melanoma Res.* 26; 205–217

The project was conceived by and designed by Dooley CM with some assistance from Geisler R. The majority of experiments were carried out by Dooley CM with some assistance of Konantz M. Most electron microscopy was carried out by Schwarz H with the remainder being carried out by Dooley CM. Mongera A assisted in both human and zebrafish rescues of *slc45a2*. Testing of albino visual acuity was carried out as collaboration together with Mueller KP and Neuhauss SC. (Fig. 2) The publication was primarily written by Dooley CM with the assistance of Nüsslein-Volhard C and Geisler R.

Curriculum vitae

Christopher Michael Dooley

born: November 11th , 1977 in Burlington, Vermont (USA)

11/2011 -	Researcher at the Wellcome Trust Sanger Institute in Hinxton, United Kingdom
04/2006-11/2011	PhD student at the Max Planck Institute for Developmental Biology in Tuebingen, Germany
09/2003-10/2005	MSc in Biotechnology at the University of Applied Sciences in Mannheim, Germany
08/2000-09/2003	Research assistant at the Max Planck Institute for Developmental Biology in Tuebingen, Germany
08/1996-06/2000	BSc in Medical Laboratory Science at the University of Vermont in Burlington, Vermont, USA
1992-1996	Essex Junction High School, Essex, Vermont, USA

List of publications

Mongera A, **Dooley CM.** Of white tigers and solute carriers. *Pigment Cell*
Melanoma Res. 2013 Nov;26(6):787-9. doi: 10.1111/pcmr.12163.

Dooley CM*, Scahill C*, Fényes F, Kettleborough RN, Stemple DL, Busch-Nentwich
EM. Multi-allelic phenotyping--a systematic approach for the simultaneous analysis of multiple induced mutations. *Methods*. 2013 Aug 15;62(3):197-206. doi: 10.1016/j.ymeth.2013.04.013.

Howe K, Clark MD, Torroja CF, et al.
The zebrafish reference genome sequence and its relationship to the human genome. *Nature*. 2013 Apr 25;496(7446):498-503. doi: 10.1038/nature12111.

Kettleborough RN*, Busch-Nentwich EM*, Harvey SA*, **Dooley CM**, de Bruijn E, van Eeden F, Sealy I, White RJ, Herd C, Nijman IJ, Fényes F, Mehroke S, Scahill C, Gibbons R, Wali N, Carruthers S, Hall A, Yen J, Cuppen E, Stemple DL. A systematic genome-wide analysis of zebrafish protein-coding gene function. *Nature*. 2013 Apr 25;496(7446):494-7. doi: 10.1038/nature11992.

Grønskov K*, **Dooley CM***, Østergaard E, Kelsh RN, Hansen L, Levesque MP, Vilhelmsen K, Møllgård K, Stemple DL, Rosenberg T. Mutations in c10orf11, a melanocyte-differentiation gene, cause autosomal-recessive albinism. *Am J Hum Genet*. 2013 Mar 7;92(3):415-21. doi: 10.1016/j.ajhg.2013.01.006

Dooley CM, Mongera A, Walderich B, Nüsslein-Volhard C. On the embryonic origin of adult melanophores: the role of ErbB and Kit signalling in establishing melanophore stem cells in zebrafish. *Development*. 2013 Mar;140(5):1003-13. doi: 10.1242/dev.087007.

Dooley CM, Schwarz H, Mueller KP, Mongera A, Konantz M, Neuhauss SC, Nüsslein-Volhard C, Geisler R. Slc45a2 and V-ATPase are regulators of melanosomal pH homeostasis in zebrafish, providing a mechanism for human pigment evolution and disease. Pigment Cell Melanoma Res. 2013 Mar;26(2):205-17. doi: 10.1111/pcmr.12053. Epub 2012 Dec 20.

Geisler R, Rauch GJ, Geiger-Rudolph S, Albrecht A, van Bebber F, Berger A, Busch-Nentwich E, Dahm R, Dekens MP, **Dooley C**, Elli AF, Gehring I, Geiger H,Geisler M, Glaser S, Holley S, Huber M, Kerr A, Kirn A, Knirsch M, Konantz M,Küchler AM, Maderspacher F, Neuhauss SC, Nicolson T, Ober EA, Praeg E, Ray R, Rentzsch B, Rick JM, Rief E, Schauerte HE, Schepp CP, Schönberger U, Schonthaler HB, Seiler C, Sidi S, Söllner C, Wehner A, Weiler C, Nüsslein-Volhard C.
Large-scale mapping of mutations affecting zebrafish development. BMC Genomics. 2007 Jan 9;8:11. PubMed PMID: 17212827; PubMed Central PMCID: PMC1781435.
*denotes shared contribution